University of Zurich[UZH]

Geomorphometric analysis of a debris flow event in Buffalora and catchment properties in the Swiss National Park

---

GEO 511 - Master's Thesis

Supervised by
Prof. Dr. Ross Purves, UZH
Dr. Isabelle Gärtner-Roer, UZH
Dr. Samuel Wiesmann, SNP

Submitted by
Fabienne Koenig
Mat. Nr. 18-724-963

July 29, 2024

Department of Geography, University of Zurich

Abstract

The Swiss National Park (SNP) is located in the canton of Grisons in the Engadin and represents a protected nature reserve where natural processes such as debris flows, erosion and deposition are left to develop naturally thus continually shaping the landscape. One significant debris flow event happened in 2022 at Buffalora, whose depositions reached the highly trafficked Ofenpass road, raising questions about future risks and predictive methods for such occurrences in the park. Geomorphometry as a quantitative land-surface analysis enables a detailed study of geomorphological processes such as debris flows through the extraction of primary and secondary terrain attributes from Digital Elevation Models. Emphasizing the importance of assessing debris flow risks in light of climate change, the significance of the Ofenpass road, and the lack of prior risk assessments for debris flow hazards in the SNP, this master thesis aims to identify debris flow-prone areas within the SNP and evaluate the feasibility of predicting such events by employing geomorphometric methods. The methodology initially focuses on applying geomorphometric parameters and indices to the area of the Buffalora debris flow event, thus applying the approved methods to the entire park. A Principal Component Analysis of all parameters and indices in all catchment areas in the SNP helped distinguish between the different catchment areas in terms of their geomorphological properties. The analysis is conducted utilizing data sets including pre- and post-Digital Terrain Models, high-resolution aerial imagery for visual geomorphological assessments and records of observed debris flow events in the SNP from 2005 to 2023. The results of this master thesis recommend integrating multiple parameters and indices for a thorough debris flow risk assessment, as each variable impacts the analysis differently. While the Principal Component Analysis effectively identified catchments less susceptible to debris flows, it could not distinguish highly susceptible catchments, indicating the results cannot be relied upon as a prevention tool. Future studies could incorporate additional variables, such as vegetation cover and soil moisture, to enhance debris flow risk assessments and validate methodologies across different regions.

Acknowledgments

There are several people to whom I would like to express my gratitude, whose support has contributed significantly to this master thesis:

Many thanks to my supervisors Prof. Dr. Ross Purves and Dr. Isabelle Gärtner-Roer from UZH who took on board my idea of writing a master thesis in the Swiss National Park. They guided me in the right direction with their expertise and constructive feedback and encouraged me throughout the entire process.

I am very grateful to the Swiss National Park for granting me the opportunity to conduct research and for the warm welcome, I received during each visit. Special thanks go to Jan Schweizer and Julia Paterno for thoroughly reviewing my work. Their invaluable inputs during the final stages of my thesis were crucial in helping me finalize this project.

My sincere appreciation goes to my supervisor from the Swiss National Park, Dr. Samuel Wiesmann. Despite not knowing exactly what lay ahead, he welcomed me with open arms and consistently made time for me, which I deeply appreciated. His unwavering encouragement and support not only boosted my confidence but also filled me with joy throughout this journey.

Further, I would like to thank my parents and my sister who always had their doors open to me during challenging times. Their care and belief in me were a constant source of motivation and resilience.

Heartfelt thanks go to my friend Ladina Honegger, who warmly hosted me at her home in La Punt. Our fulfilling conversations after long days in the Swiss National Park helped me recharge and face each new day with renewed enthusiasm.

I am grateful to my roommates and friends Hannah Kuhn and Viviane Lott, for their understanding and support during every mood swing and for their constant motivation.

The unwavering support and motivating pep talks during challenging times of my dear friends Lou Pfister and Nadine Geissmann have been a source of great strength and encouragement. Their presence and reassurance have helped me navigate the ups and downs of this journey.

I am truly thankful to my study buddy Annika Kunz, whose support has been indispensable throughout my entire geography studies. Her companionship and dedication were vital not only in navigating the complexities of the program but also in completing our master theses simultaneously. Her unwavering encouragement and shared commitment have made this journey both achievable and memorable.

Much appreciation goes to my boyfriend Andreas Huser, for his constant uplifting words and motivation which have been crucial in keeping me focused and energized throughout the process.

Thanks to my fellow master students in our masters study room, for sharing this experience and ensuring that I never faced it alone. Your camaraderie made this journey all the more fulfilling.

Contents

List of Figures

List of Tables

List of Abbreviations

AGP	ArcGIS Pro (Version 3.2.1)
CTI	Compound Topographic Index
DEM	Digital Elevation Model
DSM	Digital Surface Model
DTM	Digital Terrain Model
ERR	Elevation Relief Ratio
GIS	Geographic Information System
GSD	Ground Sampling Distance
LHN95	National height network
MRN	Melton's Ruggedness number
PCA	Principal Component Analysis
SNP	Swiss National Park
SPI	Stream Power Index
STI	Sediment Transport Index
TRI	Topographic Roughness Index
TWI	Topographic Wetness Index

1 Introduction

The Swiss National Park (SNP) is located in Switzerland in the canton of Grisons in the Engadin. It represents a reserve in which nature is protected from any human interference, particularly the entire fauna and flora, which are left to develop naturally. The SNP is designated as a Strict Nature Reserve (International Union for Conservation of Nature (IUCN) Category Ia) and forms part of the UNESCO Biosphere Reserve Engiadina Val Müstair (IUCN, 2024). Weathering, rockfall, landslides, debris flows, mountain streams, soil flow, rock glaciers, avalanches, talus cones and alluvial fans are constant features of the captivating landscape of the SNP. The processes of erosion, transport, and deposition ensure that the terrain is subject to continuous change and dynamics. Viewed over geological time scales, the current landscape of the park represents merely a snapshot (Röber et al., 2014).

Debris flows are common in the SNP area. Large parts of the geology in the SNP are composed of dolomite, which weathers more easily than crystalline rocks and thus accumulates in massive scree slopes at the base of mountains. When these scree slopes become saturated with water, such as from heavy rainfall or significant snowmelt, the water-debris mixture begins to flow down steep slopes. Typically, this mixture flows along existing channels, such as in Val dal Botsch or Val da Stabelchod along stream gullies, or the pre-existing debris flow channels in the Val Trupchun basin. Debris flows often start to slow down and eventually stop in the flatter areas of the valleys. The deposited material ranges from fine sand to large boulders. Especially in the naturally flowing streams of the SNP, the recurring debris flow events can be easily recognized by the large amount of debris and the incised channels. A debris flow as an occurring process is therefore not unusual in the SNP (SNP, 2024; Röber et al., 2014).

A significant example of such debris flow activity occurred in 2022. After a warm day, heavy rainfall on July 22, 2022, triggered a significant debris flow event at Buffalora, on the Ofenpass road. The debris flow was triggered inside the SNP and deposited partly in and outside side the park boundary. The event did not consist of a single large debris flow but rather numerous surges of varying sizes, distributed randomly and across the slope. In the upper transit area, larger surges toppled, stripped, and debarked the trees. In the lower area, the flow paths spread out, with the debris flows traversing the forest without destroying it. The rainfall event in July 2022 triggered another debris flow in the Val Naira. The Val Naira drains the western flank of Piz Nair and passes under the main road a few hundred meters northwest of Buffalora. The debris flows caused significant deposition reaching the Berggasthaus Buffalora and the main road, which was interrupted (Figure 1.1). There are no known recent events where the road was flooded, which states that the event was rather larger than usual. The frequency of the rainfall event suggests it is a 20- to 40-year occurrence, but aerial imagery indicates the recurrence interval might be closer to 100 years rather than 30 years. The height and extent of the deposits, compared with the topography and forest cover, indicate that this was a rather

rare event (Herzog Ingenieure AG, 2022).

Figure 1.1: Depositions of the debris flow event at Buffalora, reaching the Werkhof and Berggasthaus Buffalora, right at the Ofenpass road. Data: Herzog Ingenieure AG (2022), Herzog Ingenieure AG provided by AWN Südbünden on 2 August 2022, not intended for further use.

This background raises the question of where else in the SNP there is potential for such debris flow activity: Is the Ofenpass road as a vital transport route at risk? Are there other areas highly susceptible to debris flows? Is it possible to make predictions for future events based on the terrain? What methods are available for this, and how can they be applied? Additionally, how can these methods be specifically applied to Buffalora and the entire SNP?

2 Background and State of the Art

2.1 Geomorphology

To understand what methods are available for estimating predictions of future debris flow events in the SNP, it is first necessary to examine the theoretical background of such events, also concerning high mountain geomorphology and process areas.

2.1.1 High mountain geomorphology

High mountain geomorphology is concerned with the study of geomorphology in high mountain regions. This discipline analyses the origin, development and formation of landforms in areas located at high altitudes, such as mountain ranges or summit regions. High mountain regions are characterized by steep relief structures as steep slopes, cliffs and mountain peaks, which are shaped by geological processes such as tectonics, erosion, and glaciation (Mani et al., 2023). Such mountain regions are subject to a wide range of natural hazard processes (Stäubli et al., 2018). These include various gravitational processes such as rock and debris avalanches, rockfalls, landslides, and debris flows. Additionally, they face massive glacial detachments, snow avalanches, and various types of floods triggered by heavy rains or lake outbursts (Mani et al., 2023). Apart from the local relief, numerous environmental factors also contribute to the high rates of denudation in mountainous regions. These factors include low temperatures, higher precipitation levels, and distinct hydrologic and vegetational differences compared to lowland areas (Barsch et al., 1984).

2.1.2 Geomorphological processes

Geomorphological processes are physical, chemical or biological processes on the Earth's surface that erode, transport and deposit the materials of the lithosphere. Figure 2.1 shows the classification of the geomorphological process types and areas according to Dikau, Eibisch, et al. (2019). These processes can be classified as exogenous (within the Earth's surface) or endogenous (above the Earth's surface) based on the dominant physical, chemical or biological processes. In the exogenous process group, these processes are further classified into geomorphological process areas such as *gravitational, fluvial or glacial.* High mountain regions are characterized by gravitational processes (Mani et al., 2023), whose classification into different mass movements is difficult due to the high diversity of the sub-processes and the wide variety of process properties. The classification systems are based on different properties of the processes, such as process mechanism, subsurface material, degree of activity, velocity, water content or geomorphometry of the moving mass (Dikau, Eibisch, et al., 2019). Nevertheless, gravitational mass movements can be differentiated into five different process types (Dikau, Brunsden,

et al., 1996): *fall, topple, slide, spread, flow or hybrid-complex* (if the gravitational processes occur in combination or sequentially in time). The category *gravitational flow* category includes debris flows (Dikau, Eibisch, et al., 2019).

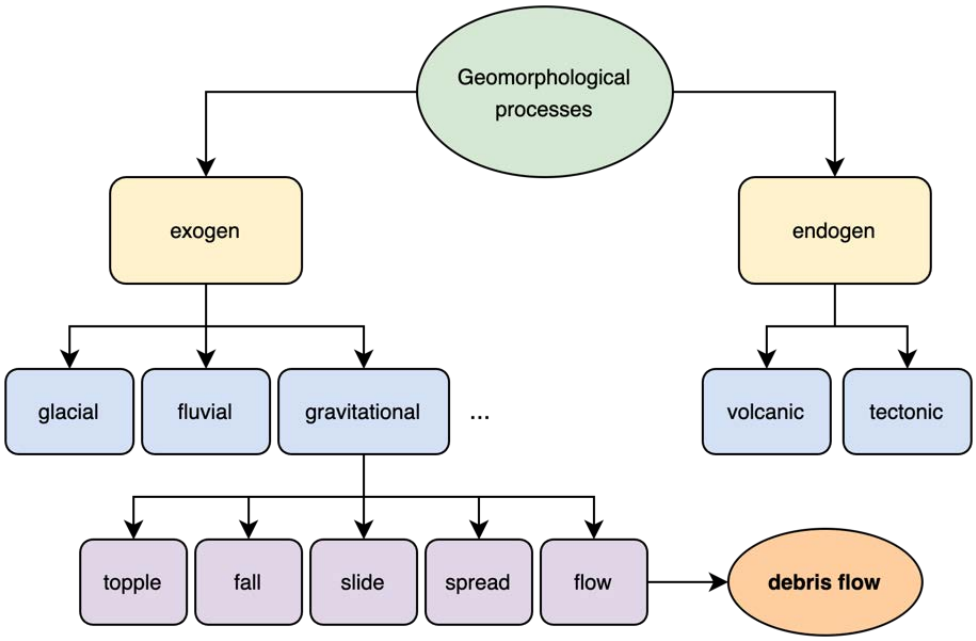

Figure 2.1: Classification of the debris flow process in the geomorphological process types and areas according to Dikau, Eibisch, et al. (2019). Own visualization.

2.1.3 Debris flow

A debris flow is defined as a form of rapid mass movement in steep mountainous terrain where a mixture of water and solid materials, such as stones, loose soil, boulders, debris or wood get driven down a slope. Debris flows are characterized by uneven flow behavior, high flow velocities, high impact forces and sudden occurrence (e.g., during thunderstorms). A prerequisite for the formation of debris flows is the presence of loose material, water and a sufficiently large slope or channel gradient. In the Alps, a lot of loose material has been deposited above the tree line in scree slopes and glacial moraines which serves as delivery material (USGS, 2006; WSL, 2006).

Debris flows depend on local climate and meteorology where water plays a decisive role in the triggering process. They are often triggered by heavy precipitation episodes and depend on the frequency and magnitude of such episodes. The time interval between precipitation and triggering of the debris flow can vary greatly, depending on the characteristics of the rain, the preceding moisture conditions and the morphometry of the affected watersheds (Borga et al., 2014). In the high alpine scree slopes, destabilization can already be achieved by underground saturation of loose material. Besides surface runoff and intensity of rainfall as contributing factors, soil saturation due to prolonged precipitation plays a critical role (WSL, 2006). Debris flows may also result from landslides, channel bed failures, moraine-dammed lake outbursts and glacial melting (Gregoretti et al., 2008). Further factors can contribute to initiating events such as basin morphology, surficial geology, hydrologic, geomorphometric and geotechnical features of the slopes, the source materials and the availability of sediments (Schumm, 1979; Harvey, 2007; Borga et al., 2014).

The interaction and ratio of solid and liquid constituents are decisive for the type of debris flow triggered. Depending on the water content, liquid floods, debris floods or debris flows can be formed (Borga et al., 2014). They take the form of a debris flood, with more water mixed in proportion to the solid material or result in erosion of unconsolidated solids when limited in water (Staley et al., 2006).

From the moment the debris flow is triggered, they develop rapidly and entrain all sediment material located in their transport zone (Borga et al., 2014). A wave-like, thrust-like flow is characteristic of the flow behavior and results in the formation of a front. The solids are concentrated at the debris flow front and are distributed evenly over the depth of the flow. Very large blocks of up to several meters in diameter can be transported within the debris flow front. Behind the front, both the flow depth and the concentration of solids decrease and the stones are transported closer to the bed (WSL, 2006). As the surge races downhill, the steep banks aside get eroded and more soil material including organic debris gets added to the flow (Hungr et al., 2014). If there are flat banks in a channel, debris flows form their lateral boundary to a certain extent by depositing material along the bed of the stream, called levées. The debris is deposited in irregular shapes on the flatter terrain. The high viscosity of the slow-flowing mixture leads to an abrupt stop of the debris flow (WSL, 2006). Affecting a forest area, debris flows can impact trees in different ways. They can erode the root plate and destabilize trees, cause abrasion scars, tear down trees into the deposition zone or clear the area where surviving trees may benefit from less competition (Meng et al., 2023). While debris flows initiate in typically small catchments of a few square kilometers, sediment transport and deposition processes may impact larger catchments (Borga et al., 2014). During major debris flows in the Alps, debris volumes of several 10'000 – 100'000 m^3 are transported downhill. The largest discharge (maximum discharge) usually occurs around the debris flow front. During debris flows in the Alps, the maximum discharge can reach 100 – 1'000 m^3/s. Flow velocities of up to 15 m/s (54 km/h) are reached and blocks weighing more than 50 tons can be transported (WSL, 2006).

2.2 Geomorphometry

Since the end of the 20th century, Geographic Information System (GIS) related applications have become frequent in physical geography and Earth sciences, including geomorphology. The combination of GIS and geomorphology is called geomorphometry and presents a modern, analytical-cartographic approach to the science of quantitative land-surface analysis. It offers various opportunities to analyze processes such as a debris flow on different analytical levels (Oguchi et al., 2011; Pike, Evans, et al., 2008). The fundamental operation of geomorphometry is the extraction of parameters and objects from Digital Elevation Models (DEMs). Values derived directly from the DEMs themselves are called primary terrain attributes, which describe the local morphology of the land surface (Pike, Evans, et al., 2008). Secondary terrain attributes are defined as values derived by combining multiple primary terrain attributes which result in indices (Chen et al., 2011). Numerous topographic parameters and indices have been proposed by the literature to represent the geomorphological characteristics of land surfaces.

2.2.1 Primary terrain attributes

According to the literature, the most basic and frequently used primary parameters include slope, aspect and curvature. Slope [*degree*] reflects the angle between the horizontal plane and the one

tangential to the surface at a given point of the topographical surface (Lehmann, 1816). Aspect [*degree*] is the direction angle of the slope to some arbitrary zero (normally north). Usually, it is measured in degrees, read clockwise from north, ranging from 0° to 360° (Gallant et al., 1996). Curvature [*degree*] is generally of two types, where the shape of the slope is displayed either through concavity or convexity: Planform Curvature (horizontal) and Profile Curvature (vertical) (Ahmad et al., 2019). Planform curvature is always perpendicular to the direction of the maximum slope and influences the ridges and drainage pattern formations. High values of planform curvature represent divergent curvatures meaning that these areas are laterally convex, rather leading to the formation of ridges. High negative values in contrast demonstrate convergent curvatures, indicating the formation of channels (flow convergence) leading to more erosion. Null values represent planar curvatures (Ahmad et al., 2019; Zevenbergen et al., 1987). Profile curvature indicates the variation in slope gradient in the vertical plane. It influences either the acceleration or deceleration of flow and, hence, determines the erosion and deposition processes. High positive values express high flow acceleration which influences the erosion process while high negative values express decelerated flow (Smith et al., 2007). The **catchment area** [m^2] serves as an important basic attribute for further secondary parameters. It includes the upslope area from a given cell and is based on flow direction and flow accumulation functions on a DEM. This parameter can give an estimation of the runoff volume of a hydrological or geomorphological event (Moore, Grayson, et al., 1991; Speight, 1980).

2.2.2 Secondary terrain attributes: indices

Going further from the primary attributes, the two most frequently used indices that are based on the catchment area are the Stream Power Index (SPI) and the Topographic Wetness Index (TWI). The SPI can be used to describe potential flow erosion and related landscape processes (Wilson et al., 2000). The literature suggests the formula for the calculation of the SPI in different versions, which are all widely used. In contrary to Wilson et al. (2000), the work from Ahmad et al. (2019) or Chen et al. (2011) refer to the formula including a natural logarithm. Nevertheless, the SPI indicates where the channels' erosive power is and how strong and great the topographical potential for deposition and erosive areas is. It is also a simple metric for the ability of a stream to incise into bedrock (Umar et al., 2014; Chen et al., 2011; Flint, 1974). Low or negative values express the topographical potential for deposition whereas erosive areas are depicted by positive values (Ahmad et al., 2019). The SPI is based on the assumption that a specific catchment area is proportional to its discharge. As the catchment area and the slope steepness increase, the amount of contributing water by upslope area and the velocity increase, leading to increased stream power and potential erosion (Gruber et al., 2008; Moore, Grayson, et al., 1991).

Given overland flow and constant transmissivity, the TWI provides information on the tendency of a location to accumulate water and can therefore be used to assess the spatial pattern of potential soil moisture in soil texture due to erosion (Chen et al., 2011). This index was developed as part of the hydrological runoff model TOPMODEL and then applied to many studies regarding soil moisture, soil chemistry or species distribution analysis (Beven et al., 1979; Marthews et al., 2015). It is now frequently used in landslide susceptibility mapping (Sevgen et al., 2019). TWI according to Wilson et al. (2000), assumes steady-state conditions and consistent soil properties. It forecasts saturation zones where the specific catchment area is large (commonly in converging landscape segments) and the local slope angle is small (at the base of concave slopes where the gradient decreases). These conditions are

typically found along drainage paths and in areas where water accumulates in the landscape. Another version of TWI is by including the soil transmissivity when the soil profile is saturated (Wilson et al., 2000). Nevertheless, Wood et al. (1990) demonstrated that the variation in the topographic component is often significantly greater than the local variability in soil transmissivity and as a result, the approach of Beven et al. (1979) is sufficient in terms of complexity for most applications.

The Sediment Transport Index (STI) is a measurement of erosion of channel flow downstream, sediment transport capacity and deposition in the plain. It is equal to the length-slope factor of the Revised Universal Soil Loss Equation (RUSLE) (Moore and Burch, 1986). Low STI values indicate low erosion risk while high values correlate to steep slopes and ridges, associated with a significant degree of soil erosion and degradation (Ahmad et al., 2019; Chen et al., 2011).

The Hypsometric Integral (HI) is a measure of the relationship between the elevation and area in a catchment. If the HI is calculated using a regular kernel (e.g., a 3x3 cell window), it is referred to as the Elevation-Relief Ratio (ERR). Both HI and ERR are defined as the difference between mean and minimum elevation divided by the relief (difference between maximum and minimum elevation) (Pike and Wilson, 1971; Otto et al., 2017). The ERR tends to be high for convex landscape patches and becomes lower with increasing concavity (Otto et al., 2017). Additionally, relief measurements indicate the potential energy of the drainage system due to its elevation above sea level, according to Strahler (1968). Especially concerning watershed relief, ERR is a measure of the potential energy within the drainage area, with higher relief values indicating stronger erosional forces due to a steeper terrain (Patton, 1988).

The Melton's Ruggedness Number (MRN) is a slope index but takes also into account the overall relief of the upslope area. MRN values help to identify channels with high versus low sediment transport capacity. In addition, the Ruggedness Number offers the possibility to distinguish basins with debris flow potential from basins where sediment transport processes are dominated by bedload (Marchi et al., 2005). A study in the Canadian Rocky Mountains carried out by Jackson et al. (1987) showed the capability of the MRN in distinguishing alluvial fans from debris flow fans. Watersheds prone to flooding had MRN values < 0.3 while watersheds prone to debris flows had ratios > 0.3. Bovis et al. (1999) determined debris flow watersheds at MRN values > 0.53 in the coastal mountains of southwest British Columbia. Wilford et al. (2004) published another study in Canada where MRN values < 0.3 characterize water flood basins, values between 0.3 and 0.6 are related to debris floods and values $>$ 0.6 refer to debris flow basins.

Corominas (1996) defined the Relief Ratio (R) as a measure to describe debris flow travel distance and event magnitude. It has been used to describe the debris flow mobility from a landslide head scarp to a debris deposition front (Rickenmann, 1999). The study of Ilinca (2021) showed that debris flow basins are characterized by $R > 0.4$ and debris flood basins by R between 0.2 and 0.4. The research conducted by Singh et al. (2020) carried out a morphometric analysis of the Ghaghara River in India to describe various surface processes. Relief ratios carried out for sub-basins in the study area ranged from 0.4 to 2, which represent low to moderate relief ratio values. They characterize high values of relief ratio as an indication of hilly regions whereas, low values are characteristic of pediplains and valleys.

The Compound Topography Index **(CTI)** examines the hydrological system of an area and represents a steady state wetness index. The CTI is a measure of soil moisture potential and differentiates areas having the potential to be saturated with water depending on its contributing neighborhood and the

local slope gradient (Buttrick et al., 2015). High positive CTI values indicate a larger vulnerability to flash flooding and inundation compared to low positive CTI values. Very low positive CTI values are also typically found along ridgelines while high positive values are often located in valley bottoms and basins with large contributing areas. Areas with very low negative CTI values characterize steep slopes highlighting the local channel system conditions. Intermediate values relate to steep slopes and water channels, which contribute most to erosion processes (Ahmad et al., 2019; Buttrick et al., 2015).

The Topographic Roughness Index **(TRI)** describes the variability of a topographical surface at a given scale, the so-called roughness. Various definitions of roughness exist, e.g., Grohmann et al. (2011) is giving an overview. The publication of Veitinger et al. (2014) chose the method developed by Sappington et al. (2007). It does not only take into account the sum of changes in elevation within an area but also the dispersion of vectors orthogonal to the terrain surface. This definition makes it possible to derive roughness directly from a DEM. The resulting index is a measure of the surface roughness with values ranging from 0 (flat) to 1 (extremely rough).

2.3 Related work in geomorphometry

The integration of geomorphometric indices within geomorphological research has been extensively explored in the literature. A comprehensive overview of such indices and their applications is provided by Otto et al. (2017). This paper outlines the fundamental principles of various parameters and indices used for analyzing landforms and geomorphological processes. It also highlights both conventional and innovative data sources essential for geomorphological mapping. By applying a selection of geomorphometric tools and indices in this alpine terrain, the authors illustrate the diverse applications of GIS in geomorphology, spanning multiple subfields.

The study of Chen et al. (2011) identified topographic features of debris flows and conditions favorable for debris-flow initiation based on geomorphological analyses of 11 river basins in Taiwan. Different morphometric indices were derived from DTMs before and after the debris flow events. Indices like the SPI, TWI, STI, ERR and parameters like form factor, effective basin area, and slope gradient have been examined. The study by Chen et al. (2011) demonstrated that debris flows typically initiate from steep slopes or landslides with higher TWI values. Debris flows are likely in basins with higher SPI and TWI. Basins with lower slope gradients and SPI but higher TWI also have a high potential for debris flow. SPI changes most significantly due to debris flow events, especially in steep basins.

Ilinca (2021) assessed the role of morphometric parameters in delineating debris flow and debris flood as different types of processes. Both are rapid mass movements in rugged mountain areas, yet they must be distinguished from one another because they require different remedial measures for effective planning. The study selected six parameters that had a substantial contribution to debris flow occurrences: melton number, basin relief ratio, basin length, basin area, fan slope and source area ratio. The results indicate that debris flow basins are defined by a Melton ratio greater than 0.55, a basin relief ratio exceeding 0.4, a basin length less than 1.7 km, and a basin area under 1.1 km^2.

Recent studies in the field of erosion and debris flow assessment have employed a variety of geomorphometric and hydrological approaches to enhance the understanding and mapping of vulnerable areas. Grelle et al. (2019) developed a streamlined GIS-based procedure to identify regions at risk of debris flows by assessing erosion and deposition in channels and alluvial fans. This methodology utilizes several morphometric parameters derived from DEMs, providing an effective framework for

initial risk assessment. Similarly, Ahmad et al. (2019) employed hydrological indices within GIS for mapping erosion-prone areas. By processing a DEM, they derived key hydrological indices, such as the STI, CTI, and SPI. These indices, along with factors like slope gradient, curvature, distance to channels, and channel density, were integrated, facilitating comprehensive erosion modeling through the combination of multiple thematic layers. In another study, Tilahun et al. (2023) utilized GIS and the Universal Soil Loss Equation (USLE) model to predict soil loss and the STI in the Ada'a watershed of the Awash River basin in Ethiopia. This research aimed to determine the mean annual soil loss, STI, and identify critical erosion-prone areas for soil conservation. The findings indicated a significant increase in soil loss, particularly in the lower regions of the watershed, underscoring the need for sustainable erosion control measures. Marchi et al. (2005) presented simple morphometric indicators for analyzing erosion and sediment delivery in several mountain basins, predominantly in the Italian Alps. These indicators, based on topographic parameters like upslope area, local slope, and distance from the basin outlet, reflect the topographic control of these processes. Their effectiveness was demonstrated through examples, such as the Melton Ruggedness Number (MRN), which showed high values on most basin slopes and along minor channels. These findings align with field observations of erosion and sediment transfer processes dominated by debris flows. Collectively, these studies underscore the importance of integrating geomorphometric parameters and hydrological indices in GIS-based methodologies for environmental hazard mapping and risk assessment, highlighting their efficacy in erosion and debris flow studies.

A notable contribution to the field of geodiversity and its intersection with geomorphological modeling is the study by França da Silva et al. (2019). Their work focuses on developing a geodiversity index through the evaluation of the relationship between various topographic variables in the state of Paraná, Brazil. This study leverages digital terrain modeling and spatial statistics to derive geomorphometric parameters, which are then analyzed using Shannon's diversity index. The resulting data are further examined through spatial correlation analysis, employing the Bivariate Moran's index as a guiding metric. This approach provides a robust framework for understanding the spatial distribution and association of geomorphometric variables, contributing valuable insights into the geodiversity of the region.

The integration of remote sensing techniques with geomorphometric indices represents a significant advancement in geomorphological research. Ortega (2012) provides a compelling example of this integration by developing a regional model to predict potential debris flows on soil and vegetation-covered hillslopes within watershed domains, focusing on the Upper Chama River watershed in northwestern Venezuela. This study utilizes a combination of remote sensing methods and morphometric and hydrological parameters, employing data from the Shuttle Radar Topography Mission (SRTM) DEM and an Advanced Spaceborne Thermal Emission and Reflection Radiometer (ASTER) scene.

2.4 Research in the SNP

The SNP has been dedicated to scientific research since its establishment, aiming to document the natural processes and changes occurring within the park. Research in the SNP has been ongoing since 1920, providing over a century's worth of continuous data, which is considered unique for such a highly protected area. Long-term research is of particular importance as it significantly enhances the understanding of natural processes. The fields of research in and around the SNP are extensive

and increasingly interconnected. They encompass the monitoring of flora and fauna, studies on visitor numbers, composition, and motivations, and investigations into the effects of climate change. Additionally, research focuses on the protection of natural processes, landscape and biodiversity changes, and the contribution of the protected area to regional development and the economy (SNP, 2024). The following provides a brief insight into research topics in the SNP.

The research on the impact of climate change on the SNP includes numerous indications from various research projects in a wide range of disciplines. As an example, the rise in average temperature was measured based on the climate station at Buffalora. This indicated an increase in the average temperature of 1.92 °C from 1917-2022. Since 1985, all years recorded have shown warmer temperatures than the average of the last 100 years (Bundesamt für Meteorologie und Klimatologie Meteoschweiz, 2014b). All the glaciers in the SNP have disappeared over the past 100 years as the permafrost is thawing in many places. This has been documented by the climate station on Munt Chavagl, which is equipped with sensors at various depths. The movement rates of earth currents are also recorded here. This is the longest continuous series of measurements of solifluction in the Alps (Rist et al., 2014). Furthermore, the increase in species on mountain peaks and the displacement of high mountain specialists are being researched. The number of plant species on selected peaks in the SNP was recorded 100 years ago. A new inventory shows that the number of species has increased by an average of 44 percent in the meantime. The GLORIA project's summit monitoring since 2002 shows that this trend is mainly because global warming has allowed more plant species to reach higher altitudes (Wipf, Rixen, et al., 2013; Wipf and Scheurer, 2016).

Researching animal behavior is certainly a big part of the research in the SNP. Research on ungulates, e.g., has a long history in the SNP, with population counts conducted since the 1920s. Extensive projects focusing on ungulates began in the 1990s. Using telemetry and GIS, researchers can track and map the movements of individual animals, aiming to gain insights into their migration patterns. In collaboration with other fields, studies also investigate the influence of ungulates on other populations (Laube et al., 2014).

Social science research in the SNP includes, for example, tourism surveys and value creation studies. Since the 1990s, the SNP has been conducting periodic tourism surveys. Since 2007, the number of visitors on hiking trails has been automatically recorded. These studies provide fundamental data on the composition, motivation, and experiences of visitors to the SNP (Lozza, 2014).

The periodical flooding of the Spöl stream is subject to constant dynamics. The construction of the Engadine hydroelectric installations in 1970 resulted in the Spöl stream carrying only residual water, causing it to lose many typical characteristics of a mountain stream. However, since 2000, the redistribution of the available residual water has enabled the initiation of small artificial floods. These floods have improved the ecological conditions in the Spöl by washing away fine sediments and benefiting organisms adapted to higher water speeds, mimicking the natural conditions of a mountain river. Regular inspections of the water are conducted before and after these floods, including data collection on the fish population (Rey et al., 2002).

Concerning the study area of Buffalora in this master thesis, the SNP is currently conducting a research project addressing the debris flow at Buffalora, but focuses more on filling the knowledge gap surrounding the impact of debris flows on plant and animal diversity in the SNP. This multidisciplinary study aims to understand how debris flows affect tree survival, vegetation succession, and animal behavior, providing crucial insights into the response of mountainous ecosystems to changing

environmental conditions. The theoretical framework of this study posits that debris flows alter physical and chemical environments, leading to changes in biodiversity and species composition. These events create new habitats and affect soil chemistry, enabling colonization by different species and providing new foraging habitats for wildlife. The use of advanced remote sensing technologies, such as drones and LiDAR, complements ground measurements, providing high-resolution data on canopy temperature and plant traits. This comprehensive approach aims to track the resilience and diversity of ecosystems following debris flows, contributing valuable insights into the long-term ecological impacts of these natural disturbances (Wipf, Rossi, et al., 2024).

3 Research framework and aims

3.1 Research motivation

As the state of the art has shown, numerous processes and effects of flora and fauna as well as on natural processes and disturbances are being researched in the SNP. Extensive knowledge exists about debris flows, including the conditions that lead to their occurrence and the reasons why such events are frequent in the park. Currently, research is focused on understanding what happens to an area after a debris flow. However, no comprehensive study has yet been conducted on the risk or susceptibility of debris flows throughout the entire SNP, presenting a research gap.

Since the SNP is generally more interested in the development of the landscape rather than in preventive measures for natural processes, such risk assessments have been of less interest. As mentioned in the introduction, the debris flow event of Buffalora in 2022 affected the Ofenpass road, an occurrence not seen in recent events. The Ofenpass road runs through the SNP and connects the Engadin with the Val Müstair leading to Italy, making it a heavily trafficked and important arterial route. Therefore, assessing the debris flow risk within the SNP, with a focus on the safety of the Ofenpass road, is of significant interest.

Adding to the aspect of global climate change, severe weather events are expected to become more extreme: Research on the impacts of climate change on alpine mass movements has led to the expectation that extreme weather events such as heavy rainfall and increased river discharge, will become more frequent. These conditions are likely to increase the frequency and intensity of debris flows posing a greater challenge for communities, infrastructure planners, and emergency responders (Stoffel et al., 2014). As debris flows become more likely, the need for a comprehensive debris flow risk assessment in the SNP becomes even more critical.

The goal of the SNP conducting scientific research, the identified research gap, the significance of the Ofenpass road, and the implications of climate change all underscore the relevance of investigating the susceptibility of the SNP to debris flows.

3.2 Main objectives

The objective of this study is to identify areas within the SNP with potential for debris flows and to assess the feasibility of predicting such events. In the context of GIS and geomorphology, the literature supposes the methods of geomorphometry. This approach provides various geomorphological parameters and indices to analyze regions based on their topographic characteristics, helping to determine if a region's terrain is conducive to debris flows.

In the first part, the debris flow event of Buffalora and its surrounding area will be described using geomorphometric methods and evaluate which approaches are of the highest relevance to describe properties of the terrain that cause a debris flow to form and correspond with the course of the happened event. The goal here is, to make an estimation and recommendation as to which geomorphometric indices are best suited for describing such terrain and predicting areas at risk of debris flows. In the second part, the findings of the analysis of the Buffalora debris flow are applied to the entire SNP to see if regions can be determined, as being in danger in terms of debris flow hazard.

With this background in mind, this thesis intends to answer the following research questions:

Which geomorphometric parameters and indices can be used to show conditions and process interrelationships of a single debris flow event (in the example of Buffalora)?

How can geomorphometric indices be applied on a larger scale to describe areas at risk of debris flow hazards (in the example of the SNP)?

4 Study area

In the following, the SNP and the area of interest at Buffalora are presented and described in more detail as the study area, where the geomorphometric analysis is being conducted.

4.1 Swiss National Park (SNP)

The SNP is located in the Engadin, in the canton of Grisons in Switzerland. The Ofenpass road runs through the SNP, connecting Zernez with the Val Müstair leading to Italy. Buffalora is located right at the border of the SNP, where the Ofenpass road leaves the park boundary (black bounding box in Figure 4.1).

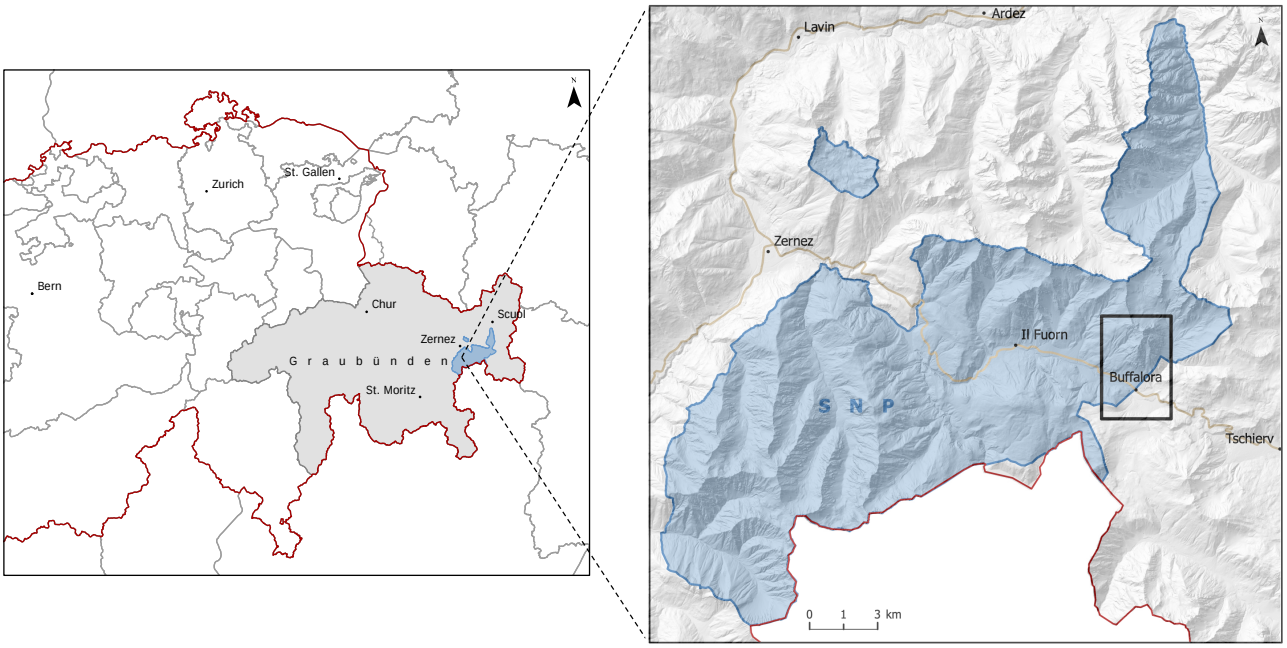

Figure 4.1: Left: Map of the SNP located in the canton of Grisons in Switzerland. Right: Zoomed in, map of the study area (black bounding box) at Buffalora at the Ofenpass road. Data: swisstopo (2023), own visualization.

The SNP lies within the mountains and highlands. The region is dominated by extreme weather conditions and high levels of erosion. In high mountain areas, the average annual temperatures are at or below zero. The minimum and maximum temperatures range between -40 and +60°C. Strong winds cause additional cooling. The dry climate and the barren dolomitic subsoil do not create favorable living conditions for plant growth in the high-altitude areas of the SNP. The vegetation, which is therefore very sparse, is no longer able to hold back the soil and loose material. Scree slopes are a

typical feature of the mountains in the SNP. The reason for this is the original rock type dolomite, which mostly collapses into coarse gravel and accumulates in the form of cones below rock faces. The explosive force of freezing water also plays a role by detaching boulders, which then thunder down steep slopes and form scree slopes (Bundesamt für Meteorologie und Klimatologie Meteoschweiz, 2014a; Furrer et al., 2014; SNP, 2024).

4.2 Buffalora

The slope affected by the debris flow is located below the Piz Nair (3010 m a. s. l.) and reaches downslope until the Ofenpass road (figure 4.2). It appears to be the first major debris flow event in this region, as the event register of the *Amt für Wald und Naturgefahren (AWN)* (Kanton Graubünden, 2024) has not recorded any other events in the Buffalora area.

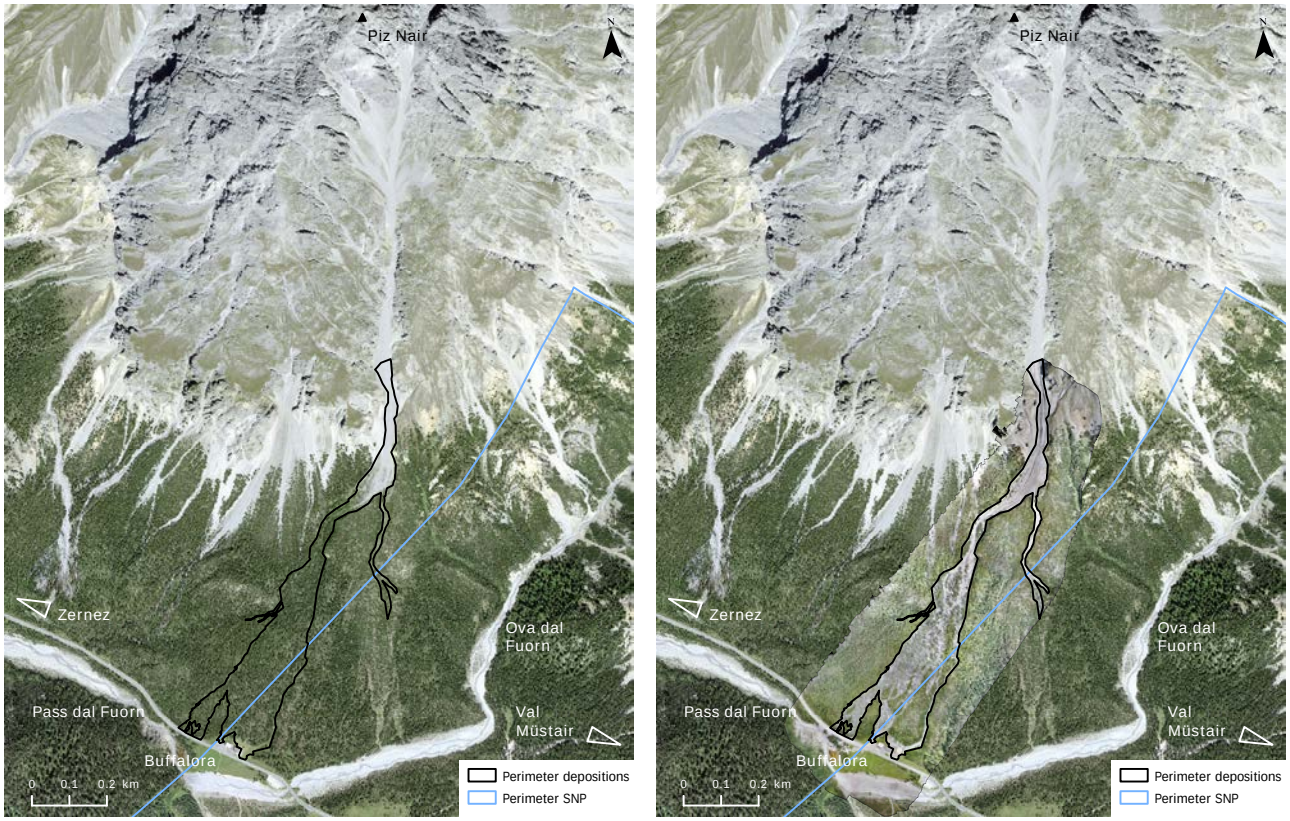

Figure 4.2: Aerial image of the area of interest before the debris flow event (left) and aerial image mosaicked with high-resolution drone imagery after the event (right). The blue perimeter shows the border of the SNP, the black border shows the deposits of the debris flow event. Data: swisstopo (2023) and SNP (2022), own visualization.

4.2.1 Geology

The geology of the study area is characterized by a clear subdivision into sedimentary rocks in the massif of Piz Nair and unconsolidated rocks below the steep rock face. The rocky area of the mountain can be seen in blue in the left illustration in Figure 4.3 and consists of biogenic sedimentary rocks and evaporites. More precisely, the right illustration in the same Figure shows that the massif of Piz Nair consists of Müschauns-Dolomite (orange areas in right illustration in Figure 4.3. Dolomite was

deposited over 200 million years ago at the edge of an ocean. This yellow-grey rock is very similar to limestone, but unlike limestone, it contains larger quantities of magnesium. It is therefore very brittle, breaks up and weathers faster than crystalline rocks. Fractures are shown downhill from the rocky area of Piz Nair (red lines in the right illustration in Figure 4.3). As the dolomite decomposes quickly, the material is removed and deposited below, which is why loose material such as slope debris, boulders, blocks, conglomerates and breccias can be found in the lower part (yellow areas in the left illustration in Figure 4.3). Moraines (till) (light green areas in right illustration in Figure 4.3), rough rock (sedimentary rock) (yellow areas in right illustration in Figure 4.3), erratic blocks (crystalline rock) (red cross in right illustration in Figure 4.3) and stream debris (dotted areas in right illustration in Figure 4.3) can also be found there. These different types of material and landforms already show that the study area is not only characterized by one process area of geomorphology but by an interplay of different process origins (Furrer et al., 2014; SNP, 2024).

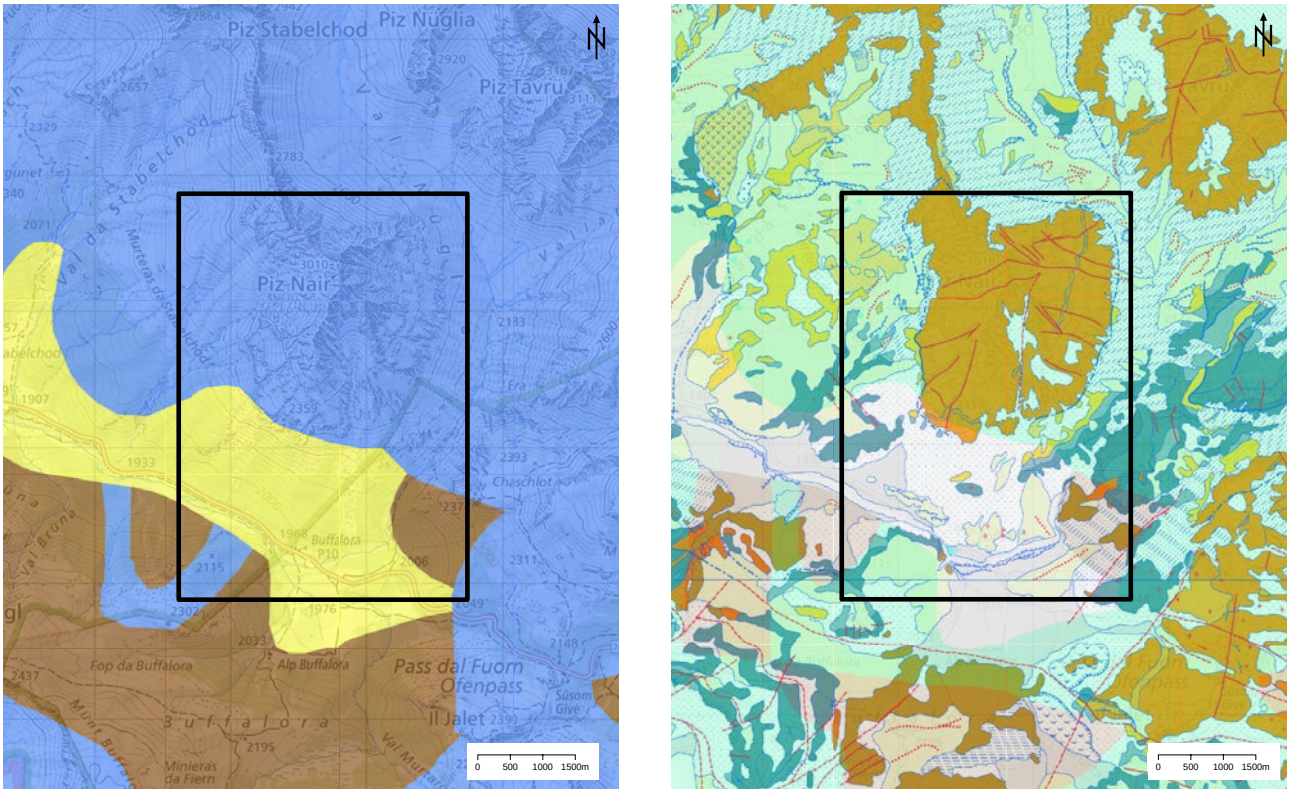

Figure 4.3: Maps of the geological subsoil of the study area. Left: Subsoil according to type of rock formation. Classes: yellow = quaternary unconsolidated rocks, brown = clastic sedimentary rocks, blue = biogenic sedimentary rocks and evaporites. Right: Geological Cover and Landforms. Relevant classes: orange = Müschauns-Dolomite, light green = Moraines (till), yellow = rough rock (sedimentary rock), red cross = erratic blocks (crystalline rock), red lines = fractures, dotted areas = stream debris. Data: swisstopo (2023)

4.2.2 Geomorphological process areas

Dominated by weather and processes like erosion, transportation and deposition, the terrain of the SNP is forced to constantly change. A detailed geomorphological map from the broader study area around Buffalora is given in Figure 4.4.

The transport of rocks, sand and very fine particles in water and ice takes place continuously and is barely perceptible to the observer. Depositional phenomena such as alluvial fans, valley fills and

moraines are the visible effects. Before material is transported, it gets weathered. This is mainly due to temperature fluctuations, frequent frost changes (frost blasting), precipitation and chemical-physical processes. The susceptibility to weathering depends on the type of rock. Large parts of the SNP are composed of dolomite, which weathers more easily than crystalline rocks. Water, wind, avalanches and ice act as an erosive power and transport the weathered material downhill. Rock load is transported from the ridge downwards through narrow, excavated gullies and in flatter terrain, the rock load loses energy and is deposited as scree.

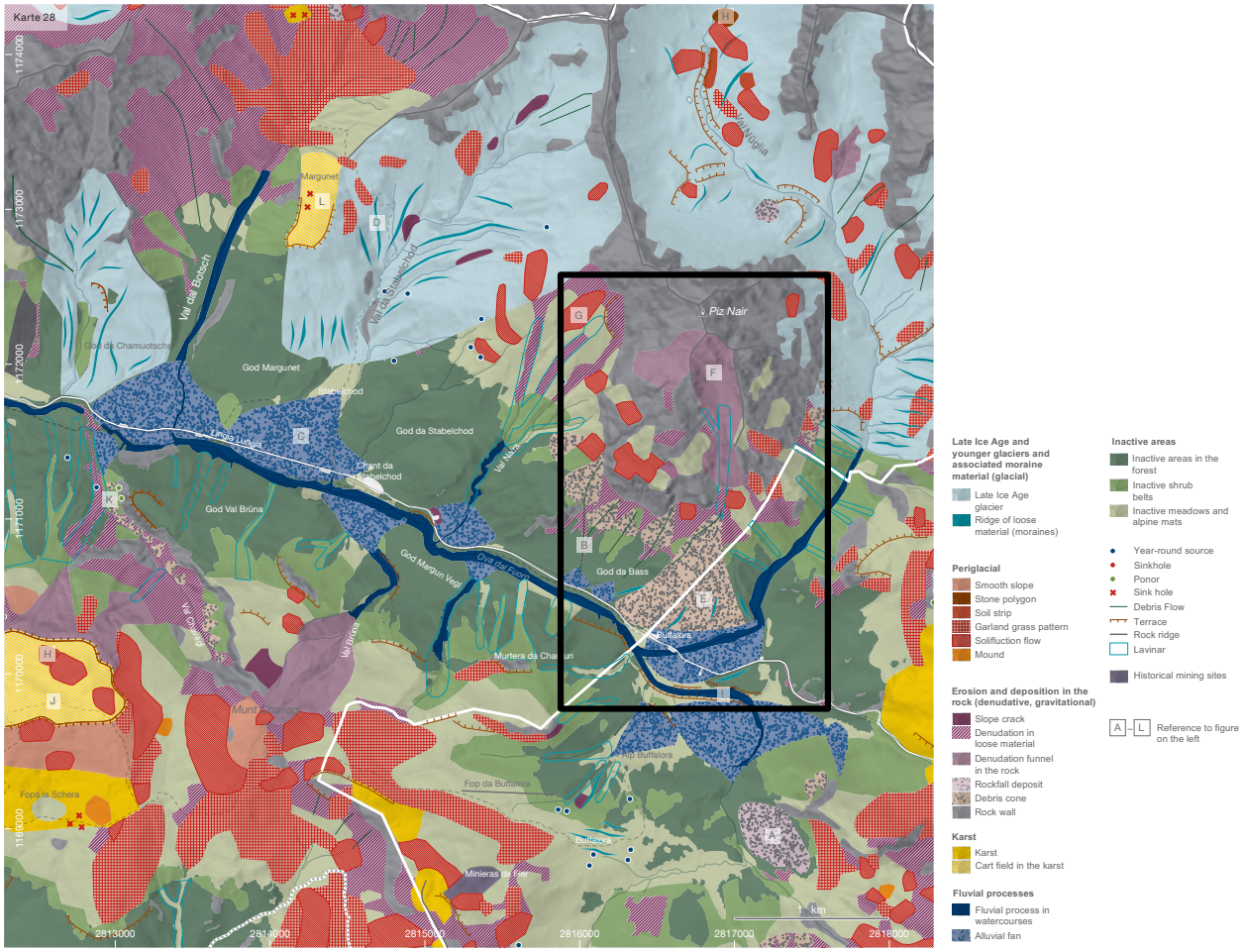

Figure 4.4: Detailed geomorphological map from the study area (black bounding box) and surrounding area in the SNP, reaching from Val Nüglia until Munt La Schera. Data: Röber et al. (2014), own visualization.

Depending on the location and type of action, these landforms and processes can be grouped into geomorphological units. The proportions of such geomorphological process areas in the SNP are divided as represented in Figure 4.5.

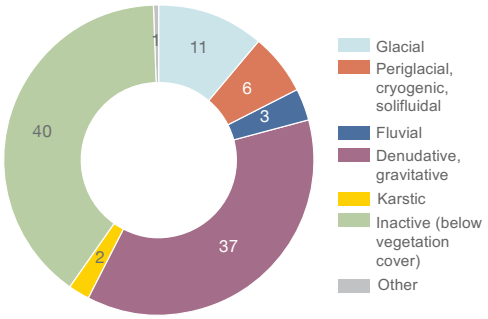

Figure 4.5: Pie chart of proportions of geomorphological process areas in the SNP in percentages (Röber et al., 2014).

It can be seen that besides inactive process areas, denudative and gravitative processes dominate in the SNP. When looking at the slope at Buffalora and the Piz Nair in the study area (black bounding box in Figure 4.4), several of those geomorphological units can be detected which result in various landforms.

The Periglacial unit describes geomorphological processes that result from seasonal thawing and freezing, very often in areas of permafrost. This unit includes garland-shaped grass patterns and solifluction flows (red checkered and striped in Figure 4.4), which are distributed at approximately the same altitude below the steep Piz Nair. Garland-shaped grass patterns arise in spring when snow is melting, the top layer of soil thaws and becomes saturated with meltwater. While the subsoil is still frozen, the water can not drain which is why the wet topsoil creeps down the slope for a few centimetres. As soon as the entire ground has thawed, the meltwater can drain away better and the movements stop. The definition does not assume a frozen subsurface, but the term is mostly used in connection with mass movements in permafrost areas. Rock faces, denudation (areal surface erosion processes) and debris cones belong to the denudative and gravitative process area of erosion and deposition in rock and are represented in our area of interest. As already mentioned above, dolomite is the dominant rock type in this region, which weathers easily and leads to loose material which results in debris cones exemplified by the slope at Buffalora ((E) in Figure 4.4). Fluvial processes include the effects of watercourses, which manifest themselves through erosion, transport or deposition, depending on the gradient, water flow and flow velocity. Below the debris cone mentioned before, fluvial processes around the river and alluvial fans are perceptible. Glacial-dominated processes exist less in the area of interest (Röber et al., 2014; SNP, 2024).

4.2.3 Weather conditions

In 2022, Switzerland experienced the fourth warmest July since measurements began in 1864, with a duration of sunshine throughout Switzerland far exceeding the norm. With its duration from the 14th to the 26th of July, it was one of the longest ever recorded heatwaves on the southern side of the Alps. Precipitation, on the other hand, remained significantly below average and mainly occurred during thunderstorms passing through. After this heat period, a cold front with thunderstorms occurred mainly along the northern slopes of the Alps and in the canton of Grisons in the night from July 25 to 26, causing the accumulated clouds to dissipate. MeteoSchweiz summarizes the event of July 25, 2022, as a line of thunderstorms that moved over the Buffalora region and the Ofenpass. At the weather station in Buffalora, 16.4 mm of precipitation was recorded within just 10 minutes. This

amount increased to 25.8 mm within an hour. The precipitation intensity over 5 minutes, derived from radar data, ranged between 80 and 90 mm per hour. Additionally, it was observed that part of the precipitation fell in the form of hail. The significant impact of hail on triggering debris flows is well known, although it has been scarcely studied scientifically so far. These weather events coincide in time and location with the Buffalora debris flow event on July 24/25, 2022 and must have been the trigger for the event (MeteoSchweiz, 2022).

5 Data

In the following chapter, all data sets used in this thesis are specified.

5.1 Digital Elevation Models (DEMs)

The data used for the geomorphometric analysis of Buffalora and the SNP consist of DEMs. DEMs are a digital representation of the elevation of a topographic surface. A Digital Surface Model (DSM) is a DEM that covers the Earth's surface including the biosphere and anthroposphere, e.g., trees and buildings. In contrast, a Digital Terrain Model (DTM) is a DEM that covers the Earth's surface without biosphere and anthroposphere, also called a "bare-earth" DEM (Guth et al., 2021). The DTM by definition above is the elevation model that serves the purpose of this work and is used for the analysis.

5.1.1 Area of interest: Buffalora

For the first part of the analysis, an elevation model before the debris flow event is needed for the area of interest of Buffalora (Table 5.1). For this purpose, the swissALTI3D from swisstopo from 2020/2021 serves as a DTM which describes the surface of Switzerland without vegetation and development and is updated every six years. As differences in terrain occur on a very small scale when analyzing debris flows, the elevation model with a resolution of 0.5 m is used for the analysis. For the analysis, the 0.5 m elevation model was then resampled to a resolution of 5 m to better recognize broader patterns and reduce computation time.

Table 5.1: Technical details of the DTM before the debris flow event of Buffalora.

	DTM pre-event
product	swissALTI3D
format	Cloud Optimized Geotiff, LZW compression
resolution	0.5 m
coordinate system	LV95 LN02
date recorded	2020/2021
source	Federal Office of Topography (swisstopo)

5.1.1.1 Volume calculation

To calculate the volume, the DTM before and after the event must have the same height reference system. The DTM after the debris flow is provided by the SNP, who took high-resolution drone images directly after the debris flow event. These images have a resolution of 1.51 cm (Ground Sampling Distance (GSD)). GSD is the distance between two consecutive pixel centers measured on the ground. The bigger the value of the image GSD, the lower the spatial resolution of the image and the less visible details (PIX4D Documentation, 2024). The DTM was resampled to 7.55 cm (5 x GSD) to avoid inertia and long calculation times for the further use of this elevation model. The drone images are in the height reference system LHN95. However, the DTM before the event, which is again the swissALTI3D from swisstopo, is always in LN02. Therefore, a DTM previously converted to LHN95 by the SNP was used for the volume calculation. The SNP had already adapted a dataset for previous purposes so that a DTM was available in LHN95. The input for this was the classified lidar point cloud from swisstopo, the SWISSSURFACE3D. It was requested in the LHN95 and then computed to a DTM. For the purpose at that time, all points were used except the vegetation. This resulted in a DTM with buildings. Since no buildings in the area of interest of this thesis are tangential, it does not interfere with the further procedure (Table 5.2).

Table 5.2: Technical details of the DTMs before and after the debris flow event of Buffalora, both in the same height reference system LHN95.

	DTM pre-event	**DTM post-event**
product	adapted DTM	high-resolution drone images
format	Geotiff, LZW compression	Geotiff, LZW compression
resolution	0.5 m	7.55 cm (5 x GSD)
coordinate system	LV95 LHN95	LV95 LHN95
date recorded	2020/2021	05.08.2022
source	SNP, Federal Office of Topography (swisstopo)	SNP

5.1.2 Area of interest: SNP

For the application of the geomorphometric analysis to the entire SNP, again the swissALTI3D from swisstopo was used but extended to the area of the entire park (Table 5.3). The purpose of the second part of the analysis is to examine the terrain as it is today using the indices to reveal potentially dangerous slopes. Therefore, the most recent DTM was used.

Table 5.3: Technical details of the DTM before the debris flow event of Buffalora.

	DTM SNP
product	swissALTI3D
format	Cloud Optimized Geotiff, LZW compression
resolution	0.5 m
coordinate system	LV95 LN02
date recorded	2020/2021
source	Federal Office of Topography (swisstopo)

5.2 Aerial imagery

To characterize the debris flow event and the existing area visually from its geomorphological perspective, high-resolution aerial images were used to compare geomorphological sections and objects of the debris flow at Buffalora over time. The orthophoto mosaic SWISSIMAGE from swisstopo is a composition of new digital color aerial photographs over entire Switzerland with a ground resolution of 10 cm in the plain areas and main alpine valleys and 25 cm for the Alps. It is updated in a cycle of 3 years. The update from 2022 provides a high-resolution image shortly before the event. Orthophotos from the drone flight from the SNP on August 22, 2022, provide a very detailed basis for analysis shortly after the debris flow event with a resolution of 1.51cm (GSD) (Table 5.4).

Table 5.4: Technical details of the aerial imagery before and after the debris flow event of Buffalora.

	Aerial imagery pre-event	**Aerial imagery post-event**
product	SWISSIMAGE	high-resolution orthophotos from drone flight
format	Cloud Optimized Geotiff (COG)	Geotiff, LZW compression
resolution	0.1 m	1.51 cm (GSD)
coordinate system	CH1903+ / LV95 (EPSG: 2056)	CH1903+ / LV95 (EPSG: 2056)
date recorded	18.07.2022	05.08.2022
source	Federal Office of Topography (swisstopo)	SNP

5.3 Zonal units: sub-catchment areas

To enable meaningful interpretation of indices calculated for the entire SNP, zonal units were established. The Topographical catchment areas of Swiss waterbodies 2 km^2 from swisstopo were used for zonal units of sub-catchments. They were extracted for the extent of the SNP. Some catchments had to be adapted by being divided by watercourses (Chapter *6.3.1 Zonal Units*). As a dataset for the watercourses, the swissTLMRegio Hydrography was used (Table 5.5).

Table 5.5: Technical details of the sub-catchment areas and watercourses for the extent of the SNP.

	Zonal units: sub-catchment areas	**Watercourses**
product	Topographical catchment areas of Swiss waterbodies 2 km²	swissTLMRegio Hydrography
format	ESRI File Geodatabase	ESRI File Geodatabase
coordinate system	CH1903+ / LV95 (EPSG: 2056)	CH1903+ / LV95 (EPSG: 2056)
data status	01.02.2019	11.10.2023
source	Federal Office of Topography (swisstopo)	Federal Office of Topography (swisstopo)

5.4 Observed debris flow events in the SNP

Similarities of the catchment areas in the SNP in terms of geomorphological properties were to be compared with debris flow events that occurred in the SNP. For this purpose, records of debris flow events from the SNP were used. These are observed events by park rangers from 2005 to 2023 that were classified as debris flows. It is important to note that these are only observed events and do not promise completeness of the events that occurred throughout that time in the SNP. Nevertheless, it gives valuable insight into the situation in the different catchments. The data was available in an Excel file, which contained the date, a coordinate of the event and further descriptions of the debris flow.

Table 5.6: Details of the dataset of observed debris flow events from 2005 until 2013 in the SNP.

	Observed debris flow events in the SNP
product	Processes in the SNP observed by park rangers and categorized as debris flows, including short description and location
format	list in Excel file
data status	2005 - 2023
source	SNP (park rangers)

6 Methodology

This chapter describes the methods used in this thesis. Firstly, a comparison of temporal landscape change of the study area Buffalora was applied, to see how the terrain evolved. Secondly, primary parameters and indices were selected according to the literature and being calculated for the study area Buffalora. Thirdly, a height difference model and the volume of the debris flow were calculated to categorize the magnitude of the debris flow. Fourthly, the approved indices were applied to the entire SNP and analyzed within the catchments. For this purpose, the value distribution was examined in the form of box- and violin plots and differences within the catchments were determined within a Principal Component Analysis (PCA). Finally, the PCA was linked to observed debris flow events in the SNP and catchment areas were categorized according to their geomorphometric properties.

6.1 Software

The geomorphometric analyses were done in ArcGIS Pro (AGP) (Version 3.2.1) and the whole workflow was carried out with model builders for two reasons. First, the steps can be retraced that way. Second, it is easier to reproduce the whole workflow with other elevation models or other areas of interest for future analyses.

6.2 Geomorphometric analysis on small scale: Buffalora

6.2.1 Temporal landscape change

The first part of understanding the history and landscape development of the research area Buffalora consists of comparison with older aerial imagery. Geomorphological processes that happened at an earlier point in time contributed significantly to the shaping of the terrain. The resulting deposition and erosion influence the spatial course, extent and further shaping of new processes. SWISSIMAGE-Zeitreise from swisstopo provided a chronological historical time series of the terrain in Switzerland in the form of aerial photographs thus providing an overview of potential earlier changes in the landscape. The data are being examined chronologically in the region of the debris flow at Buffalora and the surrounding area for the period with available imagery from 1959 to 2022. The research area was divided into 7 sections which allowed the aerial photographs to be systematically examined. The segments were selected based on landscape elements that had already been observed and could spatially easily be separated from each other. Figure 6.1 shows the division of the research area into sections, which will also be referred to in the results.

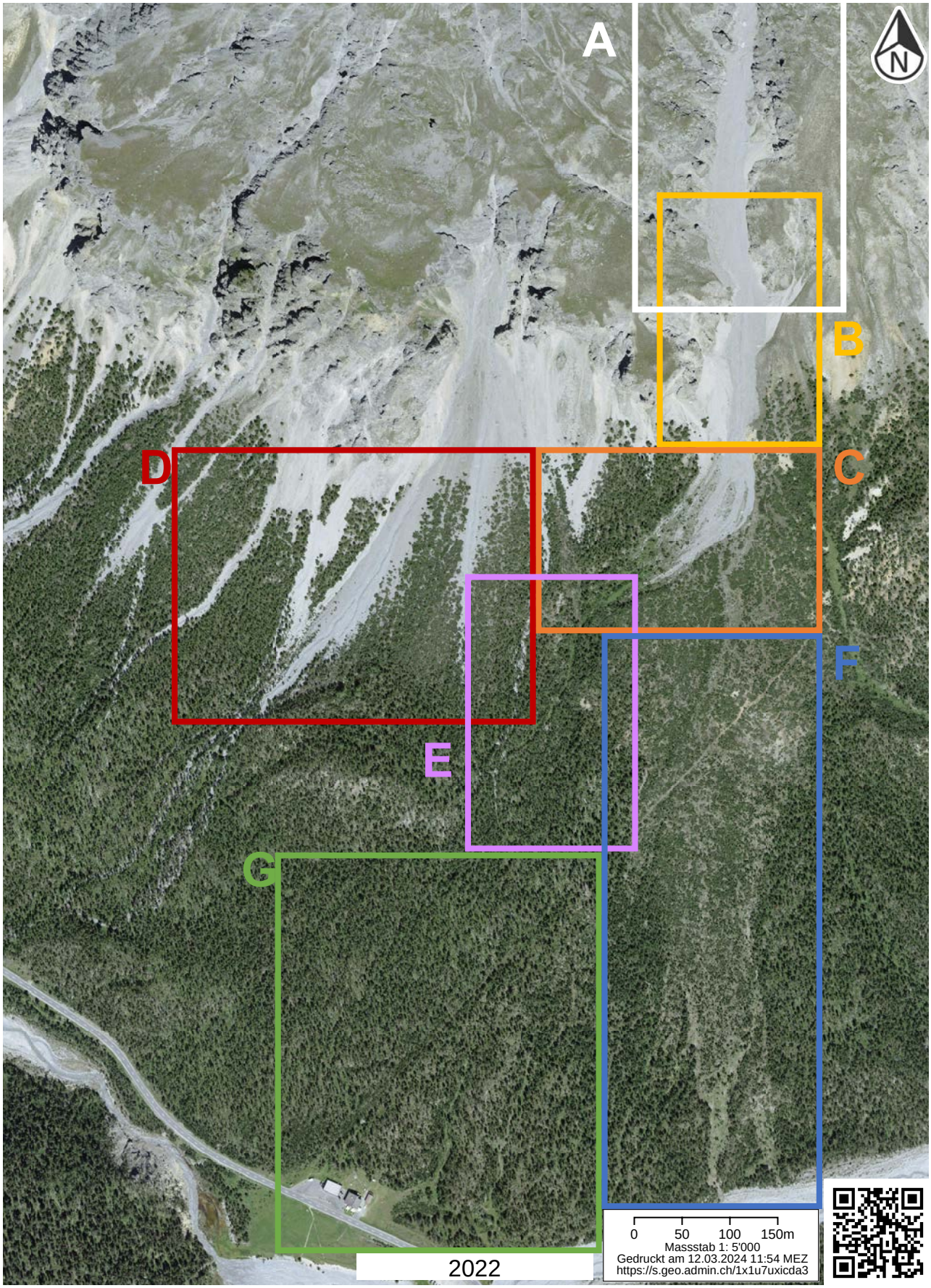

Figure 6.1: Research area of the Buffalora slope in 2022 before the debris flow event, divided into 7 main geomorphological elements which are being compared over time. Data: swisstopo (2023), own visualization.

6.2.2 Selection of parameters and indices

The geomorphometric analysis was first carried out on a small scale, which includes only the slope of Buffalora. As a first step primary terrain attributes were derived directly from the DEM itself. According to the literature, the parameters stated in Chapter *2.2.1 Primary terrain attributes* are the most commonly used geomorphometric primary parameters. They were selected because they are subsequent input for the calculation of the indices and additionally, they serve as descriptive parameters of the terrain of the debris flow event itself. Table 6.1 summarizes the chosen parameters with their unit, description and source.

Table 6.1: Name, unit, description and source of the chosen primary parameters for geomorphometric analysis of the debris flow of Buffalora.

Primary parameter	**Unit**	**Description**	**Source**
Slope	*degree*	Direction of maximum slope of tangent plane to surface at cell (calculated for some neighbourhood, typically a 3x3 window)	Horn (1981)
Aspect	*direction*	Slope direction angle, identifying the variation in the value of each cell with its neighbour	Horn (1981)
Planform curvature (horizontal), Profile curvature (vertical)	*radians / m*	Shape of the slope, either concave or convex	Zevenberger et al. (1987)
Specific catchment area	m^2	upslope area draining across a unit width of contour	Speight (1980)

Table 6.2 shows two further primary parameters derived from the DEM, showing certain ratios compared to the parameters in Table 6.1. R has to be calculated within the deposition area by definition. Nevertheless, some literature states that it also includes the delivery area of the catchment. That is why it was calculated for both cases.

Table 6.2: Name, unit, description and source of ERR and Relief Ratio.

Ratio	Formula, units	Description
Elevation-Relief Ratio (ERR) **Pike and Wilson (1971)**	$ERR = \frac{mean\ elevation - min\ elevation}{max\ elevation - min\ elevation}$	Measure of relationship between elevation and area in a catchment, calculated using a regular kernel as e.g., a 3x3 cell window
Relief Ratio (R) **Rickenmann (1999)**	$R = H/D$ *where* *H = elevation difference of deposition area* *D = horizontal distance from top to bottom of deposition area*	Identifies amount of of sediment transport capacity and possibility to distinguish debris flow basins other type of basins

This work aims to describe and identify regions in the SNP that are potential hazard areas for debris flows. As already mentioned in Chapter *2.1.3 Debris flow*, the following aspects are the main factors for the formation of a debris flow: the presence of loose material(1), water (2), sufficiently large slope or channel gradient (3) and high flow velocities (4). The STI is a measurement of sediment transport capacity and deposition in the plain. This index covers the aspect of material that is being transported during an event (1). The TWI describes the tendency of a location to accumulate water and can therefore be used to assess the spatial pattern of potential soil moisture due to erosion. Therefore, this index covers the aspect of water (2). The SPI describes the topographical potential for deposition and erosive areas. Including the slope, this index shows where the power for a stream to pass through is large and sufficiently steep and therefore covers the factor of a large slope or channel gradient (3). Last, the TRI derives the roughness of a terrain, where low values indicate flat areas and high values indicate rough areas. The lower the TRI value, the higher the flow velocities get (4). Table 6.3 presents the indices that were chosen to be calculated in this work, to represent the four factors mentioned above.

Table 6.3: Name, unit, description and source of the chosen secondary parameters for geomorphometric analysis of the debris flow of Buffalora.

Index	Formula, units	Description
Stream Power Index (SPI) **Wilson et al. (2000)**	$SPI = ln(As*tanB)$ *where* As = *specific catchment area* B = *local slope angle*	Measure of erosive power given overland flow and constant transmissivity
Topographic Wetness Index (TWI) **Beven et al. (1979)**	$TWI = ln(\frac{As}{tanB})$ *where* As = *specific catchment area* B = *local slope angle*	Predicts saturated zones given overland flow and constant transmissivity
Sediment Transport Index (STI) **Moore and Burch (1986)**	$STI = (m+1) * (\frac{As}{22.13})^m * sin(\frac{B}{0.896})^n$ *where* As = *specific catchment area* B = *local slope angle* m = *contributing area (constant)* n = *slope exponent (constant)*	Measure of erosivity of channel flow downstream, sediment transport capacity and deposition in the plain
Topographic Roughness Index (TRI) **Sappington et al. (2007)**	$TRI = 1 - \frac{\sqrt{(\sum x)^2+(\sum y)^2+(\sum z)^2}}{n}$ *where* $z = 1 * cos(slope)$ $xy = 1 * sin(slope)$ $x = xy * cos(aspect)$ $y = xy * sin(aspect)$ n = *cell neighborhood*	Measure of surface roughness as variability of a topographical surface at a given scale

6.2.3 Applying primary parameters

6.2.3.1 Slope, aspect, curvature, catchment area

Figure 6.2 shows the workflow of the calculation of the primary parameters. Slope, aspect and curvature were carried out with the tool *Surface Parameters (Spatial Analyst)* in AGP, which determines the parameters of a raster surface. As *Local Surface Type* was always chosen the option *Quadratic and Neighborhood Distance* according to the resolution of the DEM. As the indices afterward are calculated using trigonometric operations, the slope and aspect parameters have already been converted to radians.

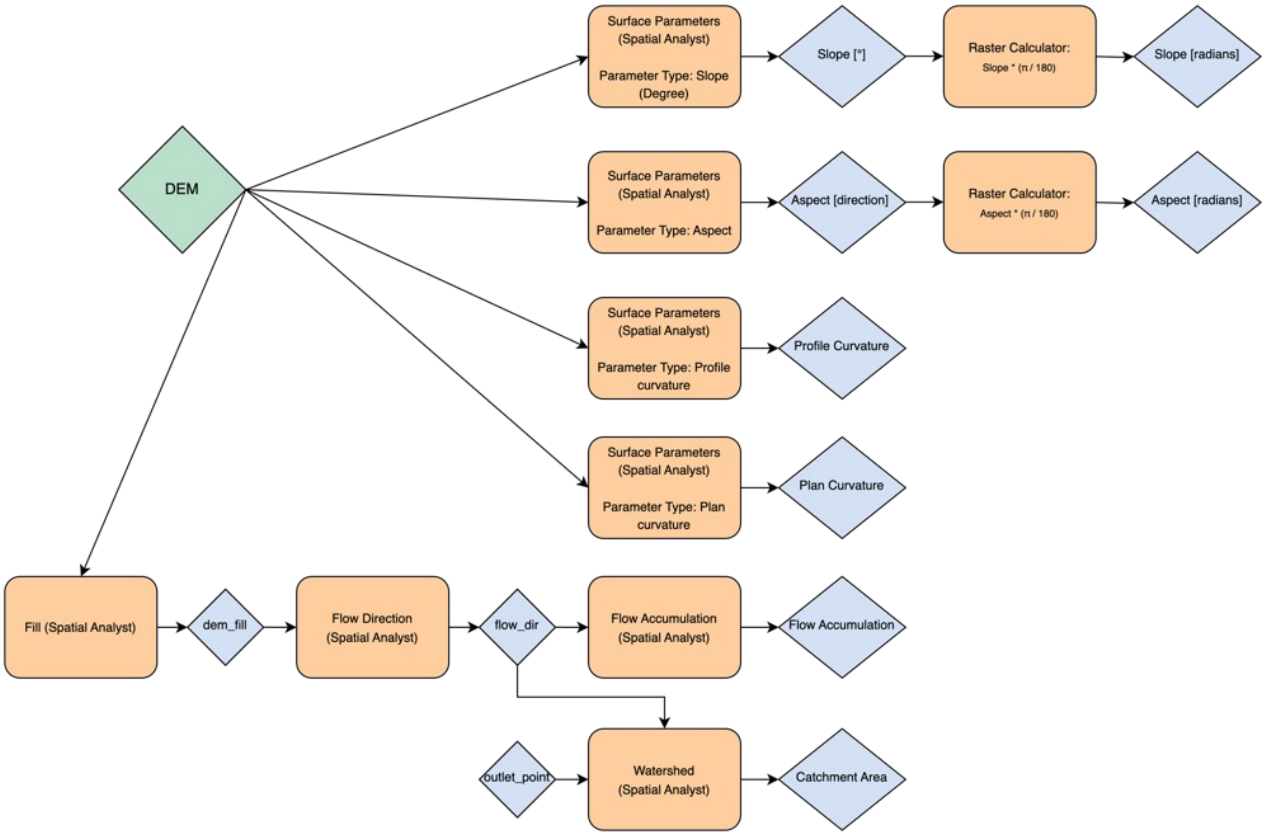

Figure 6.2: Flowchart of the calculation of the primary parameters. DEM as input data in green, executed operations in orange, intermediate and resulting parameters in blue.

To perform the calculation of flow accumulation, the tool *Fill (Spatial Analyst)* had to be applied first, to fill sinks in a surface raster to remove small imperfections in the data. The filled elevation raster could then be used to perform the *Flow Direction (Spatial Analyst)* tool, which creates a raster of flow direction from each cell to its downslope neighbor, or neighbors. In this case, the D8 method was chosen. The flow direction raster then serves on one side as the input data to execute the *Flow Accumulation (Spatial Analyst)* tool, and on the other side as input data for the catchment area. For the catchment area, additionally, the pour point at a certain point of interest had to be defined. It is important to note here that the pour points have to be located exactly on a cell that belongs to the flow accumulation. Otherwise, the next tool can not calculate a watershed, because it is based on the course of the flow accumulation lines. If the accumulation lines are not visible enough, the symbology can be adapted. In this work, the pouring point was chosen at the top of the deposition which gives an insight, into how much area contributed to the erosion and deposition of the debris flow. Finally, the catchment area was then performed with the *Watershed (Spatial Analyst)* tool, which needs the flow accumulation raster and the pour points as input data.

6.2.3.2 Elevation-Relief Ratio (ERR) and Relief Ratio (R)

For the Elevation-Relief Ratio, the tool *Focal Statistics (Spatial Analyst)* was used to calculate the average, minimum and maximum height in the elevation raster. This tool calculates for each input cell location a statistic of the values within a specified neighborhood around it. In this case, a 3x3 neighborhood was chosen. According to the formula from Pike and Wilson (1971), the resulting rasters

were then combined in the Raster Calculator (Figure 6.3 for workflow).

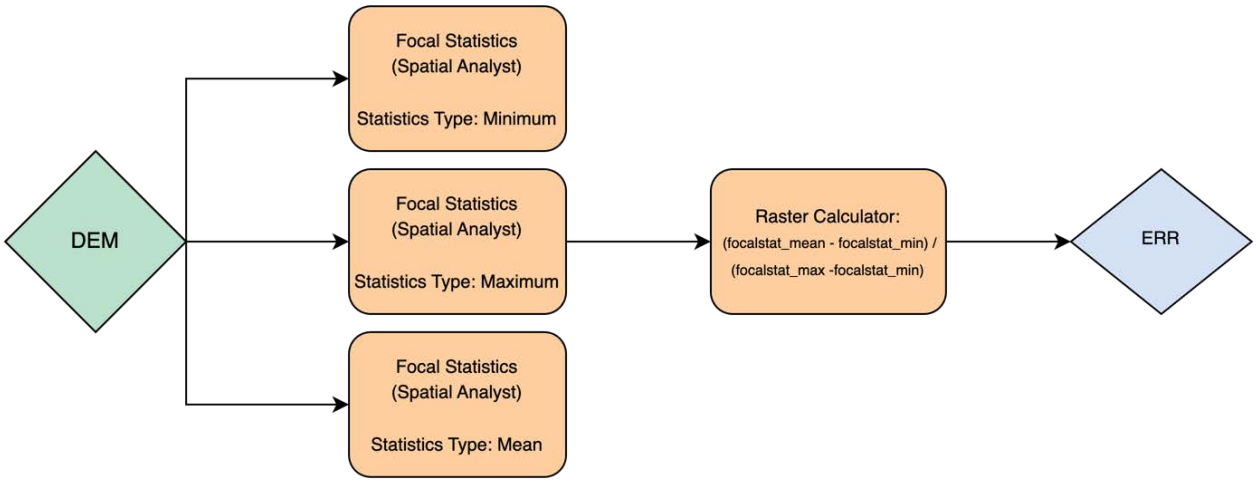

Figure 6.3: Flowchart of the calculation of the Relief Ratio (R). DEM as input data in green, executed operations in orange, resulting parameters in blue.

The Relief Ratio (R) is limited to the delivery and accumulation area of the debris flow and not, like the ERR and other following indices, to the wider surrounded area. Therefore, the area of interest in the DEM was extracted by a mask with the tool *Extract by Mask (Spatial Analyst)*. To determine R, the highest and lowest points in this area had to be identified first. They could be found out with the tool *Find Highest Or Lowest Point (Defense)*. The horizontal distance (D) between these two points could then be measured with the *Measure* tool (Figure 6.4 for workflow). The elevation difference (H) between these two points could then be calculated by subtracting the two elevation values at these points. The ratio could then be carried out.

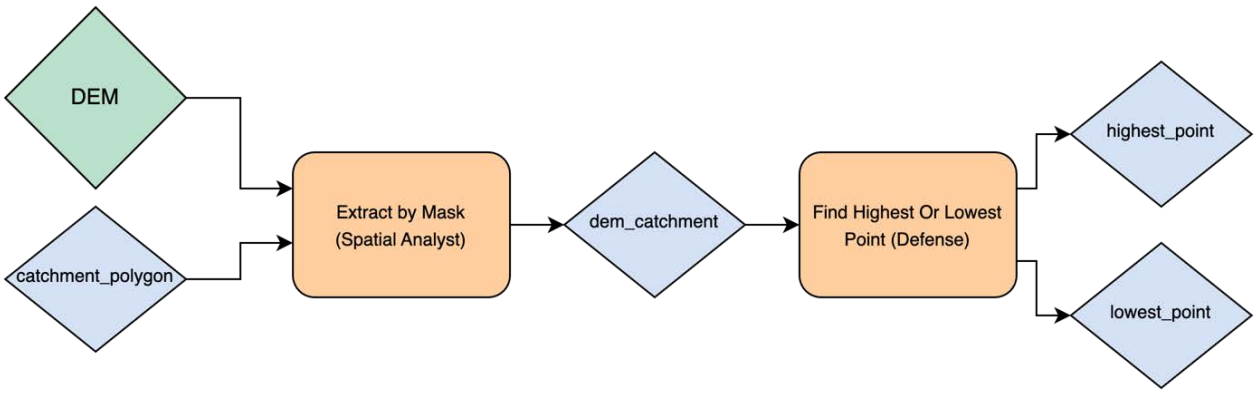

Figure 6.4: Flowchart of the calculation of the Relief Ratio (R). DEM as input data in green, executed operations in orange, resulting parameters and interim inputs and results in blue.

6.2.4 Resolutions of DTMs

The parameters and indices listed above were calculated with the swissALTI3D, with a resolution of 0.5m. When calculating the indices, it occurred that the resolution was too high to recognize coarser patterns and hotspots and that the noise was too high. Related Work as from Chen et al. (2011) used DEMs with a 10m resolution whereas Ahmad et al. (2019), França da Silva et al. (2019) or

Sappington et al. (2007) even used a 30m DEM. These resolutions are too low to see any detailed patterns in one slope, why it was decided to resample the DEMs to 5m. That resolution seemed to offer a suitable scale, to see detailed patterns and still a coarser overview over one slope. When analyzing all the catchments in the SNP, the resolution has to remain the same to compare the slopes with one another.

To resample the swissALTI3D from 0.5m to 5m the cubic resampling method has been chosen. Cubic interpolation considers more neighboring cells (usually 16) than other methods and applies a cubic polynomial to estimate the new cell value. This method produces smoother results than bilinear interpolation and can better preserve elevation changes, making it a suitable choice for DEM resampling, especially in areas with gradual terrain transitions (Minh et al., 2024).

6.2.5 Applying secondary parameters: indices

The selected indices according to Table 6.3 were then derived from the calculated primary parameters using the formulas suggested by the literature. The following sections describe in more detail how the geomorphometric indices were calculated.

6.2.5.1 Preparation of index calculation: Flow Direction Type Model

When calculating those indices that consisted of flow accumulation, many negative values appeared. Since the DEM has a very high resolution and many rough surfaces, there are many convexities (flow accumulation = 0) and in addition many low flow accumulation values. If small flow accumulations get multiplied with a trigonometric function of small slope values, the cell values result negatively. These negative values are correct, but also partly an artifact of the data. It was then discovered that flow direction type D8 generates particularly a lot of low flow accumulation values. To eliminate such negative values, the flow direction type D-Infinity was used, which still generated negative values, but much less than with the flow direction type D8 (Figure 6.5 for comparison of the flow direction type models). Those values that still appeared negative in the index were then set to NoData values. This procedure was applied in the following for the SPI, TWI and STI indices.

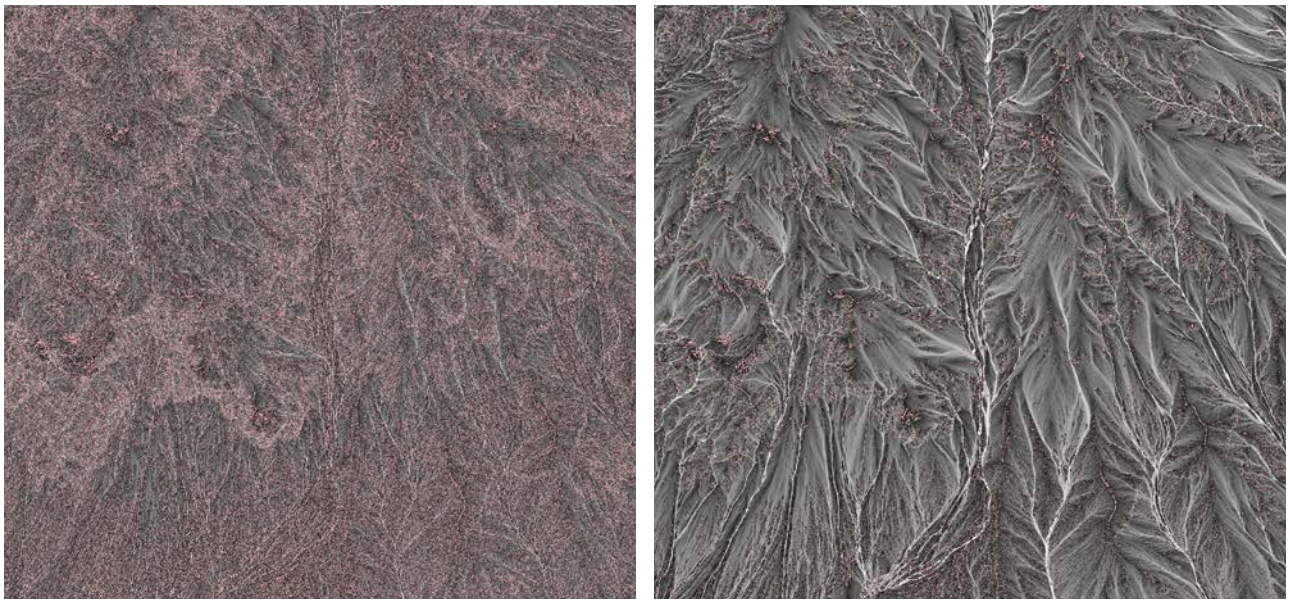

Figure 6.5: Comparison of flow direction type models with flow accumulation as output. Flow accumulation is based on the flow direction type model D8 (left) and flow accumulation is based on the flow direction type model D-Infinity (right). Negative values are colored in red.

6.2.5.2 Stream Power Index (SPI)

The SPI is derived from the slope in radians and flow accumulation with the D-Infinity flow direction type as a base. The literature suggests the formula for the calculation of the SPI in 2 versions, which are both widely used: The product of the specific catchment area and the tangent of the slope with or without the natural logarithm. In this work, the variant with a natural logarithm was chosen. When applying the ln function, it transforms the scale of the number from linear to logarithmic. Small changes in the original number result in proportionally smaller changes in the ln value and therefore stabilize the variance of data. The tangent function demands its input to be in radians, to ensure correct operation of the trigonometric function. The specific catchment area As is being defined here as the flow accumulation multiplied by the cell size of the DEM, in this case, 5m. The calculation of the SPI was executed within the raster calculator (Figure 6.6 for workflow).

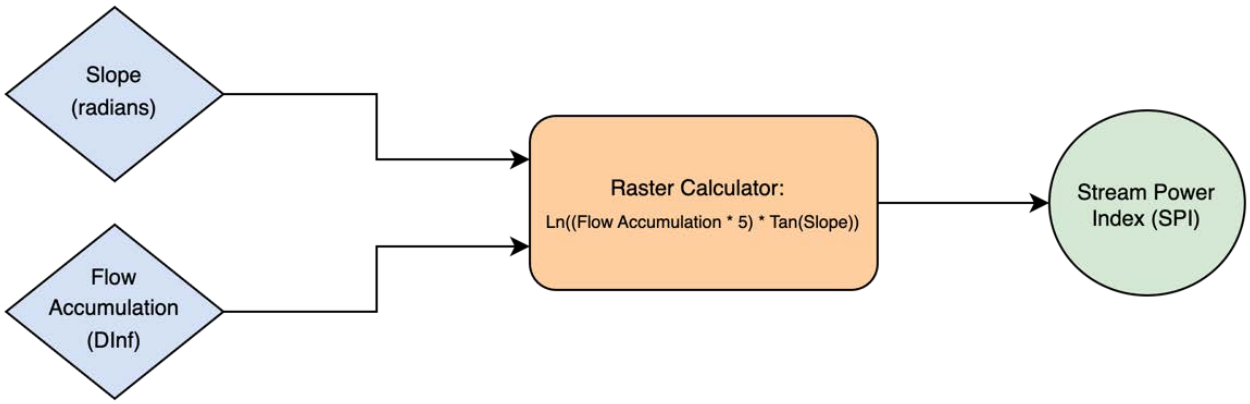

Figure 6.6: Flowchart of the calculation of the SPI. Primary parameters as input data in blue, executed operations in orange, resulting index in green.

6.2.5.3 Topographic Wetness Index (TWI)

The TWI follows the approach of Beven et al. (1979) and is derived similarly to the SPI, except for dividing flow accumulation by slope instead of multiplying. Again, the slope is supposed to be in radians and the flow accumulation with the D-Infinity flow direction type as a base multiplied with the grid cell as the specific catchment area. The study area is located in the high mountains, on a steep slope. The equation of the TWI demands conditions that are usually encountered along drainage paths and in zones of water concentration in landscapes (Wilson et al., 2000) (Chapter *2.2.2 Secondary terrain attributes: indices*). This would exclude high mountain areas as the study areas are located in. Despite its theoretical limitations, the TWI can offer valuable insights into potential hazard zones in high mountain areas, especially because conclusions about debris flow hazards are derived not from this index alone but through a combination of the other indices. See Figure 6.7 for the workflow executed in the raster calculator.

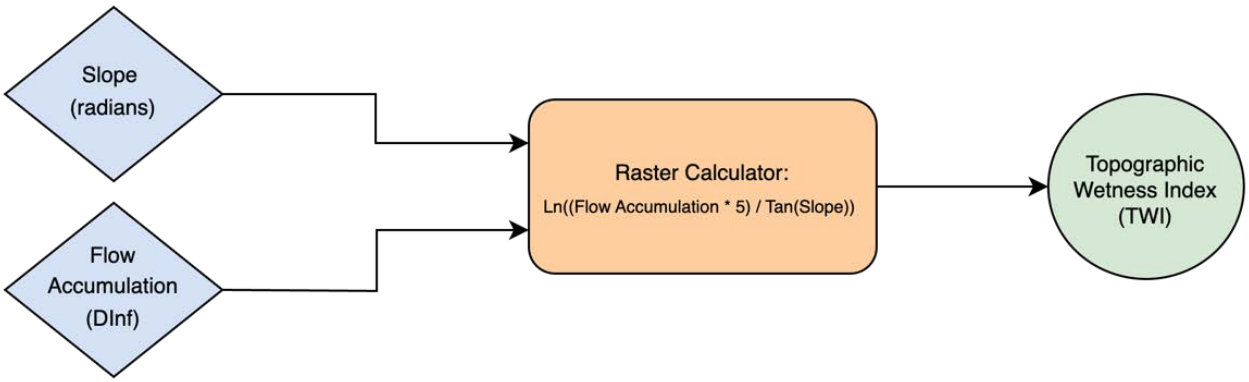

Figure 6.7: Flowchart of the calculation of the TWI. Primary parameters as input data in blue, executed operations in orange, resulting index in green.

6.2.5.4 Topographic Roughness Index (TRI)

The TRI follows the vector ruggedness measure developed by Sappington et al. (2007) and is based on the vector approach proposed by Hobson (1972). First, normal unit vectors of every grid cell of the DEM have been decomposed into x, y, and z components based on trigonometric operations of slope and aspect. Then, a resultant vector was being obtained for every pixel by summing up the single components of a center pixel and its neighbors within a 3x3 cell window. Because the DEM has already been resampled to 5m, a 3x3 cell neighborhood seemed enough small to still obtain details. The resultant vector is then normalized by the number of grid cells n (here 3 x 3 = 9) and then subtracted from 1 (Figure 6.8 for workflow).

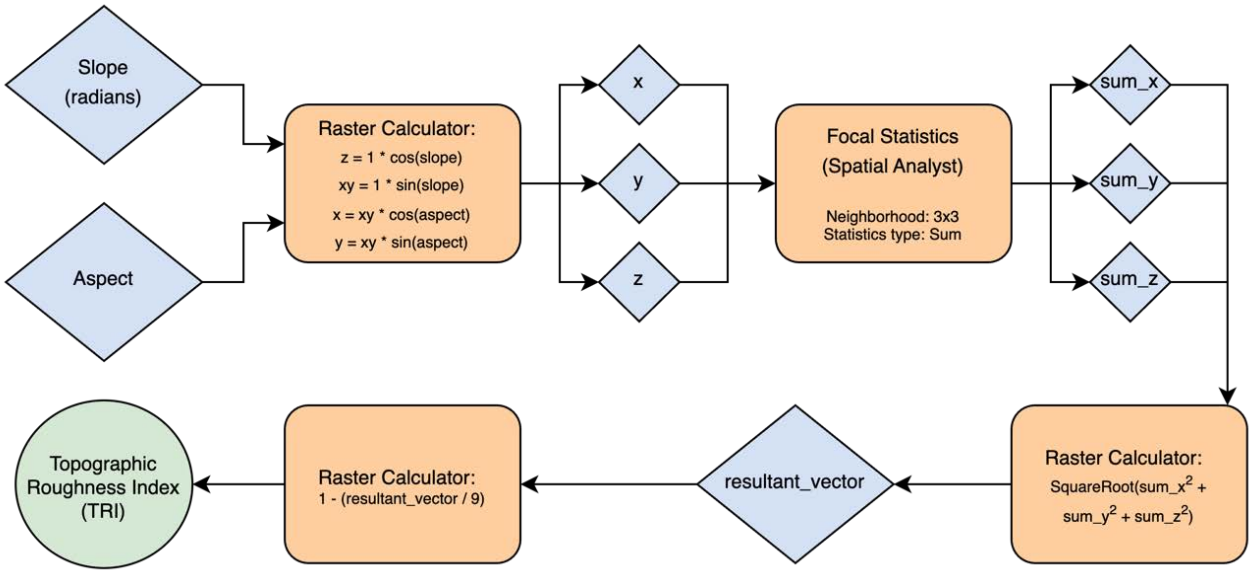

Figure 6.8: Flowchart of the calculation of the TRI. Primary parameters as input data and intermediate parameters in blue, executed operations in orange, resulting index in green.

6.2.5.5 Sediment Transport Index (STI)

The STI follows the equation according to Moore and Burch (1986). It is derived from the slope in radians and flow accumulation with the D-Infinity flow direction type as a base. Many papers propose to set the contributing area exponent m to 0.6 and the slope exponent n to 1.3, which was also implemented here. The specific catchment area As is again defined as the flow accumulation multiplied by the cell size of the DEM. The calculation of the STI was executed within the raster calculator (Figure 6.7 for workflow).

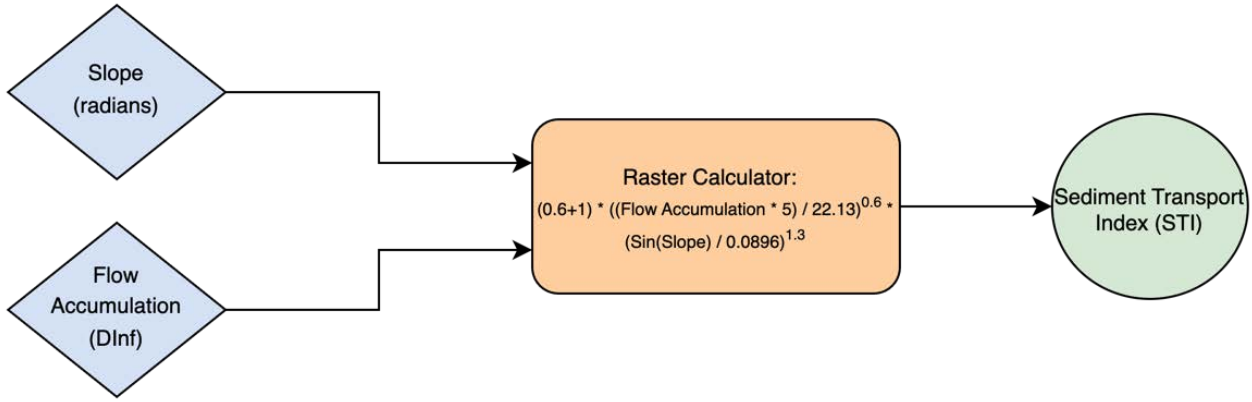

Figure 6.9: Flowchart of the calculation of the STI. Primary parameters as input data in blue, executed operations in orange, resulting index in green.

6.2.6 Correlation matrix

In a further step, the correlation between the selected parameters and indices was examined. In this way, indices that correlate strongly can be identified and excluded for further investigation of debris flow endangered regions in the SNP. For this purpose, pairwise linear relationships were established

between all parameters and indices using the Pearson correlation coefficients in a correlation matrix. This analysis measures the strength and direction of association between two continuous variables. The Pearson Correlation Coefficient (r) ranges from -1 to 1, where -1 indicates a perfect negative linear relationship, 0 indicates no linear relationship and 1 indicates a perfect positive linear relationship. According to Kuckartz et al. (2013), a weak correlation is defined when r is between (-)0.1 and (-)0.3, a moderate correlation when r is between (-)0.3 and (-)0.5, a high correlation when r is between (-)0.5 and (-)0.7 and a very high correlation when r is between (-)0.7 and (-)0.9. The correlation matrix was carried out in RStudio. All parameters and indices were added into RStudio in *.tif* format. First, a *RasterStack* object had to be generated, which is a collection of raster layer objects with the same spatial extent and resolution. Each spatially identical pixel from each raster object is arranged side by side in a table. The correlation matrix could then be generated using the *ENMTools package*. The command *raster.cor.matrix* takes a raster stack and returns a data frame with Pearson correlation coefficients between the contained rasters. Finally, the correlation matrix could be displayed as a correlogram using the *corrplot package*.

6.2.7 Height Difference Model (HDM)

To calculate the accumulated and eroded material, a Height Difference Model (HDM) was calculated in the Raster Calculator by subtracting the pre-event elevation model from the post-event elevation model. Thus, all positive values represent accumulation and all negative values are erosion. Erosion was colored in blue and accumulation in red, each in different gradients. The area indicating no change in elevation cannot be set exactly to 0, as different elevation models were used for the calculation. Inaccuracies arise both within and between the elevation models, which are very important for obtaining accurate results, especially with a HDM. The height accuracy is +/- 10 cm, which is also declared by swisstopo for the swissSURFACE3D model that serves as a database for the swissALTI3D being used (swisstopo, 2024). Therefore, the class that should represent no changes in elevation in the HDM was defined between -0.1 and +0.1 and colored neutral in grey.

6.2.8 Volume

The HDM could further be used for the volume calculation. To evaluate the volume deposited by the debris flow, all values greater than 0.1 in the HDM were extracted using the raster calculator *(Con(HDM > 0.1, HDM))*. They were then multiplied by the cell size to obtain the volume per cell ($HDM\_positive \times 0.5 \times 0.5$). With *Zonal Statistics as Table*, the sum of all grid cell values located within the perimeter of the depositions was then created which resulted in the deposited volume.

6.3 Geomorphometric analysis on larger scale: SNP

The second part of this thesis focuses on the application of the selected methods on a larger scale. The parameters and indices are being calculated for the entire SNP in the same way as for Buffalora (Chapter *6.2.5 Applying secondary parameters: indices*). They form the foundation for the further evaluation of unknown slopes at risk of debris flows.

6.3.1 Zonal Units

To identify unknown slopes at risk of debris flows, units are being defined in which hotspots in indices can be detected and then being compared with each other. For this purpose, the SNP is divided into its sub-catchments. In hydrology, a catchment is the area where water converges and flows towards a specific point, called the outlet of the watershed (Olaya, 2009). This usually includes rivers along with all its tributaries. Such catchment areas typically cover individual slopes, and in most cases are identical to catchment areas of debris flow events. Therefore, catchment areas are well suited as zonal units for detecting slopes prone to debris flows.

When examining the data set *Topographical catchment areas of Swiss waterbodies 2 km² (Federal Office for the Environment FOEN)*, it was noticed that some of the sub-catchment areas contain watercourses that extend through the entire sub-area. This results in catchment areas that include two slopes. Concerning debris flows, one slope has nothing to do with the other and has to be analyzed separately. This is why such catchment areas must be separated for this study and the data set had to be adapted. To do that, the watercourses located within the SNP were taken from the *swissTLMRegio Hydrography (Federal Office of Topography swisstopo)* dataset. Catchments through which these watercourses run were split along this depth line using the *Split* tool. This results in two polygons; orographically left and right. Catchments that start inside the SNP boundary but go beyond the boundary are left as they are and are not cut at the park border.

6.3.2 Distribution of the indices values across the catchments

To obtain a rough idea and overview of the values that resulted in the indices, the distributions of each index per catchment area were visualized. All rasters of indices were imported into RStudio as *.tif* files and the catchment areas as *shapefiles*. The values of the indices were extracted cell by cell and assigned the according to catchment area. In the end, 5 data frames resulted, where all cell values of an index per catchment area were summarized. With the package *ggplot2*, box- and violin plots were then created for each catchment for each index.

6.3.3 Principal Component Analysis (PCA)

To find out which catchments within the SNP are susceptible to debris flows, it is necessary to find out how the catchments differ from each other. For that, the number of dimensions necessary to describe the data have been reduced, to visually identify associations between the data points. This approach was implemented by applying a Principal Component Analysis (PCA). PCA is a statistical approach used to reduce a data table of cases and variables into its core elements, known as principal components. These components are linear combinations of the original variables that capture the maximum variance in the data. By doing so, PCA represents the original data table using only these key components, significantly simplifying the data while retaining its most important information (Greenacre et al., 2022).

The following components were assessed as relevant dimensions and therefore included in the PCA: all indices (SPI, TWI, STI, TRI, ERR), area, slope and altitude. The area was calculated per catchment in m^2. With the tool *Zonal Statistics as Table (Spatial Analysis)* the median of all indices, slope and altitude per catchment area was determined. The PCA was conducted in RStudio. As all variables

have different scales, they had to be normalized first. With the *FactoMineR package* the PCA could then be conducted. The results were then plotted with a scree plot to visualize the importance of each principal component and could then be used to determine the number of dimensions to retain. With a biplot, it was possible to visualize the similarities and dissimilarities between the catchment areas and further show the impact of each attribute on each of the first two principal components.

6.3.4 Observed debris flow events in the SNP

Data about observed debris flow events in the SNP should be included in the analysis. The SNP provided a data set about observed debris flow events in the park since 2005, documented by park rangers. This data set had to be modified as coordinates first. In cases where the description of the location by the park rangers was clear, a coordinate was set within the corresponding catchment area. In four cases, the park rangers' descriptions were too imprecise to identify in which catchment the event occurred. Therefore, four of the 152 registered events were omitted. Finally, the 148 events were recorded as a point dataset in AGP. The tool *Summarise Within (Analysis Tools)* was used to count the number of events per catchment area and was added to the catchment area layer as a new attribute. A new column was also added to the catchment layer to indicate whether an event has taken place per catchment or not (yes/no).

6.3.5 Synthesis: Combined map of PCA and observed debris flow events

As a last step, the synthesis of the analyses should be summarised in a map that links the PCA as well as the debris flow events per catchment. As described in Chapter *6.3.3 Principal Component Analysis (PCA)*, a biplot with the first 2 dimensions was created from the PCA. The intersection of the Principal Component 1 (PC1) and Principal Component 2 (PC2) axes creates four quadrants. Each data point (here catchment areas) in the biplot is projected into one of these quadrants based on the signs (positive or negative) of its PC1 and PC2 scores. Each catchment therefore belongs to one of these 4 quadrants. The position of each catchment in a specific quadrant helps in understanding its characteristics relative to the principal components in our case the geomorphometric parameters and indices chosen for the PCA. Catchments with similar properties were therefore also localized in the same quadrant. For this reason, the catchments were colored in the respective quadrants in the combined map. In addition, the observed debris flow events in the SNP since 2005 (Chapter *6.3.4 Observed debris flow events in the SNP* for digitization) were included in the map. The catchments were colored according to whether an event was observed or not. Additionally, the number of observed events per catchment was represented by a dot of varying size. This results in a map from which statements can be made about the similarities of the catchment areas in the SNP based on similar geomorphological characteristics and linked to the number of observed debris flow events.

7 Results

The following chapter presents the results, which are divided into two main parts. Firstly, the results of the analysis of the debris flow event at Buffalora are demonstrated. This includes the findings of the temporal landscape change, the resulting plots of the calculated parameters and indices, the resulting correlation matrix of the applied parameters and indices, the height difference model of pre- and post-elevation models and a calculated volume of the debris flow event. Secondly, the results of the application of the indices to the entire SNP are being presented. They involve box- and violin plots of each index per catchment area, the applied PCA and the integration of observed debris flow events, resulting in a map where a categorization of the catchment areas based on their geomorphometric properties is illustrated.

7.1 Geomorphometric analysis on small scale: Buffalora

The following subsections reveal results regarding the study area of the debris flow event in 2022 at Buffalora according to Figure 4.2.

7.1.1 Temporal landscape change

The following sections demonstrate the findings of the temporal landscape change analysis, presenting the periods during which geomorphological processes became visible, thus providing an approximate estimate of how long certain landscape traces have existed. Only the periods in which changes were observed are mentioned below. The following figures show the seven geomorphological areas according to Figure 6.1. They are displayed over four periods, with spatial changes described for the years 1959, 1973, 2003, and 2019.

Figure 7.1 shows the temporal development of the debris flow source area A. The main channel and the side channels have existed since at least 1959 and there are active and inactive channels, which do not change much throughout the years. In some cases, it can be seen that trenches have eroded more and more silt or sediment flows have likely accumulated. The displaced loose material appears to originate from the side channels of the rocky gullies of Piz Nair (Chapter *4 Study area*), probably being displaced into the slopes and the bottom of the main channel due to fall and flow processes during and between precipitation events.

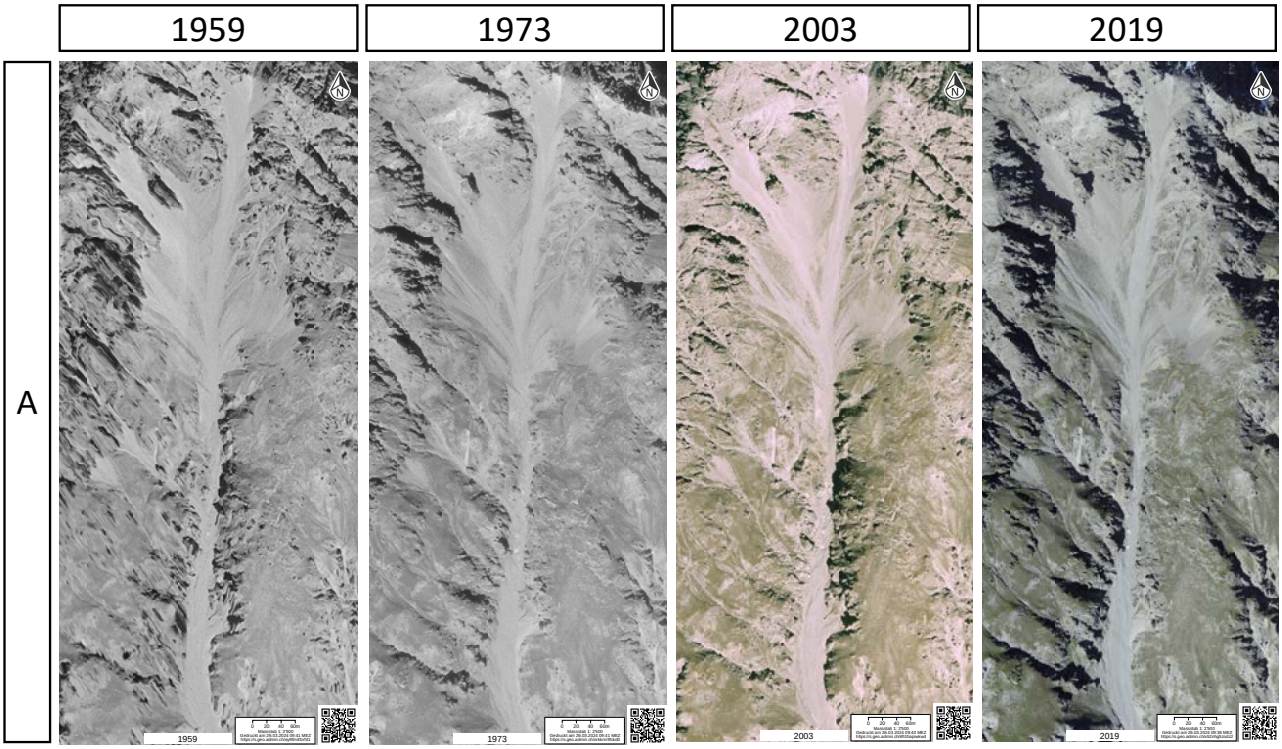

Figure 7.1: Geomorphological element A (according to Figure 6.1) compared over 4 periods. Data: swisstopo (2023)

Figure 7.2 shows the transient area B, which is the following section of the delivery area A in Figure 7.1. The imagery from 1959 already shows the major existing channel in which material is collected and channeled from the upper delivery area. This channel then flows into section C, where the material continues to erode and in some cases already accumulates. In 1973, either erosion by water or further small debris flows emerged, making their way through the gully. There seem to be no major changes until 2003. Between 2003 and 2019, a channel in the middle of the deposits seems to be more accentuated and forms a main flow line. At the eastern upper edge, brighter and therefore more recent deposits are visible.

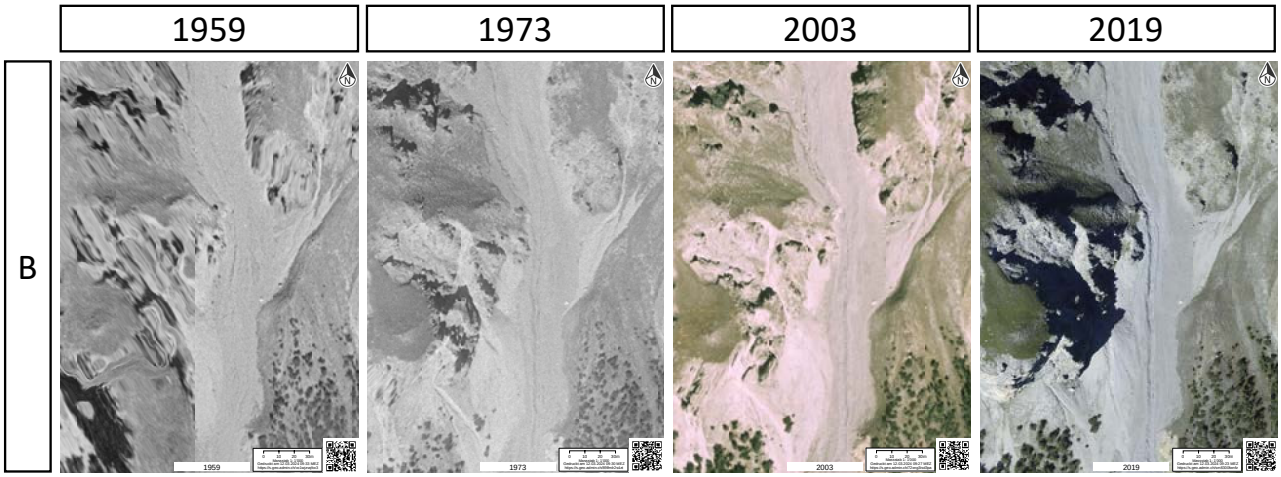

Figure 7.2: Geomorphological element B (according to Figure 6.1) compared over 4 periods. Data: swisstopo (2023)

Figure 7.3 shows section C, where erosion areas and deposits get wider. The imagery from 1973 shows

recent events: a flow of sediment can be seen at the northern and southern edges of the deposits, running along the forest boundary. In 2003 even a new arm of deposited sediment was visible there at the eastern forest boundary. In the last image, it seems like the eroded areas have been filled up more with material, but have not flowed further south. Vegetation plays an important role in events like debris flows as it prevents the deposits from further expanding. The vegetation in area C seems to erode more over the years and could not recover from recent abrasions events.

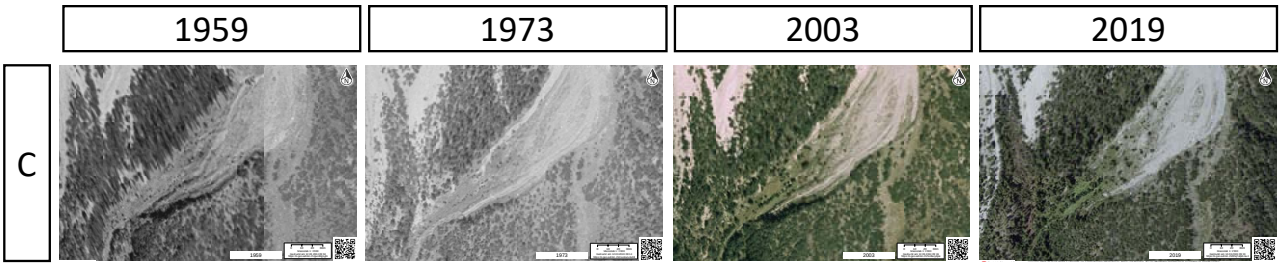

Figure 7.3: Geomorphological element C (according to Figure 6.1) compared over 4 periods. Data: swisstopo (2023)

Section D in Figure 7.4 shows the side slopes west of Buffalora. Similarly, here, plenty of eroded areas are recognizable, which generally indicates an active region. Many slope processes are taking place and loose material is available that erodes the slope, in particular the existing forest. In 1973, it seems that the deposits on the side slopes have become larger, which indicates that past processes must have occurred between those years and caused further erosion and deposition. There seem to be no major changes until 2003. The last image shows that the notches on the side slopes in the section seemed to have been filled up with material and the deposited areas appear to reach further down.

Figure 7.4: Geomorphological element D (according to Figure 6.1) compared over 4 periods. Data: swisstopo (2023)

Starting from the deposits in section C (figure 7.3), a long notch extends from earlier erosion into section E (figure 7.5). This channel coincides spatially with the course of the Buffalora debris flow event of 2022. The second image shows the long notch more accentuated. Considering the new deposits in the side slopes (section D in Figure 7.4), material may have accumulated and flowed down the slope between 1959 and 1973 along this gully and has therefore accentuated the notch. There seem to be no major changes until 2019.

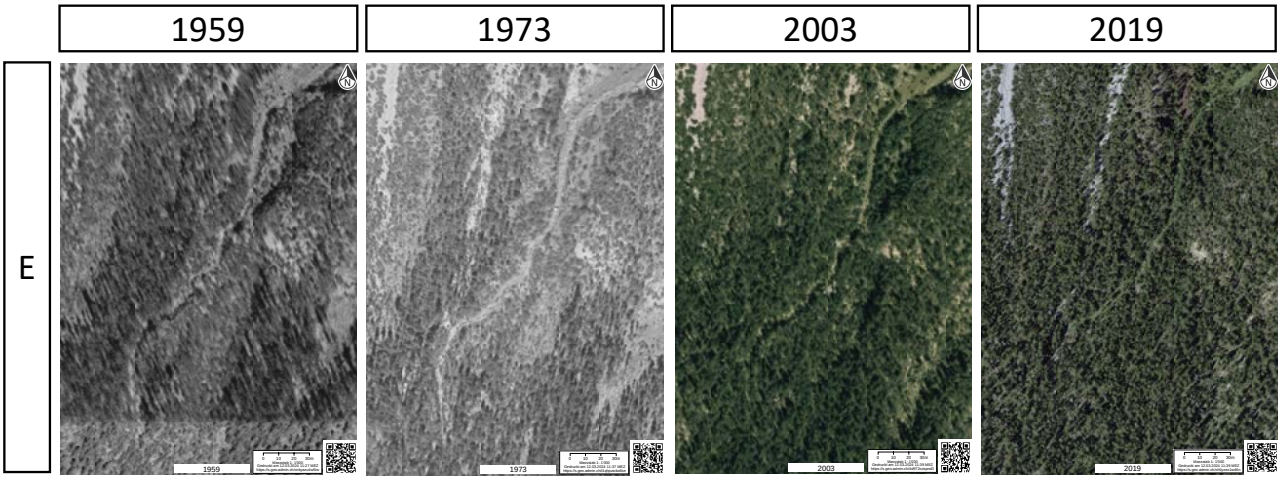

Figure 7.5: Geomorphological element E (according to Figure 6.1) compared over 4 periods. Data: swisstopo (2023)

Section F in Figure 7.6 shows large-scale abrasion of the forest down to the river, which can be allocated to a major slope event. The process must have occurred several years before 1959, given the already advanced stage of natural forest regeneration. No channels or levees can be identified clearly, which would be indicators for a debris flow. However, the extensive abrasion of vegetation could suggest an avalanche. The largely eroded aisle seems to have overgrown again more with vegetation throughout the periods. In 2003, the lower part of the eroded area showed lighter patches visible. Perhaps, more slope processes have happened and have led to more erosion there. Between 2003 and 2019 no significant changes other than the regrowth of the vegetation can be seen. Compared to section C (figure 7.3) it seems that in this area, the patch could recover and regrow the vegetation again without disturbing abrasion processes.

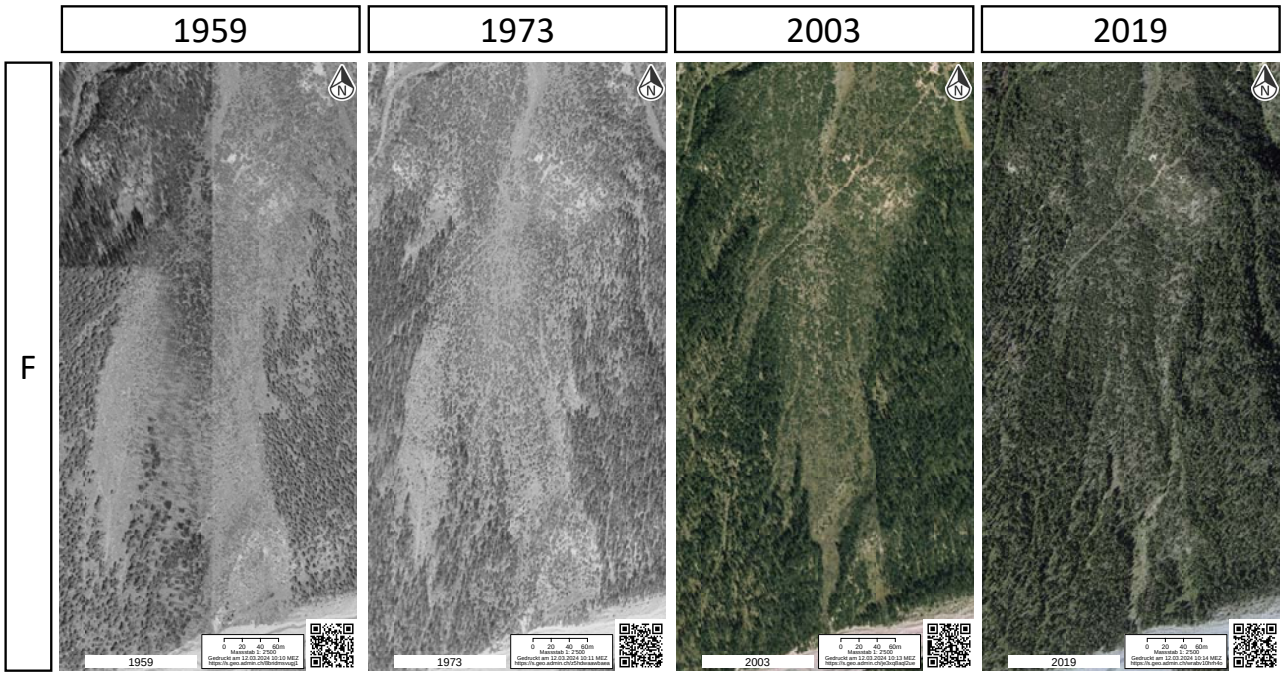

Figure 7.6: Geomorphological element F (according to Figure 6.1) compared over 4 periods. Data: swisstopo (2023)

Section G in Figure 7.7 shows a large clearcut of the vegetation from the upper right edge of the image towards the lower left edge. This is the former SNP border and is not related to the former slope processes. Apart from that, a few gaps in the form of lines perpendicular to the slope inclination indicate probably water or sediment flow down the slope. Until 1973, the SNP border got more covered with vegetation, the street got wider and more houses were added, which are positioned in direct line of fire for subsequent slope processes. The image from 2003 shows clearer indentations in the gullies between the small hills at the slope, which paves the way for water and material to accumulate and flow down the slope. Until 2019 no significant changes can be seen.

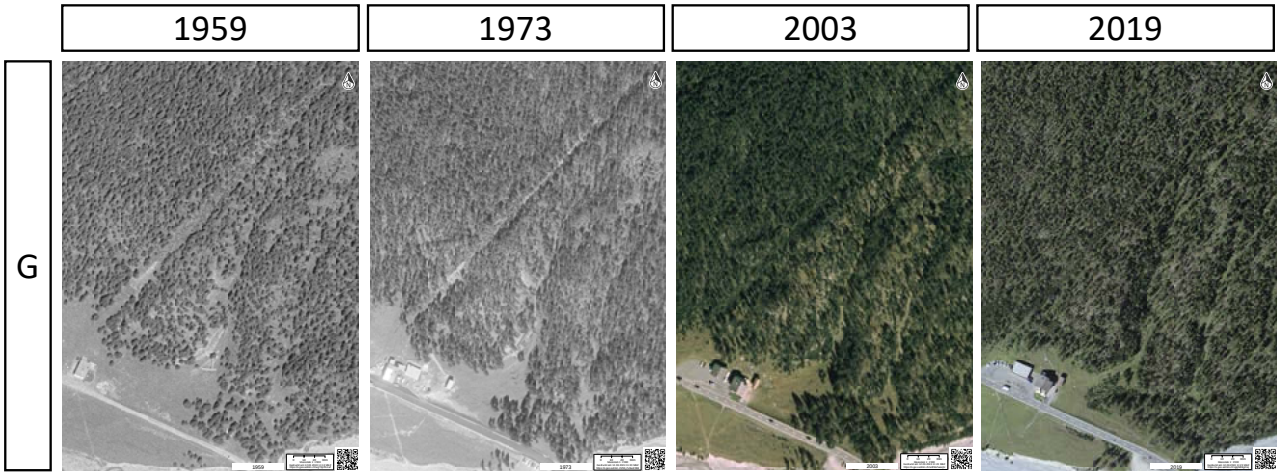

Figure 7.7: Geomorphological element G (according to Figure 6.1) compared over 4 periods. Data: swisstopo (2023)

The temporal landscape analysis shows that the study area is generally characterized by erosion, accumulation, fluvial - and gravitational processes and natural forest regeneration. Comparing these earlier imageries with the event of 2022, it appears that the above-mentioned terrain features directed the deposition of the 2022 event along the pre-existing paths, resulting in the observed course: The source area supplies material from the Piz Nair massif, accumulating and transporting it through the eroded gully until the erosion and deposition spread out and a branch diverges. Over a long period, erosion and accumulation have taken place there and gravitational processes have shaped the landscape. The terrain has created a foundation for the Buffalora debris flow event to traverse through in 2022.

7.1.2 Primary parameters

In the following, the application of selected geomorphometric parameters is presented. This was carried out in the study area of Buffalora according to Figure 4.2 as well.

Figure 7.8 shows the flow accumulation of the study area, which is a prerequisite for creating the catchment area and secondary indices. The flow accumulation represents the accumulated upstream area draining through each cell (esri, 2024). The plot brings out the Ova dal Fuorn as the main river around the mountains. The smaller rivers and gullies that flow orographically from the left and right into the Ova dal Fuorn are getting visible. The flow accumulation also clearly shows where the water and sediment for the debris flow originate. In the basin below the Piz Nair, many small rivers come together from the crests of the delivery area to form one larger river, which runs straight into the

deposits of the debris flow event. The flow accumulation then follows the shape of the deposits very closely, in particular the curve that steers the deposits more to the south-west. In the lower part of the deposits, the flow accumulation lines seem to enclose the deposits.

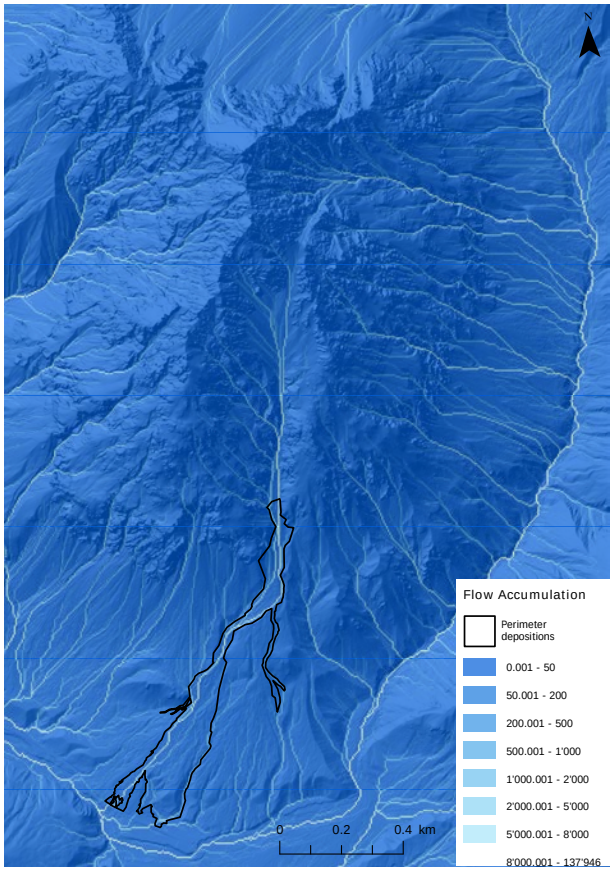

Figure 7.8: Resulting map of the flow accumulation of the study area Buffalora. Perimeter of depositions as black border, unit in sum of flow (cells) that come together at each point according to the flow direction. Data: swisstopo (2020)

The image in Figure 7.9 shows the catchment area (blue), outlet point (orange) and main flow line (red). The catchment area, which was derived from the flow accumulation includes the upper basin of the Piz Nair, whose area is around 253'788.2 m^2, which is considered to be quite large in comparison to the area covered by the deposits which counts 80'805.71 m^2. The main flow line was measured to provide an order of magnitude of the length of the course where the debris flow occurred. For that, the catchment area and the deposits were measured. The flow line within the catchment area, i.e. from the uppermost point to the pour point, is 1'077.85 m. The flow line from the pour point to the lowest point is 1'870.12 m. In total, this results in a main flow line of 2'947.97 m.

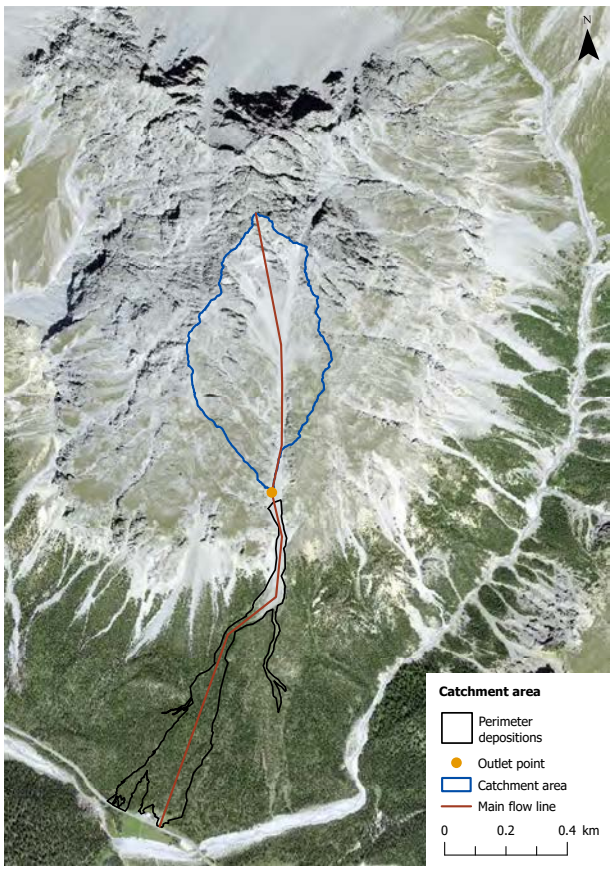

Figure 7.9: Resulting map of the catchment area, outlet point and flowline of the study area Buffalora. Data: swisstopo (2023), own visualization.

Figure 7.10 shows the slope gradient of Buffalora in degrees. Steeper areas can be seen in the upper part of the catchment area, which often coincides with the rocky outcrops. The channel leading from the catchment area into the perimeter of the debris flow deposits is visible. The course of the debris flow generally leads from a rather steeper to a flatter region. This also roughly corresponds to the shape of the deposits, which run out towards the flatter part and therefore become wider.

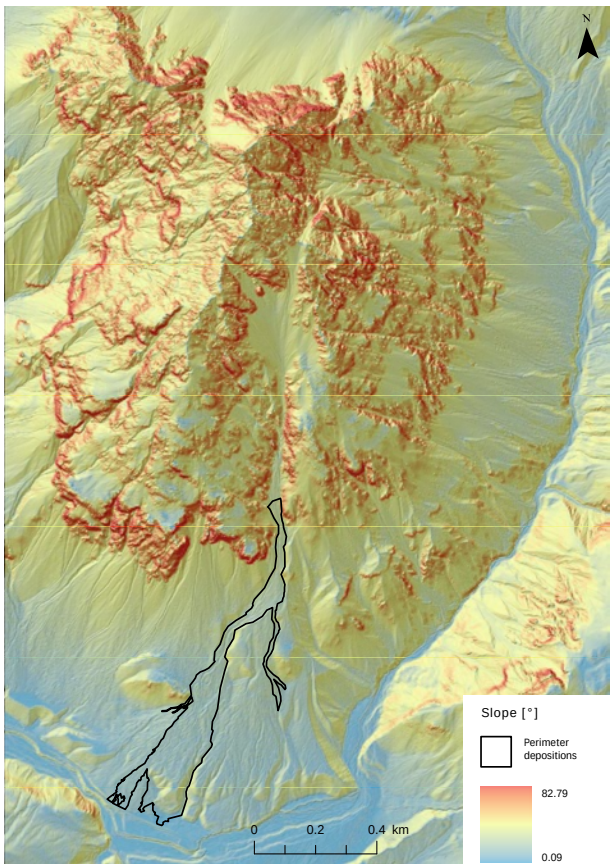

Figure 7.10: Resulting map of the primary geomorphometric parameter slope of the study area Buffalora. The perimeter of depositions as black border, unit in degrees, small slope inclination in blue, and large slope inclination in red. Data: swisstopo (2020)

The parameter aspect in Figure 7.11 offers an overview of the orientation of the terrain. The debris flow and the associated channel upstream are located on a slope that is oriented between southeast and southwest.

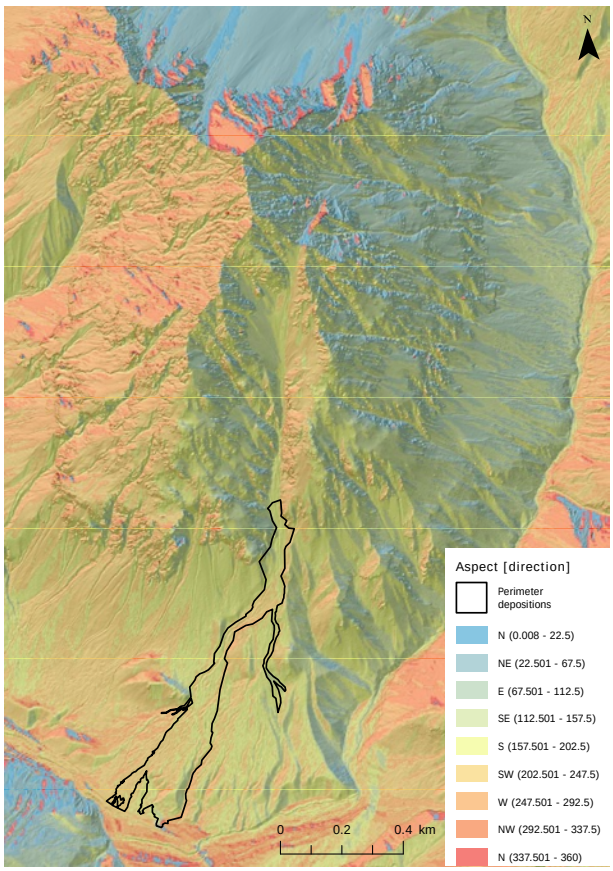

Figure 7.11: Resulting map of the primary geomorphometric parameter aspect of the study area Buffalora. Perimeter of depositions as a black border, orientation indicated in cardinal directions. Data: swisstopo (2020)

The visual appearance plot of the profile and plan curvature is very similar (Figure 7.12). High positive values in profile curvature stand for high flow acceleration and high negative values express decelerated flow (Smith et al., 2007). The left plot therefore shows the ridges of the terrain with high positive values (red) in areas and the channels and the riverbed with high negative values (blue). The left plot shows the platform curvature. High planform curvature values show divergent curvatures, which rather leads to the formation of ridges (Ahmad et al., 2019). Such ridges are recognizable in the right plot as red areas and correspond to the existing ridges. The boundary of the catchment area of the debris flow is well emphasized by these ridges. Low planform curvature values show convergent curvatures indicating the formation of channels (flow convergence) leading to more erosion (Ahmad et al., 2019). Such areas are easily recognizable as blue areas that correspond to the existing riverbed and channels. Some channels lead to the deposition of the debris flow and outline the shape of the terrain.

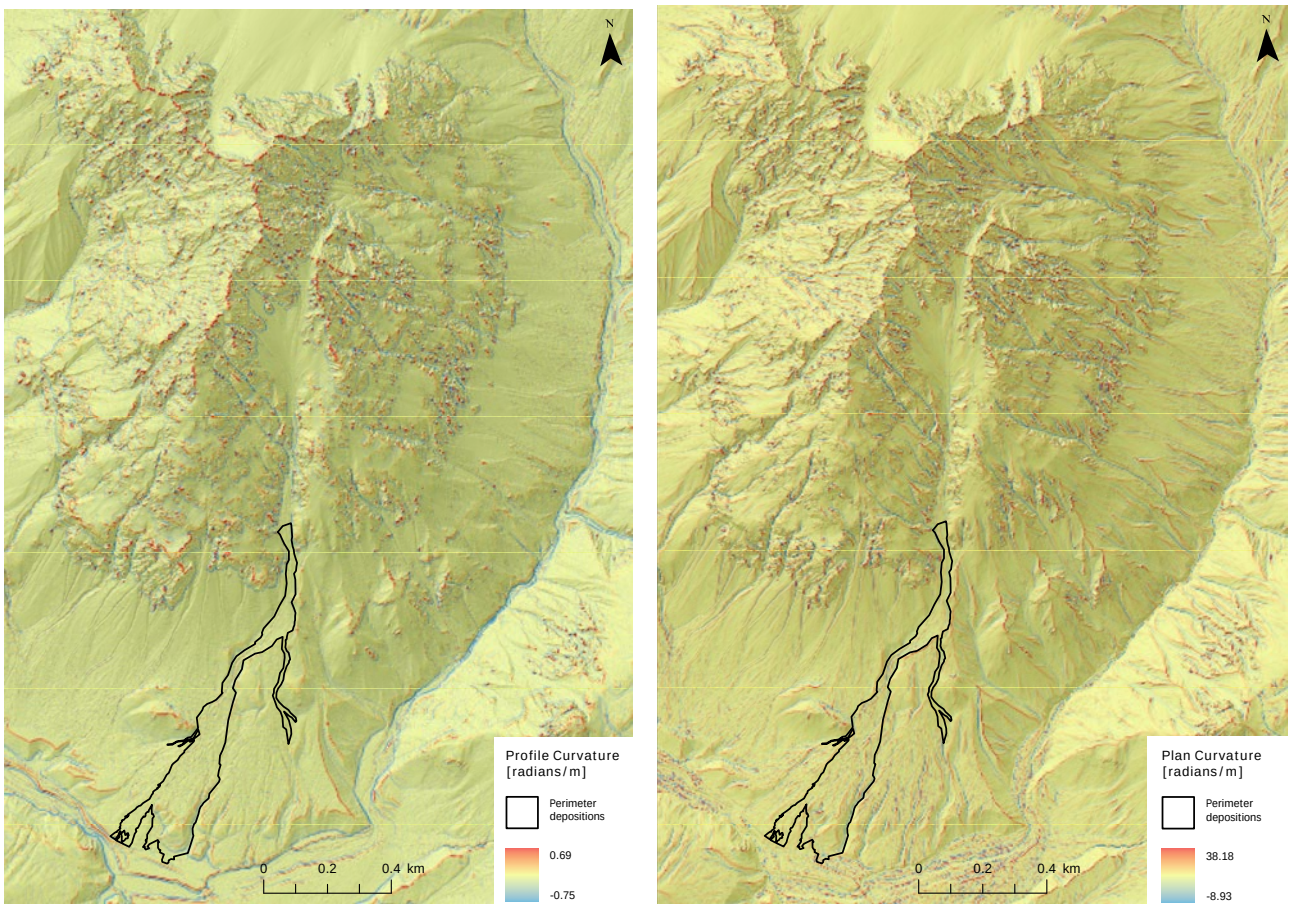

Figure 7.12: Resulting maps of the primary geomorphometric parameters profile and plan curvature of the study area Buffalora. Perimeter of depositions as black border, unit in radians per meter, small curvature in blue and large curvature in red. Data: swisstopo (2020)

Figure 7.13 represents the ERR. This ratio tends to be high for convex landscape patches and becomes lower with increasing concavity (Otto et al., 2017). Concave terrain features describe topography that is curved inwards as hollow or indented shapes and correspond, e.g., to valleys or lakes. Convex landforms represent outwardly curved topography such as hills or mountain ranges. The larger or smaller the value, the more pronounced the corresponding shape. In Figure 7.13 these shapes can be recognized: the river within the valley is characterized by low values. The mountains around Piz Nair are characterized by a mixture of high and low values, which is due to the rocky and uneven terrain in which hollows, ridges and rocky outcrops balance each other out. In the catchment area and the deposits of the debris flow, however, average values can be seen, which reveals a terrain without remarkable terrain features and indicates flatter and evened-out terrain. This gave the debris flow a free path to accumulate material and the possibility to deposit again at the bottom of the slope.

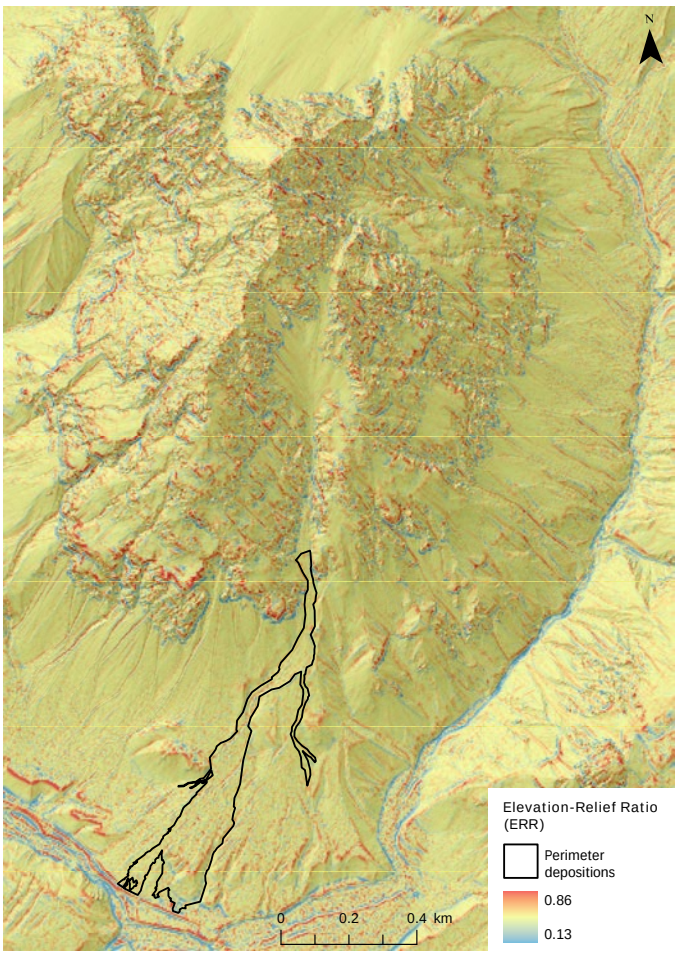

Figure 7.13: Resulting map of the ERR of the study area Buffalora. Perimeter of depositions as black border. ERR values indicate how much the terrain varies to its horizontal extent. Data: swisstopo (2020)

Table 7.1 shows the results of R. Comparing the calculated results to the values of the study of Ilinca (2021), mentioned in Chapter *2.3 Related work in geomorphometry*, the event of Buffalora can be categorized somewhere between a debris flow and a debris flood.

Table 7.1: Results of R of the study area Buffalora.

	Highest point	**Lowest point**	**H**	**D**	**Relief Ratio (R)**
with delivery area	2987.98 m a. s. l.	1963.49 m a. s. l.	1024.49 m	2103.38 m	**0.49**
within deposition area	2364.69 m a. s. l.	1963.49 m a. s. l.	401.2 m	1170.88 m	**0.34**

7.1.3 Secondary parameters: indices

In the following, the application of selected geomorphometric indices is presented. This was carried out in the study area of Buffalora according to Figure 4.2 as well.

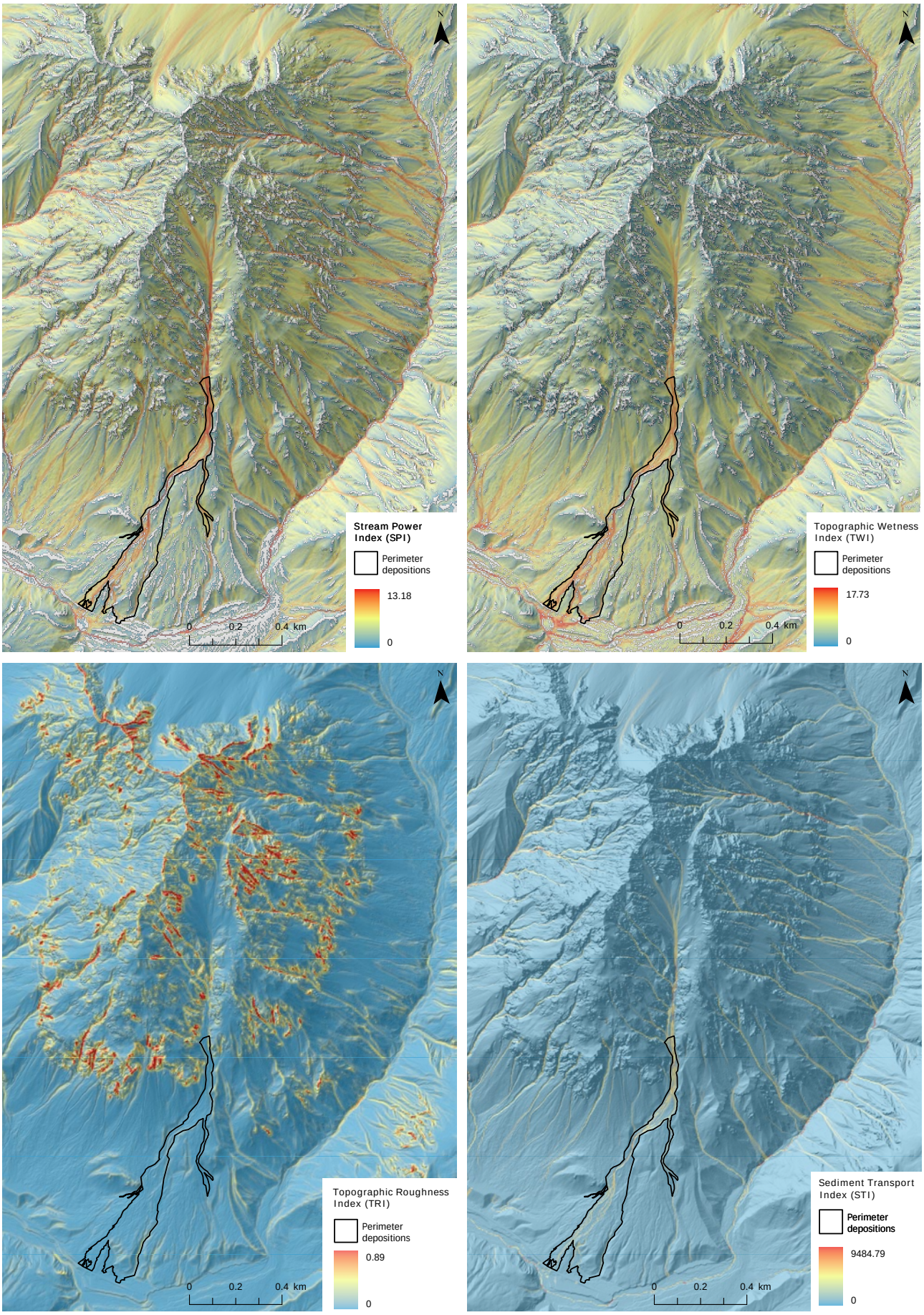

Figure 7.14: Resulting maps of geomorphometric indices of the study area Buffalora: SPI, TWI, TRI, STI. Low values are indicated in blue and high values are indicated in red. Due to the distribution of TRI values concentrated in very low values, the plot is shown with the standard deviation. Data: swisstopo (2020)

Figure 7.14 represents the resulting geomorphometric indices: SPI, TWI, TRI and STI. The SPI generally highlights the crests with low- and gullies with high stream power values, as water and sediments flow orographically down the slope to the left or right. High stream power can be recognized in the delivery area of the debris flow, composed of several small arms coming down from all side slopes, resulting in a large arm flowing into the depositions of the debris flow. The delivery area is a significant erosion and accumulation area for the Buffalora event. Very high values are shown inside the deposits and follow the shape of the deposits quite precisely. The upper part of the deposits in particular shows very high values, as the majority accumulates there from the delivery area and forms a channel. Very similar patterns to the SPI can also be seen in the TWI. Compared to the side slopes, the study area of the Buffalora debris flow stands out strongly. Again, it shows clearly that the delivery area channels the side flows into one stream. The TRI stands out visually from the other indices. High roughness is visible in the mountain range of the Piz Nair. It is striking that starting from the delivery area of the study area in the direction of the debris flow, the channel shows very low to no roughness. The entire lower part of the Piz Nair massif does not appear to be rough, including the region where the debris flow descended. The STI shows clearly the small valleys of the terrain, in which a lot of water can flow down a slope. The patterns seem to be similar to the SPI and the TWI but are more concentrated on the individual gullies which stand out in comparison to the rest of the values. Within the perimeter of the depositions, the STI is particularly high compared to the side slopes, which means that the potential for sediment transport in the area of the debris flow that has passed was or is still high. Nevertheless, similar patterns to the SPI and TWI can be seen: high sediment transport in the delivery area, which leads directly into the deposits of the debris flow. The STI also shows a branch leading from the side slope into the deposits.

This chapter examines geomorphometric parameters and indices of Buffalora, highlighting key terrain features and the debris flow path. The flow accumulation map traces the origin and path of the debris flow along the Ova dal Fuorn river. The slope gradient map reveals the steeper upper catchment transitioning to flatter debris deposit regions, while aspect analysis shows the debris flow oriented between southeast and southwest. The curvature map identifies ridges and channels, indicating areas of erosion and deposition. The ERR and R maps show flatter terrain suitable for material accumulation and classify the event between a debris flow and a debris flood. Indices such as SPI, TWI, TRI, and STI further highlight erosion, sediment transport, and low roughness along the debris flow path, indicating high erosion and deposition in the delivery area.

7.1.4 Correlation matrix

Figure 7.15 shows the pairwise Pearson Correlation Coefficients of the resulting correlation matrix for all parameters represented as a correlogram. Between SPI, TWI and STI a moderate-high positive correlation occurs: SPI and TWI with a correlation coefficient of 0.66, SPI and STI with a correlation coefficient of 0.61 and TWI and STI with a correlation coefficient of 0.5. This may be because all three indices are based on specific catchment area (flow accumulation) and slope. In addition, the indices already showed spatial similarities visually, which was to be expected insofar as they all aim for the same surface property. The TRI shows a weak negative correlation with the SPI and TWI and none with the STI. The ERR shows no correlation with any other index.

In connection with the primary parameters, further correlations emerged. They are mentioned in the following, however, they are not considered for the elimination of further indices or parameters.

Slope and TWI show a moderate negative correlation. Aspect does not seem to be related to other parameters. Plan and profile curvature show weak to moderate negative correlation to SPI, TWI and STI. Flow accumulation shows a weak to moderate positive correlation to SPI, TWI and STI. As these indices are all based on flow accumulation, the correlation was expected to be larger. To a certain extent, they also have similar predictions: if the flow accumulation, which represents the accumulated upstream area, increases, the sediment transport, wetness and stream power increase as well.

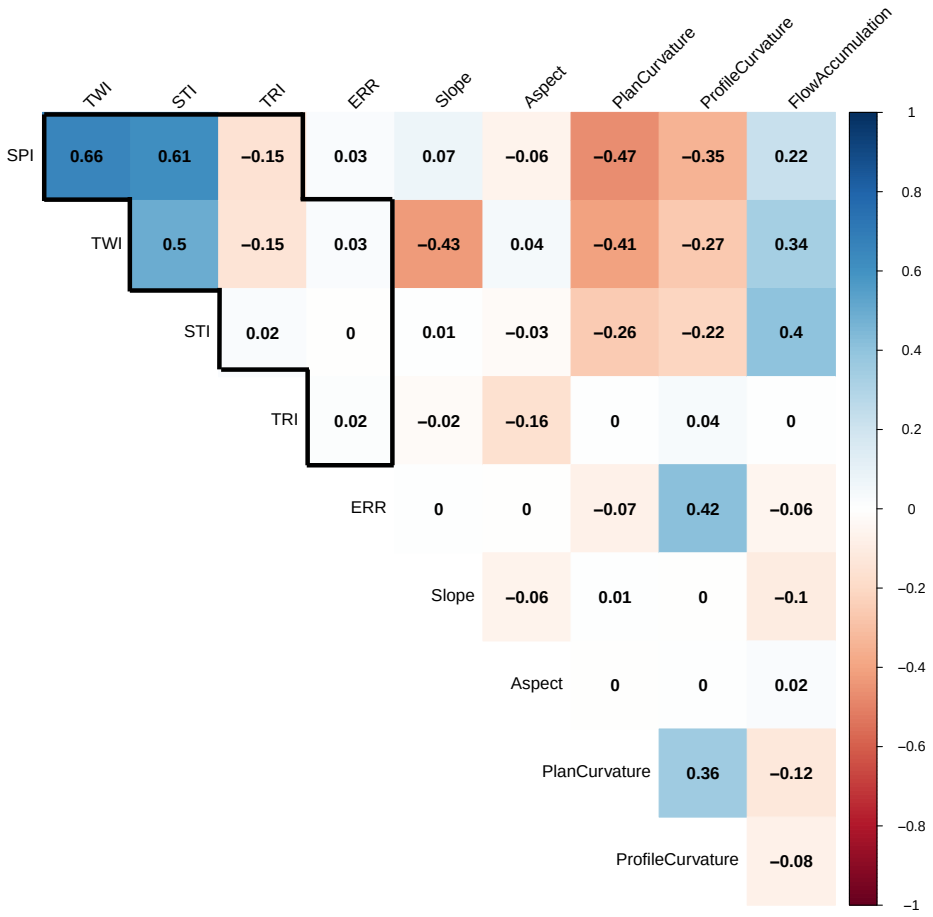

Figure 7.15: Pairwise Pearson correlation coefficients of the resulting correlation matrix represented as a correlogram. Included are primary parameters and indices: SPI, TWI, STI, TRI, ERR, slope, aspect, profile curvature, profile curvature and flow accumulation. The indices are framed in black. Values between -1 and 0 mean negative correlation, values = 0 mean no correlation, values between 0 and 1 mean positive correlation and values = 1 meaning perfect positive correlation. The correlations are colored according to the color scale.

Almost all of the parameters and indices exhibit moderate to weak correlations, indicating that they do not significantly overlap in the information they provide. Each index captures distinct and essential geomorphological aspects of a debris flow, making them all valuable for a comprehensive analysis. Understanding the correlations among these indices helps to interpret the data more accurately, but does not necessarily mean the exclusion of any. Therefore, it is justified to retain all indices in the further analysis to ensure a holistic and detailed understanding of the geomorphological processes involved.

7.1.5 Height Difference Model (HDM)

Figure 7.16 shows the resulting HDM of pre-and post-event elevation models of the study area Buffalora. Regions considered to have no change in elevation are colored in grey (including an uncertainty range of −/+ 10cm). Regions with an increase in mass (accumulation) are colored in gradients of red respectively regions with a decrease in mass (erosion) are colored in gradients of blue. The black outline shows the perimeter of the depositions, also excluding regions, where the debris flow did not leave any deposits, hence it is assumed it did not traverse through those regions. It is noticeable that the values are strongly negative where the debris flow left no deposits. This is due to the two different DEMs. The pre-event elevation model was generated from a point cloud that was recorded with lidar, in contrast to the post-event elevation model, which was created from RGB images using photogrammetry. The lidar data can estimate the ground more accurately from the automatically classified point cloud, compared to the drone images, which in our case tended to underestimate the ground in places where the trees have remained dense. When subtracting them from each other, areas with strongly negative values result. Therefore, only those regions located within the perimeter of the deposits are considered for the interpretation of erosion and accumulation. The edges of the map are also not to be taken into account. With drone data, the images at the edges are always distorted because images from the sides are missing for overlapping references. This is also the reason for the high maximum and minimum values in the HDM (−90.33 and +19.26).

A clear erosion channel can be seen in dark blue at the beginning of the perimeter in the upper area. At this point, the slope is steeper than below (Figure 7.10) and roughness is very low (Figure 7.14). According to the temporal landscape analysis, there has already been a gully and the material is the most concentrated there. Accumulations can be seen to the east and west of this erosion channel, which has been pushed to the sides and deposited there. The material also accumulated in the curves further south. Further erosion continues down the slope until the deposits can expand in width, slow down and therefore begin to deposit more broadly. The deposits are most noticeable at the very bottom of the tongue of the depositions.

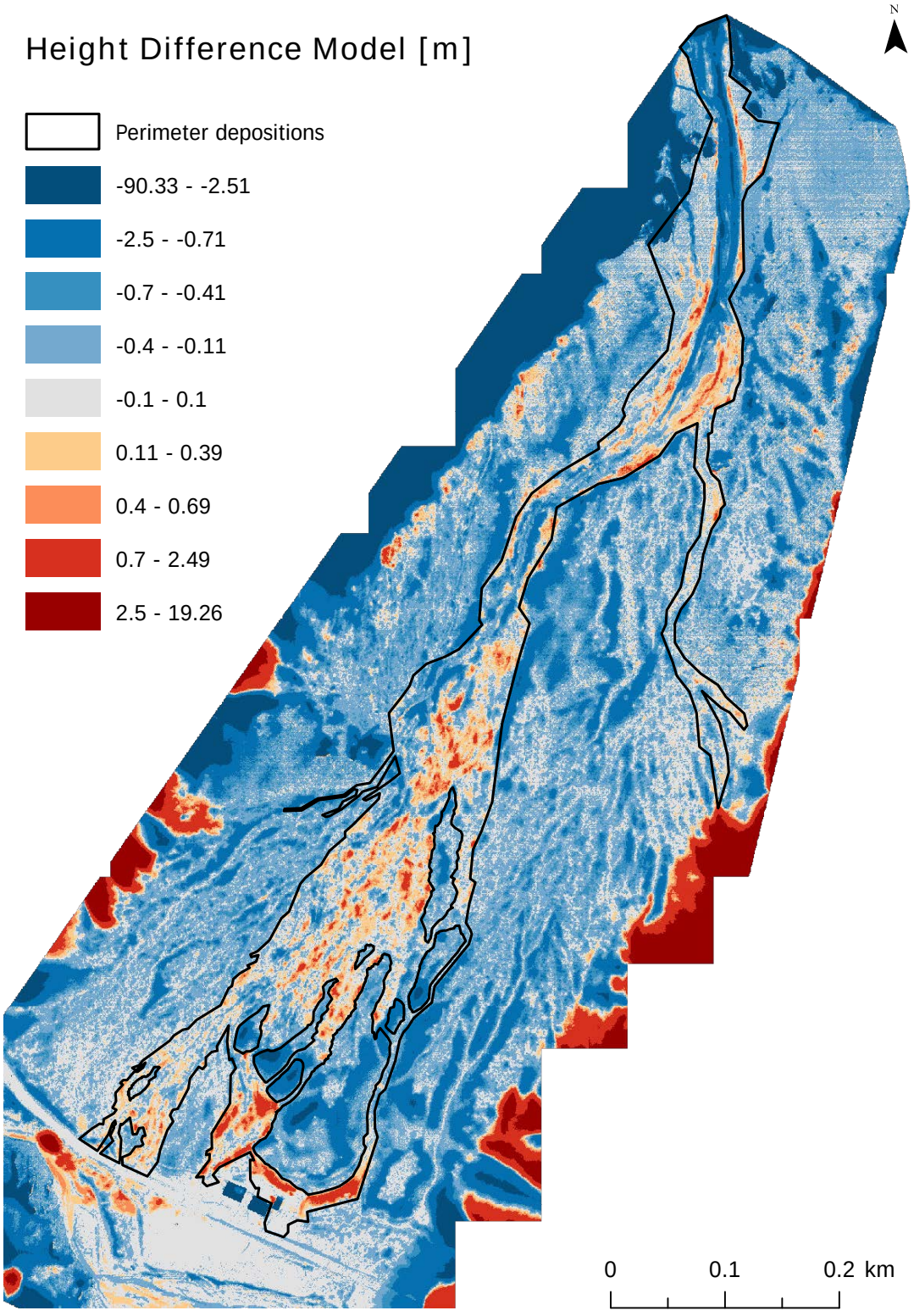

Figure 7.16: Resulting height difference model of pre-and post-event elevation models of the study area Buffalora. The perimeter of depositions in black, excluding those regions, where the debris flow did not leave any deposits. Regions considered to have no change in elevation are colored in grey (including the uncertainty range of −/+ 10cm). Regions with an increase in mass (accumulation) are colored in gradients of red respectively regions with a decrease in mass (erosion) are colored in gradients of blue. Data: swisstopo (2020) and SNP (2022)

The HDM shows areas of erosion and accumulation of the debris flow event area at Buffalora. Erosion

is concentrated in steep, low-roughness regions with old gullies, while accumulation occurs along the edges of these channels and in curves further downhill. As the debris flow moves down the slope the speed decreases, and deposits more material, with the largest depositions at the bottom.

7.1.6 Volume

The calculation of the deposited volume of the Buffalora debris flow event resulted in 8'882.3 m^3. As already mentioned in Chapter *2.4 Research in the SNP*, debris flows can transport volumes of several 10'000 - 100'000 m^3 downhill. The well-known Bondo landslide in 2017 triggered several debris flows in Val Bondasca, with a total of around 500'000 m^3 of material being transported to Bondo (WSL, 2018). Further, the Swiss Federal Institute for Forest, Snow and Landscape Research (WSL) has been observing spontaneously occurring debris flows in the Illgraben since 2000, an exceptionally active catchment area near the village of Susten (Leuk) in Valais (WSL, 2024). Figure 7.17 shows the volume of debris flow events at Illgraben from 2019 to 2022. The last bar in orange represents the calculated debris flow volume of Buffalora. Compared to the debris flow events at Illgraben and Bondo, the calculated volume of the Buffalora debris flow can be classified as rather small.

Nevertheless, when the volumes are considered in relation to the catchment sizes, the volume of the Buffalora event is not as small by comparison: The Illgraben catchment area includes two sub-drainage basins: the Illbach Valley to the east, which covers 5.7 km^2, and the Illgraben Valley to the west, which spans 4.7 km^2 which makes a total catchment area of 10.4 km^2 (McArdell and Sartori, 2021). As stated in Chapter *7.1.2 Primary parameters*, the catchment area of Buffalora is around 0.25 km^2. This means that the Buffalora catchment is about 40 times smaller than the two compared at Illgraben. Considering also having debris flow volumes of the Illgraben with similar size as the Buffalora debris flow volume, the calculated volume is rather moderate in relation to its catchment size.

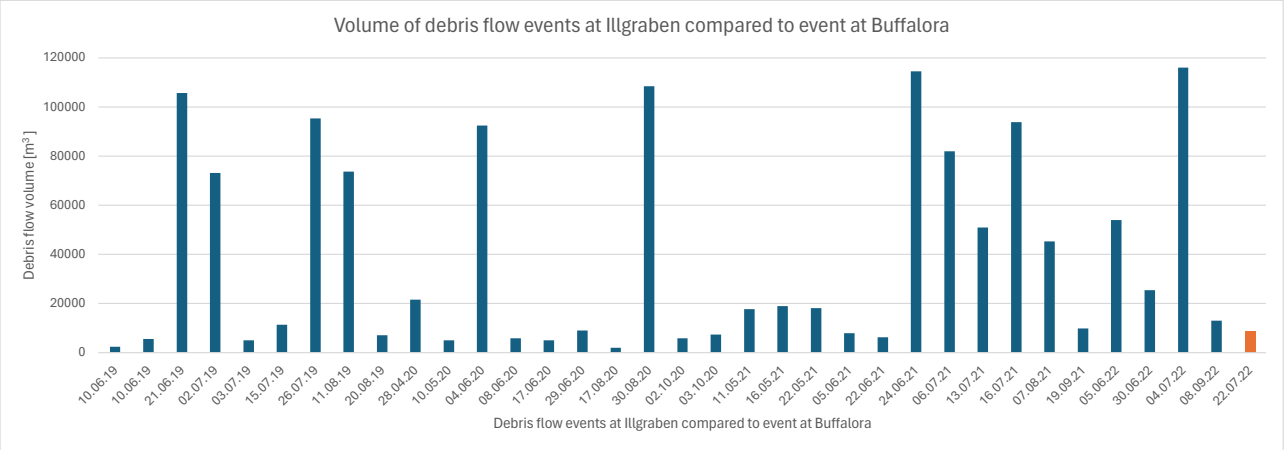

Figure 7.17: Volume of debris flow events at Illgraben from 2019 to 2022 sorted by date, bars colored in blue. The last bar in orange represents the calculated debris flow volume of Buffalora. Data of debris flow volumes at Illgraben: McArdell, Hirschberg, et al. (2023)

7.2 Geomorphometric analysis on larger scale: SNP

Selected geomorphometric parameters and indices have been applied to the whole SNP. The analysis was conducted within the resulting 111 catchment areas within the SNP. The following chapter first

presents the distribution of the index values within the catchments in the form of box- and violin plots. Then the results of the PCA including parameters and indices are presented. In the end, the resulting map of the categorization of the catchment areas within the SNP based on their geomorphometric characteristics and observed debris flow events is illustrated.

7.2.1 Distribution of data within the catchments

The following section presents box- and violin plots for all geomorphological indices (SPI, TWI, STI, TRI, ERR) across all 111 catchments in the SNP. Each set of boxplots provides insights into the distribution, central tendency, and variability of these indices within the catchments. The addition of violin plots as a density function allows for a more detailed examination of the value frequency of the data.

The violinplots of the SPI in Figure 7.18 overall all follow a multimodal distribution. The interquartile range (IQR), which is represented by the box, is approximately situated in the lower third of the occurring SPI values, between around 2 and 5. There are many outliers at the top, which are not shown for the sake of simplicity. Peaks in the violin plots can be observed at SPI at 0 and around 3. The most frequent values therefore occur in the lower third of the existing SPI value range. The peaks in the violin plots differ slightly between the catchments. Compared to the others, catchment numbers 51, 76, and 107, for example, have less broad peaks around an SPI value of 3. On the contrary, the largest peak in the violin plot is distributed over a larger range in catchments number 13 or 27, for example.

The visualization of the TWI values in Figure 7.19 follows a very similar distribution as those of the SPI. They also follow a multimodal distribution with a range in the lower third of the data. The peaks of the violinplots are at 0 and around 5.

The box- and violin plots of the STI (figure 7.20) and TRI (figure 7.21) show a different distribution than SPI and TWI. Overall, the violin plots show a strongly right-skewed distribution of the data, which means that there are a large number of low values and a few high outliers. In both indices, the median is very close to 0, indicating that more than half of the data points have very low values. The long upward whisker indicates values that are significantly higher than the rest of the data. Because the majority of the data points are concentrated in a narrow range near the zero point here, the maximum value was set much lower to better visualize the distribution of the data: for STI, the max. value of 1250 was set to 60 and for TRI, the max. value of 0.6 was set to 0.025. It can be seen then that in some catchment areas, the violin plots of the STI are multimodal distributed. Catchments number 51 and 107 still appear strongly right-skewed distributed. The other catchment areas seem similar in distribution. Some violinplots of the TRI have more cell values with higher TRI values and therefore appear wider at the top end: catchment numbers 11, 17, 49, 57, 67 and especially 111.

The distribution of the ERR data is symmetrical and normally distributed, displayed in the box and violin plots in Figure 7.22. The boxplot shows that the median is in the center of the IQR and the data range, approximately at an ERR of 5. The IQR is also positioned symmetrically around the median in the center. The whiskers that extend upwards and downwards from the box of the boxplot are also symmetrical and show that the data are evenly distributed and that there are few or no outliers. The violin plot is symmetrical about the vertical and horizontal axis, which is typical of a normal distribution. The widest point of the violin plot is in the center, around the median, which represents

the highest density of data points. The width of the plot decreases evenly when moving up and down from the median, indicating the decreasing density of the data.

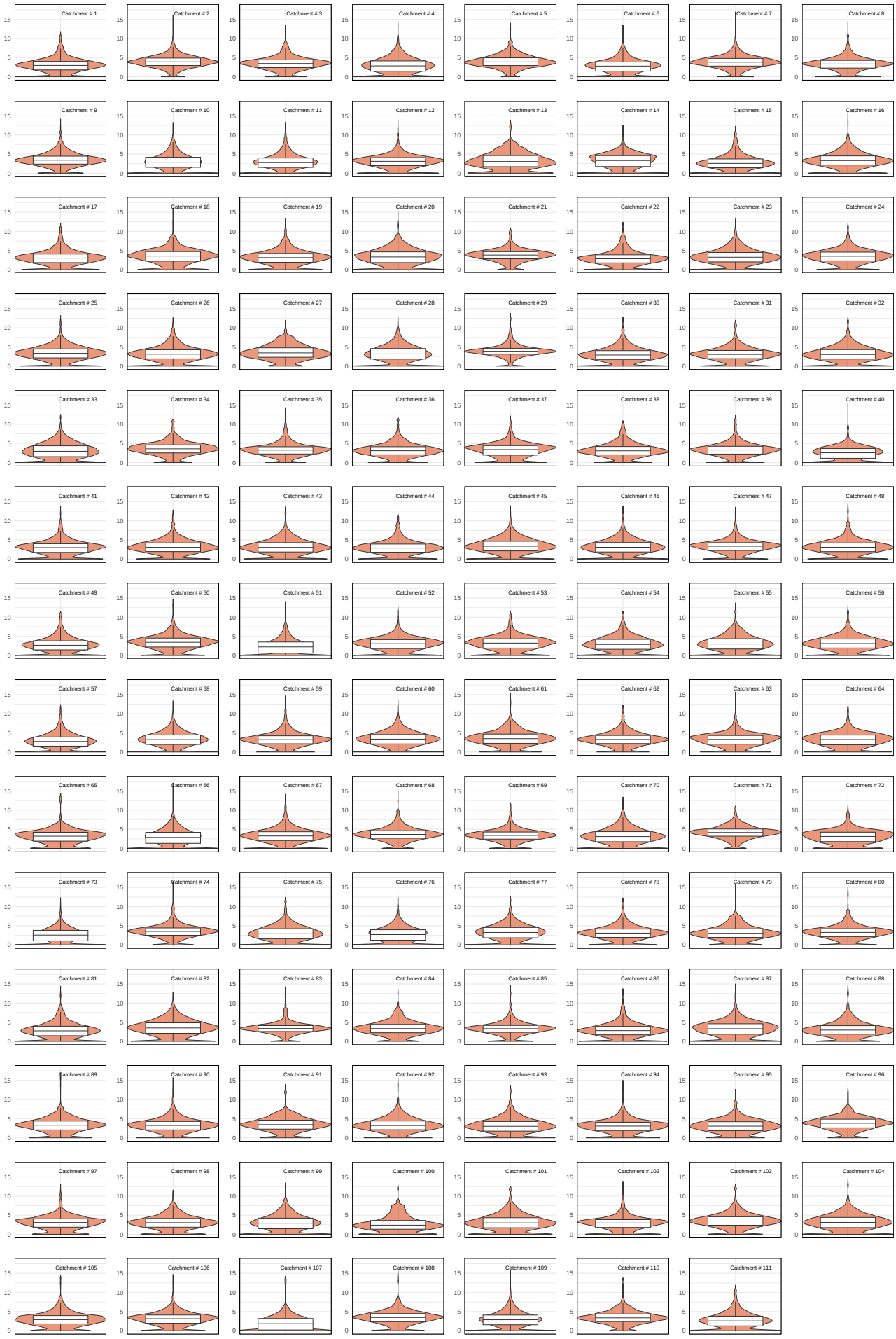

Figure 7.18: Box- and violin plots of Stream Power Index (SPI) for 111 catchments in the SNP.

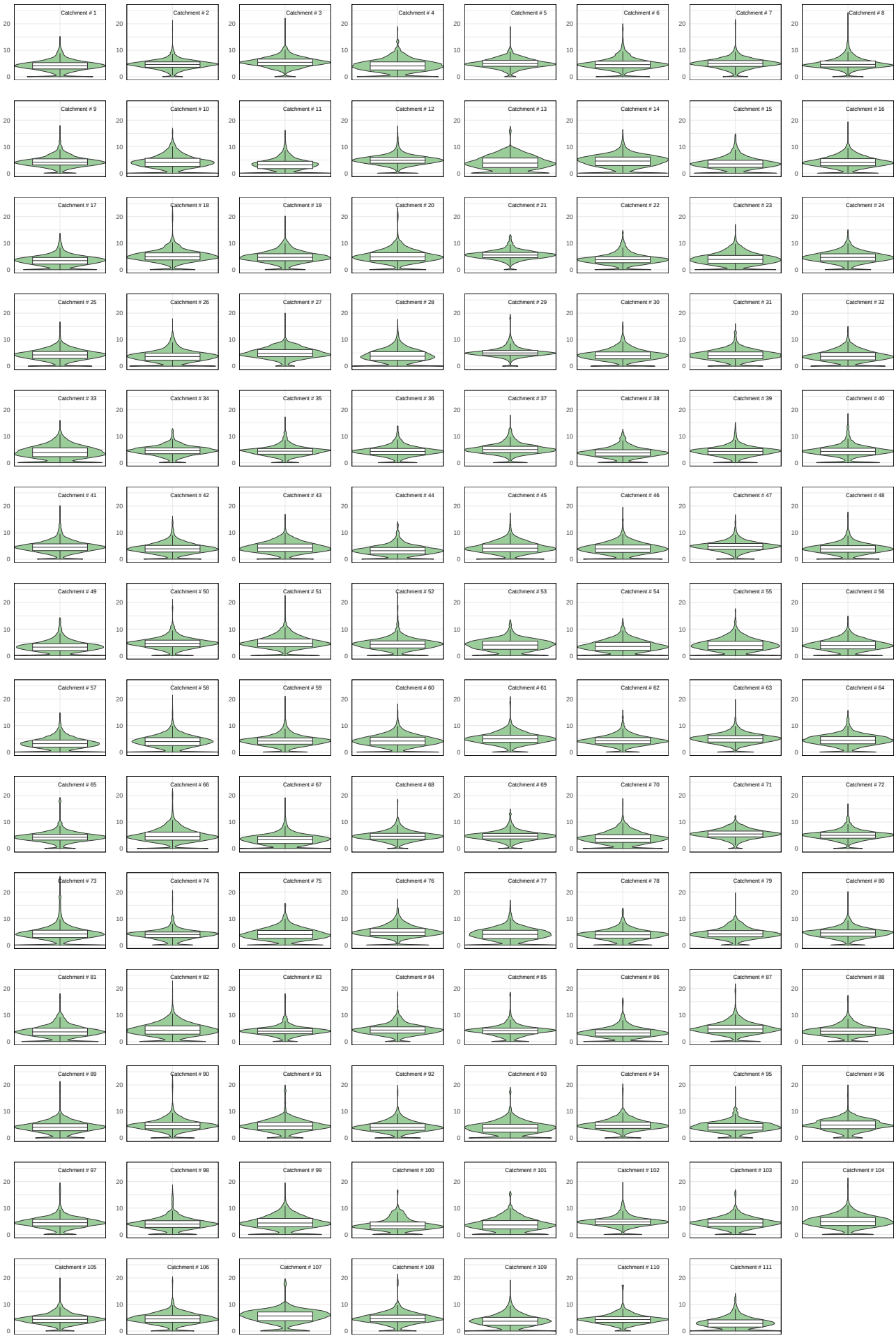

Figure 7.19: Box- and violin plots of Topographic Wetness Index (TWI) for 111 catchments in the SNP.

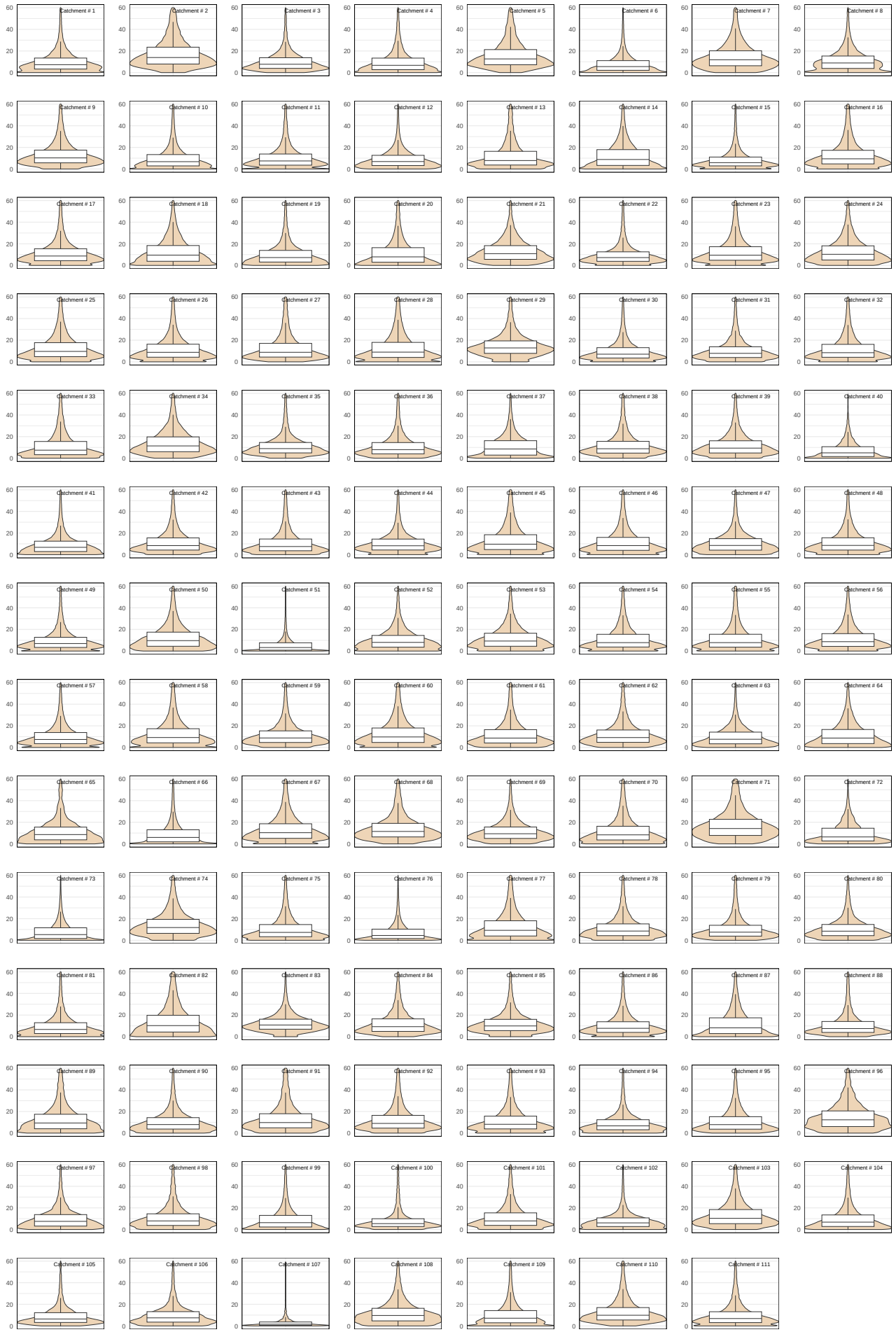

Figure 7.20: Box- and violin plots of Sediment Transport Index (STI) for 111 catchments in the SNP.

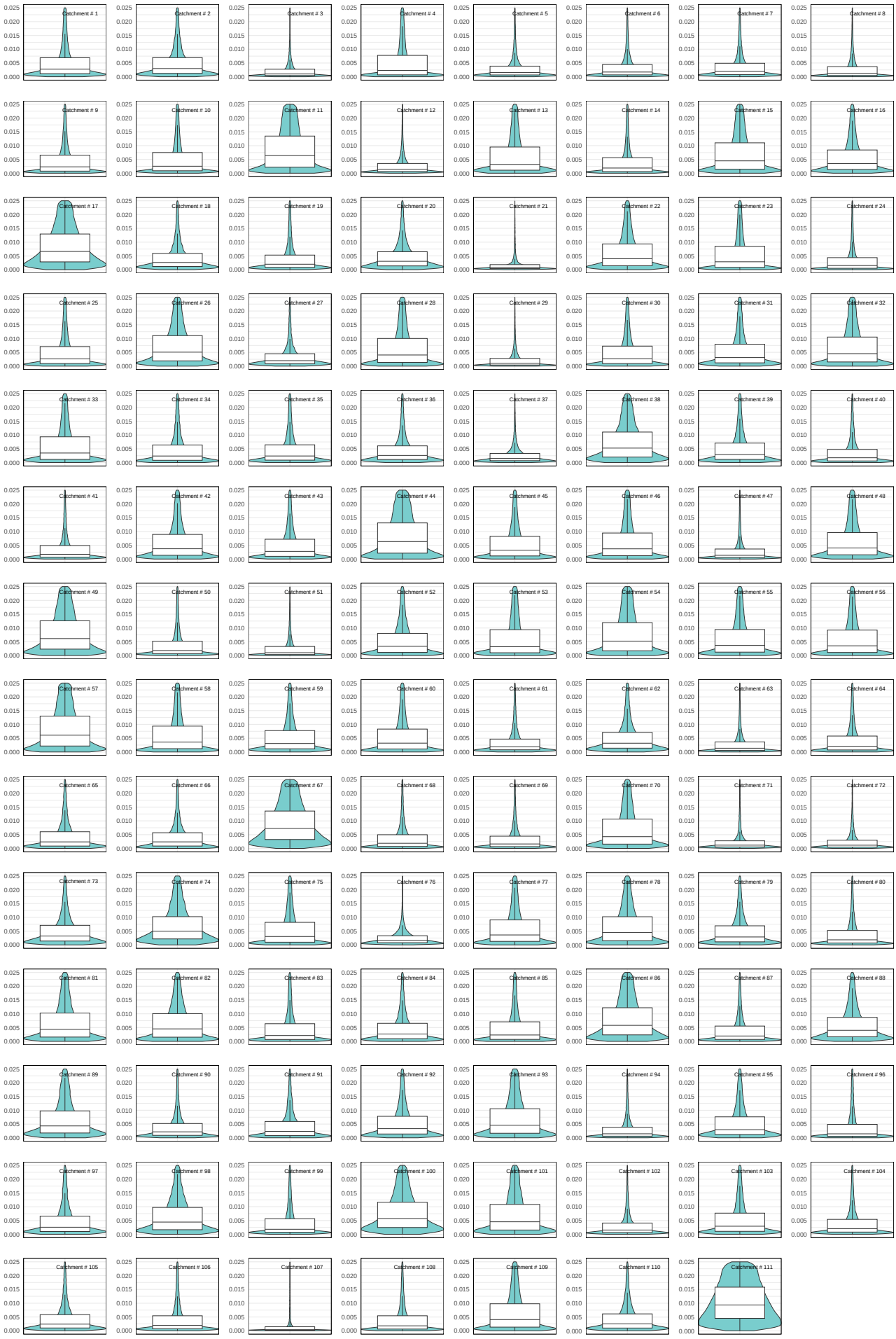

Figure 7.21: Box- and violin plots of Topographic Roughness Index (TRI) for 111 catchments in the SNP.

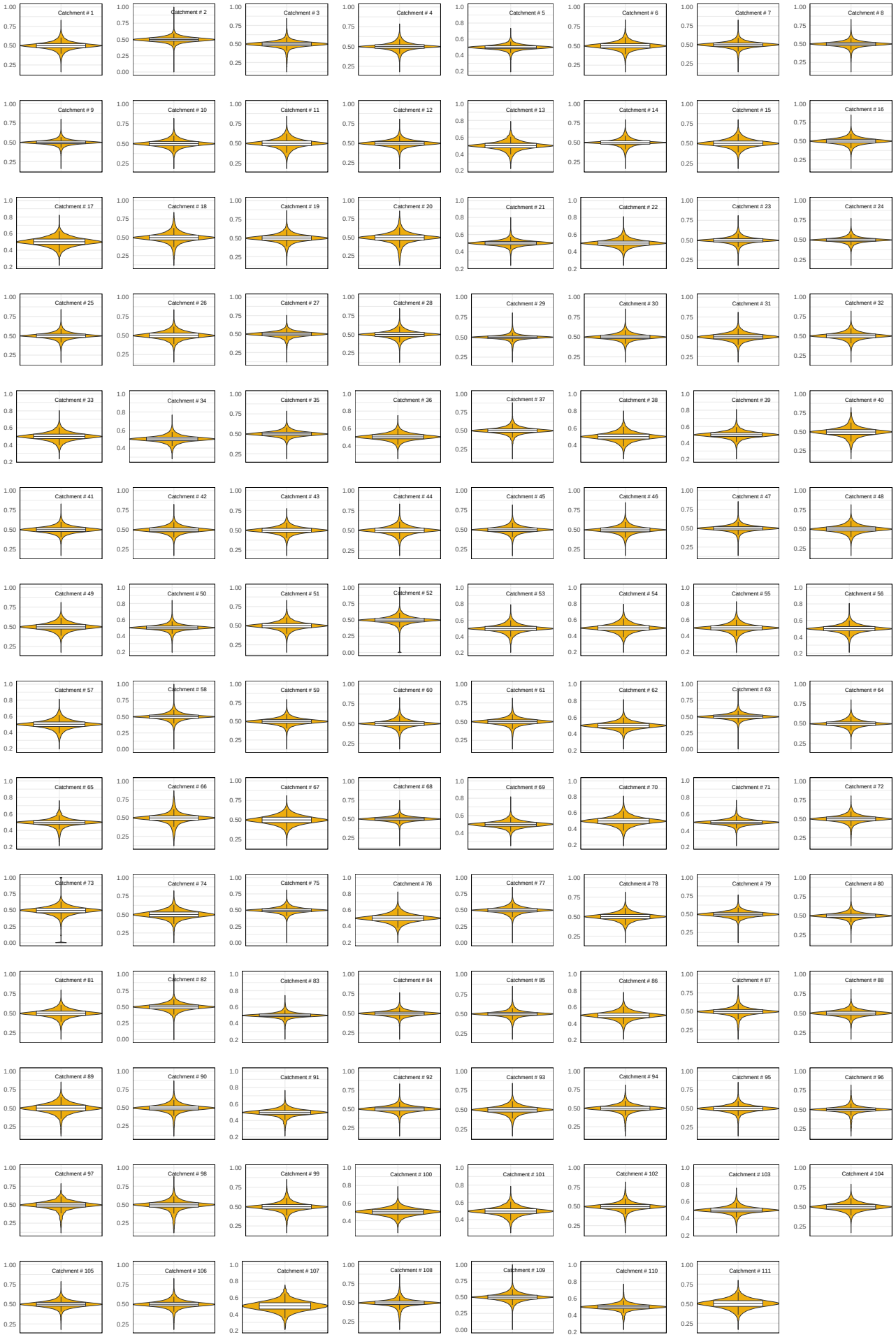

Figure 7.22: Box- and violin plots of Elevation Relief Ratio (ERR) for 111 catchments in the SNP.

Overall, the SPI and TWI follow a multimodal distribution, the STI and TRI a right-skewed distribution and the ERR a normal symmetrical distribution. Certain catchment areas stand out due to their data distribution, nevertheless, the plots do not sufficiently allow us to distinguish between strongly differing catchment areas.

7.2.2 Principal Component Analysis (PCA)

Figure 7.23 shows the summary of the conducted PCA. Each component explains a percentage of the total variance in the data set. The Proportion of Variance section shows that component 1 explains 40.8% of the total variance in the dataset while component 2 explains 26.5% of the total variance. Figure 7.24 shows a screeplot that visualizes the contribution to the variances of all dimensions. The Cumulative Proportion section in Figure 7.23 therefore summarizes that the first two components together explain 67.3% of the total variance of the data. There is no accepted objective way to decide how many principal components are enough to represent the data accurately (Peres-Neto et al., 2005). In this case, a large part of the variance of the data is explained by the first two dimensions. The analysis will continue in a qualitative way, which is why it was decided that the first two principal components accurately represent the data.

```
Importance of components:
                          Comp.1    Comp.2    Comp.3     Comp.4     Comp.5     Comp.6     Comp.7      Comp.8
Standard deviation     1.7990988 1.4504794 1.0571085 0.84614625 0.73652484 0.42017160 0.15186629 0.108455694
Proportion of Variance 0.4082727 0.2653771 0.1409547 0.09030903 0.06842505 0.02226864 0.00290913 0.001483696
Cumulative Proportion  0.4082727 0.6736498 0.8146045 0.90491349 0.97333853 0.99560717 0.99851630 1.000000000
```

Figure 7.23: Summary of the PCA analysis conducted in RStudio: standard deviation, proportion of variance and cumulative proportion of all 8 components.

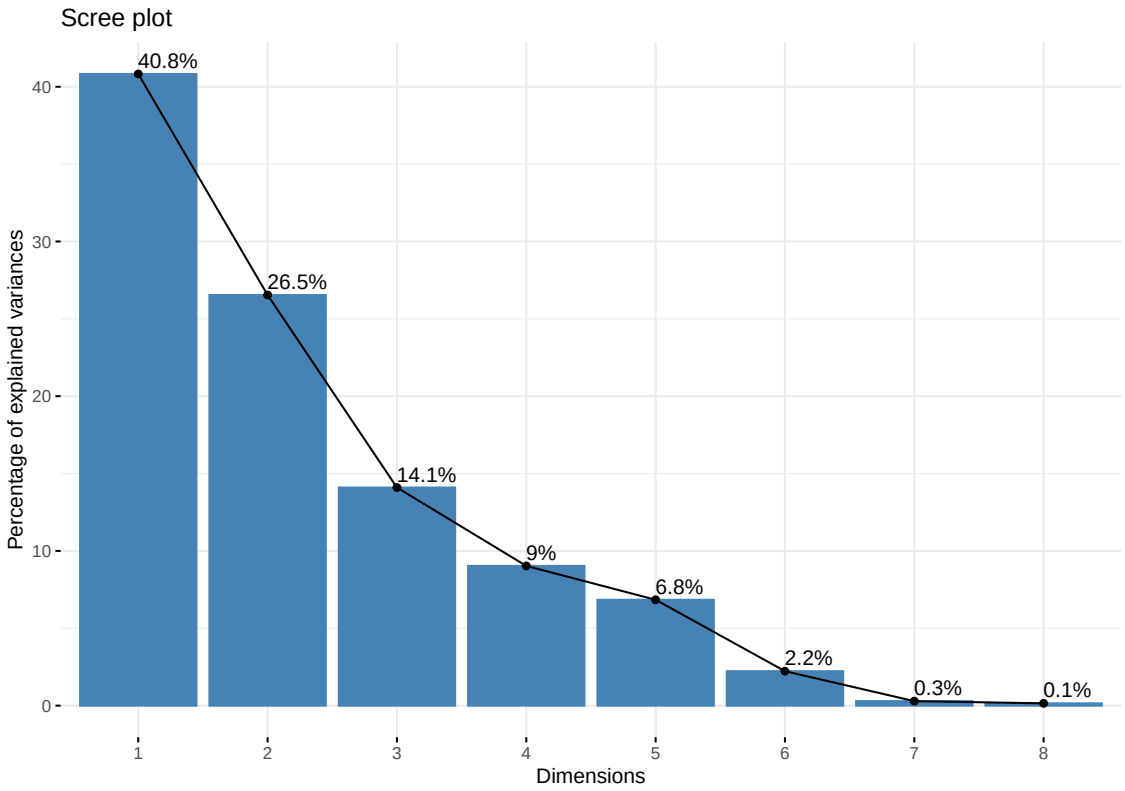

Figure 7.24: Scree plot showing the percentage of explained variances associated with each principal component.

Figure 7.25 displays the loadings of each variable on the principal components (PC or Comp. in the following Figures), which indicate the strength of the relationship between each variable and the components. The first principal component (Comp. 1) shows high positive loadings for the TWI and high negative loadings for the TRI, ERR, slope, and height. Specifically, the high positive loading for TWI suggests a strong positive correlation with PC1. Conversely, the negative loadings for ERR, slope, and height indicate a strong negative correlation with PC1. The first principal component captures significant portions of the variance for the variables TWI, TRI, ERR, and slope, reflecting their contributions to this component. In contrast, the remaining indices, STI and SPI, have stronger contributions to the second principal component (Comp. 2). Thus, the first two principal components collectively account for a substantial portion of the variance in the main indices, suggesting that these two dimensions are sufficient to represent the data effectively.

```
Loadings:
       Comp.1 Comp.2 Comp.3 Comp.4 Comp.5 Comp.6 Comp.7 Comp.8
SPI            0.675                      0.274  0.654  0.194
TWI     0.506  0.150  0.133 -0.286         0.396 -0.169 -0.656
STI            0.671                     -0.118 -0.694  0.202
TRI    -0.493 -0.117 -0.188  0.166         0.805 -0.179
ERR    -0.338        -0.127 -0.883 -0.282
AREA   -0.147         0.826        -0.527
SLOPE  -0.487  0.238 -0.152  0.256 -0.119 -0.308  0.135 -0.700
HEIGHT -0.343         0.471 -0.183  0.788

               Comp.1 Comp.2 Comp.3 Comp.4 Comp.5 Comp.6 Comp.7 Comp.8
SS loadings     1.000  1.000  1.000  1.000  1.000  1.000  1.000  1.000
Proportion Var  0.125  0.125  0.125  0.125  0.125  0.125  0.125  0.125
Cumulative Var  0.125  0.250  0.375  0.500  0.625  0.750  0.875  1.000
```

Figure 7.25: Covariance matrix from PCA loadings. This matrix illustrates the covariances between the original variables and the dimensions after performing the PCA. Small loadings are conventionally not printed (replaced by blank spaces), to draw the eye to the pattern of the larger loadings.

Figure 7.26 represents a biplot created from the PCA. The dimension 1 forms the x axes, the dimension 2 forms the y axes. The vectors represent the original variables. Their directions and lengths indicate the contributions of the original variables to the principal components. The longer the vector, the greater the loading of that vector. Each point in the biplot represents a catchment in the SNP. The points are colored according to whether a debris flow event has occurred in this catchment or not. The labels on the points correspond to the number given to each catchment. Vectors that are grouped are positively correlated to each other. Therefore, STI and SPI are correlated as well as slope, TRI, area, height and ERR together. TWI stands out, pointing in the opposite direction as TRI, meaning it is negatively correlated to TRI. Height, area and ERR are poorly represented compared to the other variables. The catchments are distributed around the zero point quite evenly, with some points slightly further away from the origin. Looking at the counts of catchments with and without debris flow events in each quadrant (small boxes in Figure 7.26) one can also see that the catchments spread quite evenly throughout all the quadrants. Out of 111 catchments in total, there are between 25 and 32 catchments in each of the 4 quadrants. Clear clusters are not explicitly recognizable. In addition, the coloring of the catchments according to events is quite scattered among the whole plot and it is rather difficult to say with which variables a catchment is prone to debris flows. Nevertheless, the positions of the catchments can be used to determine which values of the indices are higher in which catchments. Further, what can be seen, is in which quadrant of the biplot some catchments are rather not prone to debris flow events. This is the case in the lower right quadrant, where the points are positive in the first dimension and negative in the second dimension. This quadrant has the least catchments with observed debris flow events (3/25). The catchments positioned there have low values in all parameters, except the TWI.

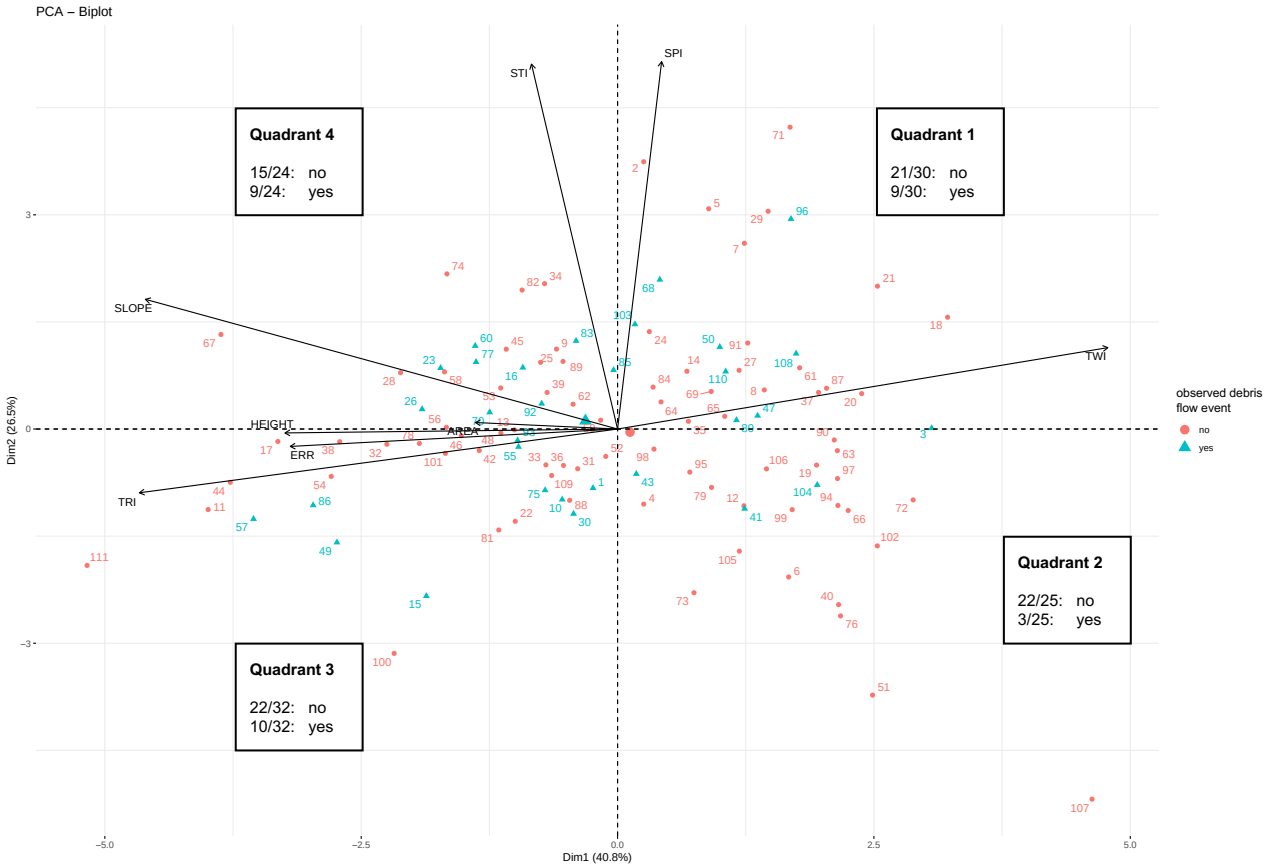

Figure 7.26: PCA Biplot. Each point represents a catchment in the SNP, here in a multidimensional space with the principal components forming the axes (dimension 1 forming the x axes, dimension 2 forming the y axes). The points resp. catchments are colored according to whether a debris flow event has occurred in this catchment or not (blue meaning event occurred, red meaning event did not occur). The labels on the points correspond to the number given to each catchment. The directions and lengths of the vectors indicate the contributions of the original variables to the principal components.

The PCA reveals that the first two dimensions account for 67.3% of the total variance, which covers enough to represent the data accurately. The loadings show that the first component is positively correlated with TWI and negatively with TRI, ERR, slope, and height, while the second component is influenced by STI and SPI. The biplot illustrates that catchments are spread across all quadrants without clear clustering. However, it helps to identify catchments in the lower right quadrant, which have low values in all parameters except TWI and the least observed debris flow events. Therefore, with the method of PCA, it was possible to determine which catchments are rather less prone to debris flows based on the effect of the geomorphological indices.

7.2.3 Synthesis: Combined map of PCA and observed debris flow events

Map 7.27 combines the findings of the PCA and observed debris flow events in a map and illustrates a categorization of the catchment areas based on their geomorphometric characteristics combined with observed debris flow events of catchment areas at the example of the SNP. The bold black border shows the boundary of the SNP. The grey lines separate the catchments from each other. There are 111 catchments in total, which are numbered accordingly. The coloring of the catchments is based on the performed PCA. Figure A on the map shows a simplified form of the biplot resulting from the PCA. The PCA reduced 8 chosen parameters down to 2 PCs, building the y and x axes in the

biplot. The intersection of the zero point of both axes creates four quadrants. Each point in the biplot represents a catchment in the SNP and is positioned in one of the 4 quadrants according to their values in indices resp. PC scores:

Quadrant 1 (positive in Dim. 1 and Dim. 2)

- high values in SPI, STI, TWI
- low values in slope, height, ERR and TRI

Quadrant 2 (positive in Dim. 1 and negative in Dim. 2)

- low values in SPI, STI
- rather high values in TWI
- low values in slope, height, ERR and TRI

Quadrant 3 (negative in Dim. 1 and Dim. 2)

- low values in SPI, STI, TWI
- high values in slope, height, ERR and TRI

Quadrant 4 (negative in Dim. 1 and positive in Dim. 2)

- high values in SPI, STI
- rather low values in TWI
- high values in slope, height, ERR and TRI

Catchments with similar geomorphological properties are therefore localized in the same quadrant and are classified into a class and colored accordingly. The number of observed debris flow events per catchment is shown with a yellow dot. The more debris flows observed, the larger the dot. Catchments without an event are shown without a dot. For visual differentiation, all catchments in which a debris flow event has already been observed are shown with stripes and all catchments that have never recorded one are shown without stripes.

Catchments of the class Q1 are distributed throughout the SNP but tend to be located in the eastern part of the park. They are grouped north of Livigno and the Ofenpass road, but also near Val Trupchun along the park border. Those catchments that show observed debris flow events are mainly grouped around the Munt la Schera and the Ofenpass road.

Class Q3 includes catchments that are grouped in the southwestern part of the SNP along the park border and right next to it in the area between Quattervals and Val Trupchun (especially Val Müschauns). They are also scattered in the Val dal Spöl, in the area of Piz Nair (Buffalora) and the Val Minger. This class contains two out of 3 catchments with the most debris flow events. It should be taken into account that these catchments are located in the Val Minger and Val dal Botsch, both of which are very well-accessible and frequently hiked valleys, which may contribute to a higher number of observations. Additionally, it has to be considered that these areas also tend to be large. The larger an area, the greater the probability of a debris flow event occurring there.

It is visually striking that overall the catchments of class Q4 are very large. However, the number of observed debris flow events differs throughout the catchments. Spatially, the catchments are concentrated in the western part of the SNP, in the areas of Val Cluozza, Val Sassa, Val dal Diavel, Val da l'Acqua and Val Tantermozza. There are also many Q4 class catchments in the Val Trupchun. Catchments with observed events are mainly located in the Val Cluozza and Val Trupchun.

Compared to the other quadrant classes, the Q2 class is characterized by catchment areas with few to no debris flow events. Spatially, they are clustered along the Ofenpass road, along the Spöl and southern of the Munt Chavagl. In comparison to class Q4, catchments of class Q2 are throughout quite small catchment areas. The different classes are spatially not completely separated from each other, but it can be said that the catchments with similar characteristics also cluster spatially.

The catchments in which debris flow events have occurred are clustered spatially in the SNP. The Val Minger, the Ofenpass area, the Val Trupchun and the Val Cluozza are particularly affected. These affected areas cannot be assigned to just one class, as events occur in all classes. Class Q2, however, shows significantly fewer events and concentrates on the Ofenpass road, along the Spöl and south of the Munt Chavagl.

Using the example in the SNP, it was therefore possible to prove that catchments in class Q2, i.e. with low values in SPI, STI, slope, height, ERR and TRI, tend to have a low to no risk of debris flows.

Last, we take another look at the case study of the Buffalora event from the beginning of this thesis. The event at Buffalora stretches across two catchment areas. It originated in catchment number 81 and was mainly deposited in catchment number 99. It was the first debris flow observed at this location, hence only a small yellow dot. Interestingly, catchment number 81, where the debris flow began, belongs to class Q3, which is a class with rather debris flow-promoting properties. However, catchment number 99, where it was deposited, belongs to class Q2, which rather indicates a low debris flow risk. This comparison of the results with a recent event shows how an approximation to the real situation in nature can be made with the applied method in this thesis. It is important to emphasize here that the results are only an approximation to reality and by no means can be used as a prediction tool or risk map for debris flow events. Although the Buffalora event did not originate in catchment number 99, such deposits in the event of this kind also pose a big danger. Therefore, a catchment with class Q2 cannot be considered a safe area per se. Nevertheless, it is striking that this case study showed that the source area belongs to the more dangerous area of class Q3, and the deposition area, with lower debris flow velocities and smaller hazards, belongs to class Q2, with a smaller debris flow risk.

The resulting map of this thesis (Map 7.27) integrates PCA findings with observed debris flow events, categorizing catchments based on their geomorphometric characteristics. Classes Q1, Q3, and Q4 reveal different spatial patterns and debris flow occurrences, with Q2 showing fewer events and generally smaller catchments. Class Q2, characterized by lower values in key indices, tends to have a lower risk of debris flows. The Buffalora event exemplifies this, with the debris flow source area in Q3 (higher risk) and the depositions in Q2 (lower risk). This shows how the PCA method provides valuable insights into debris flow risks, offering an approximation of risk levels across different catchments, even though it is not a definitive predictive tool.

Map 7.27: Catchment areas in the Swiss National Park categorized by geomorphometric attributes and recorded debris flow events

Perimeter
- National border
- Perimeter SNP
- Catchment area
- Artificial lake
- Perimeter depositions debris flow event Buffalora 2022

1-111 Catchment area numbers

Quadrants based on PCA (see figure A)
- Q1
- Q2
- Q3
- Q4

Number of observed debris flow events since 2005
- 0
- 1 - 3
- 4 - 7
- 8 - 10
- 11 - 15
- 16 - 22

Observed debris flow event
- yes
- no

Scuol
Lavin
Susch
Macun
Zernez
S-chanf
Pass dal Fuorn
Lago di Livigno
Parco Nazionale dello Stelvio
E n g i a d i n a B a s s a

0 1 2 km

Figure A

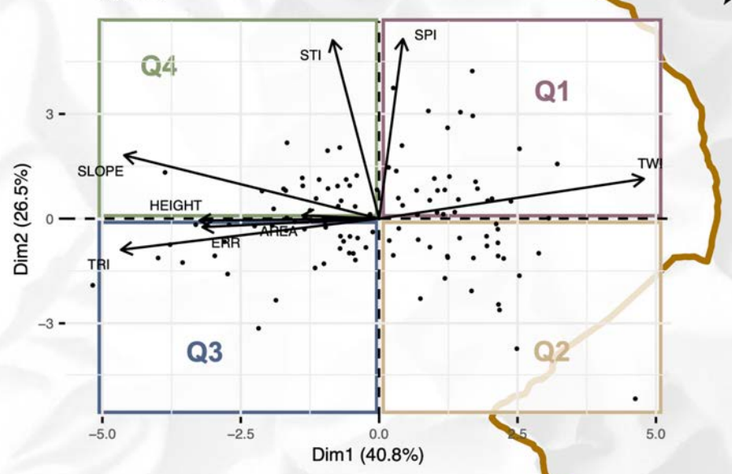

Figure A: Simplified biplot created from a Principal Component Analysis (PCA). PCA is a statistical approach to reduce multidimensional data into its core dimensions, known as Principal Components or Dimensions (PCs or Dim). Here, PCA reduced 8 chosen indices down to 2 PCs, building the y and x axes in this figure. These components are linear combinations of the original variables that capture the maximum variance in the data. The vectors represent the original variables. Their directions and lengths indicate the contributions of the original variables to the principal components. The intersection of the PC axes creates four quadrants. Each point in the biplot represents a catchment in the SNP and is positioned in one of the 4 quadrants according to their values in indices resp. PC scores. Catchments with similar geomorphological properties are therefore localised in the same quadrant. Classes Q1, Q3, and Q4 revealed different spatial patterns and debris flow occurrences, in comparison to Q2, showing fewer events and generally smaller catchments. Therefore, class Q2, characterized by lower values in key indices, is assumed ito nclude catchments with lower risk of debris flows.

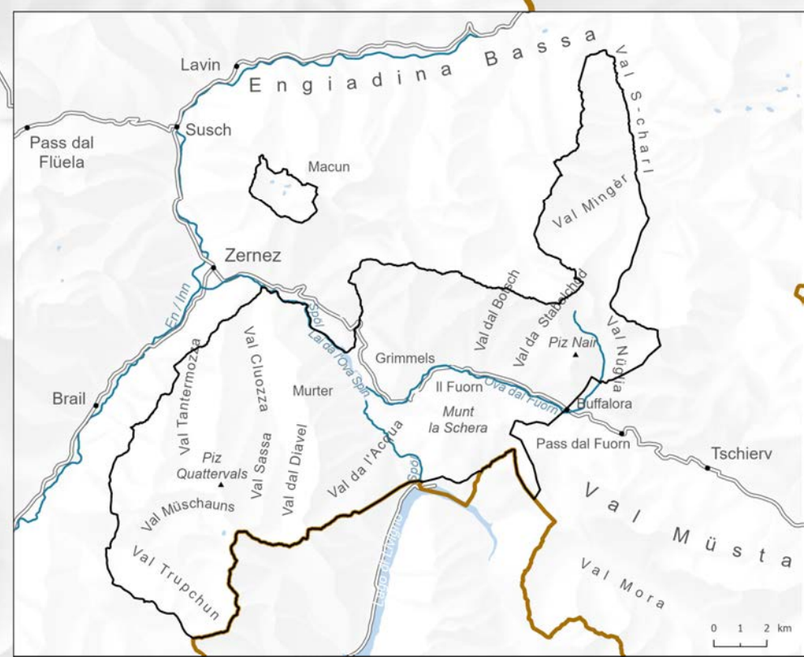

Author: Fabienne Koenig
Purpose: Master Thesis, Department of Geography, UZH
Date: 29.07.2024

8 Discussion

As Oguchi et al. (2011) mention, geomorphometry as a quantitative land-surface analysis has only become common since around the end of the 20th century. It is remarkable what can already be done nowadays, while it is to be expected that the methods, approaches and implementations will continue to develop much further in the near future. As also conducted in this thesis, the majority of geomorphometric analysis is based on only one DEM. On the one hand, this demonstrates that meaningful analyses can be conducted with minimal data input, making it accessible to a wide range of users. On the other hand, the analysis is more prone to errors since it relies entirely on a single data source. If the elevation model is of poor quality or contains inaccuracies, the entire analysis will be flawed.

The reliance on a single DEM for most geomorphometric analyses underscores the importance of data quality and resolution. Finer resolutions in elevation models lead to greater variances in subsequent analysis. This is because higher-resolution DEMs capture more detailed variations in the terrain, which can introduce more variability and complexity into the analysis. In contrast, coarser resolutions may smooth out these variations, potentially leading to less detailed but more stable results. Choosing the right resolution is a very crucial part and plays a central role. There is always a trade-off to be found between recognizing as many details of a region as possible and visualizing a rough pattern. The most fine resolution is not always the best option to choose, as it depends on the purpose of the analysis. Another difficulty poses insider knowledge as data base. It was already mentioned in Chapter *5.4 Observed debris flow events in the SNP* that the counted debris flow events from the SNP are only observed events by park rangers who categorized them as debris flows and therefore do not promise any completeness. It would certainly be worthwhile to collect such data sets consistently and without any gaps, as they provide valuable insights and enable interesting analyses. However, it should also be emphasized that the availability of such data from the SNP is rather rare and only possible because park rangers patrol the park every day, which gives valuable insights. Even when such data are not completely accurate, it is what makes analyses conducted in this thesis possible in the first place. Hence, it is important to be aware of the quality and background source of used data. This is not only the case with insider knowledge-based data, but also with data from official providers. The zoning of the SNP into sub-catchments provided by swisstopo had to be adjusted as described in Chapter *6.3.1 Zonal Units*. This case has shown that data from official providers such as swisstopo, are not always completely reliable. It is crucial to handle the data with caution and to assess their validity and suitability for the intended analysis while acknowledging that the data may not have been acquired for local analysis. The literature often emphasizes the utility of high-resolution DEMs in geomorphometric analyses. My research supports this notion, as the use of high-resolution DEMs was crucial for the accurate calculation of indices and the overall assessment of debris flow risks. However, the incorporation of historical and qualitative data from the SNP into the geomorphometric

analysis represented an innovative step forward, underscoring the value of combining quantitative data with local knowledge for a more robust hazard assessment.

The methodology of this master thesis was guided by own interests and the available resources. The motivation stemmed more from a genuine interest in conducting research within the context of the SNP and exploring geomorphometric analysis techniques. The first approach of a geomorphometric analysis of a debris flow in the SNP therefore leaned more towards an intrinsic and explorative approach. The focus lay on utilizing available resources and existing knowledge, as the SNP provided data about a debris flow event in 2022 and the literature supposed various geomorphometric methods as the calculation of indices. By exploring the data and methods, flexibility could have been allowed to let the research process guide its way. Retrospectively, the subsequent procedure made sense: First, the smaller test area (Buffalora) was set into the context of the region, geology and geomorphological process areas to get some background information. The previously researched parameters and indices were then applied to the small study area. That way the indices could first be tested on a small scale and then validated with the background information. When realizing the parameters and indices are accurate and useful, the approach was applied on a larger scale, to see if any patterns throughout the SNP occur. Such hotspots did not come out clearly, which is why somehow the different indices had to be reduced or brought together. That is when PCA was applied, to reduce the dimensions and find clusters within the catchments. With the previously smaller test area Buffalora, the theory of endangered and less endangered catchments could then be validated again in the end.

8.1 Geomorphometric analysis at Buffalora

Before starting to apply the geomorphometric parameters and indices, background information about the historical and temporal landscape change at Buffalora was gathered. It revealed that a sub terrain was formed over 60 years ago, which is or could be decisive for further slope processes in the research area. The period between 1959 and 1973 must have been a geomorphologically active year, as new accumulations of material can be recognized in some places on the aerial photographs from 1973. In years before 1959 and 2019, slope movements appear to have occurred, which contributed to the spatial course of the debris flow at Buffalora. The study area is generally part of a geomorphologically very active region. Steep slopes and dolomite as parent rock (Chapter *4.2.1 Geology*), in combination with heavy precipitation, provide the ideal basis for the passage of slope processes (Chapter *2.1.3 Debris flow*). As already stated in Chapter *4 Study area* the dry climate and dolomitic subsoil do not create favorable living conditions for plant growth in the high altitude areas, which is why succession is generally very slow in the Engadin and vegetation recovers and regrow slowly over a long period.

Applying the primary parameters to the DEM section of Buffalora was the first part of the analysis. It has been shown that they reflect the shape of the course and deposition of the debris flow quite well. The rough terrain can be visualized and it is helpful for a first impression of the terrain. However, they differ in terms of impact and importance. The parameter slope clearly shows where the terrain is flatter and steeper. This emphasizes channels and rock faces. Slope is also used for almost all further indices and is therefore the most important parameter and indispensable. The flow accumulation shows where the water is channeling, allowing a possible course of a debris flow to be determined. The flow accumulation also serves as the basis for most indices and is therefore very relevant. In the case of the Buffalora debris flow, it ran exactly along the shape of the deposits and in

this particular case counted as a valuable parameter. The parameter aspect reveals the orientation of the slopes, which could be relevant from where tributaries converge and are part of the composition of the Roughness Index. The catchment area becomes very important for zoning into sub-catchments. The other primary parameters curvature (plan and profile), relief ratio and ERR were no longer used in the further analysis and were therefore of little importance. The PCA also revealed that ERR did not contribute strongly to the principal components and therefore does not play a major role in the variances of the catchment areas (Chapter *7.2.2 Principal Component Analysis (PCA)*).

As well as the primary parameters, the selected indices represented the course and shape of the debris flow at Buffalora and were useful to visually describe the shape and characteristics of the terrain. According to the state of the art, SPI and TWI are the most widely used indices. In terms of describing a single event, they also seemed to cover most of the course and shape of the Buffalora debris flow event. However, it seemed clear that they were very similar to each other. This was shown visually (Chapter *7.1.3 Secondary parameters: indices*) but also in the Correlation Matrix (Chapter *7.1.4 Correlation matrix*) where they showed the highest correlation in the entire matrix. First, this led to the conclusion that only one of the two should be used for further analysis. However, the PCA showed that the two indices contribute strongly to the first two components, but in different directions and thus cover different variances of the catchments. Therefore, both indices are very relevant despite their similarity. STI was visually very similar to SPI and TWI, and most similar to SPI in the PCA. However, as it uses a slightly different approach to the other two indices, it counts as an important contribution to the analysis. The TRI brought a different aspect of the terrain into the analysis. It was the only index, where aspect besides slope was included. Visually, it stood out from the other 3 indices. The lower part of the Piz Nair massif including the region where the debris flow descended did not appear to be rough, which favors the unimpeded flow and speed of the debris flow and thus also the extent of the event. When calculating indices based on flow accumulation, many negative values appeared, as described in Chapter *6.2.5.1 Preparation of index calculation: Flow Direction Type Model*. It was found to be due to an unfortunate combination of flow direction type D8 and the DEM with very high resolution and many rough surfaces. It did not seem obvious at the beginning that the different flow direction types made such a big difference. Checking this in advance would have saved a lot of additional correction work, however, a lot could also be drawn from this. By replacing the D8 Flow Direction Type with DInf, still negative values occurred, but much less than with D8, which opposed an accurate compromise. As already mentioned before, this case showed that the finest resolution of a DEM is not always an advantage. The 4 chosen indices (SPI, TWI, STI, TRI) were selected due to the prerequisites for the formation of debris flows: the presence of loose material, water, sufficiently large slope and high flow velocities (Chapter *6.2 Geomorphometric analysis on small scale: Buffalora*). It seemed to be a good approach to cover the basic requirements for a debris flow, but of course, it is far from complete. As described in Chapter *2.1.3 Debris flow*, the inclusion of further properties could add valuable aspects: basin morphology, surficial geology, hydrologic, geomorphometric and geotechnical features of slope, source material and availability of sediment.

The integration of geomorphometric indices into debris flow risk assessment has been extensively documented in the literature. For instance, Otto et al. (2017) and Chen et al. (2011) demonstrated the relevance of indices like the SPI and the TWI across various geographical settings. This thesis affirmed these findings, where indices such as SPI and TWI have proven effective for delineating areas prone to debris flows. Nevertheless, this thesis also identifies limitations of certain indices frequently

cited in the literature. The study of Chen et al. (2011) found that debris flows are likely in basins with higher TWI. However, in this study, high TWI values were observed in quadrant 2 in the Biplot of the PCA, which comprises catchments with fewer debris flow events than in other quadrants. This discrepancy suggests that while TWI may be effective in other contexts, its applicability in high-altitude, rugged terrains like the SNP is limited. This finding suggests that TWI's effectiveness may be context-specific, reducing its applicability to regions where moisture and wetness are more directly linked to debris flow risks.

Recent advancements in geomorphometric analysis, as highlighted by Ilinca (2021) and Grelle et al. (2019), have expanded the range of parameters and indices used in assessing debris flow risks. This thesis incorporated, to use not only the most popular indices in literature as SPI and TWI, but also include roughness and sediment transport. By integrating TRI and STI, this research builds on the foundational insights of França da Silva et al. (2019) and Tilahun et al. (2023), who emphasized the importance of using complex indices to better capture the diverse factors influencing geomorphological hazards.

The HDM gives insight within the perimeter of the debris flow deposits that primary parameters and indices could not give. It is a valuable addition to describe and recognize the dimensions of a debris flow. However, caution is required in terms of the elevation models. Lidar data and drone data were used for the HDM of the Buffalora debris flow. Compared to lidar data, drone data underestimates the ground in places where the trees have remained dense, which is why in the case of this work the regions outside the debris flow deposits appeared strongly negative. Since we were only interested in the areas within the perimeter of the deposits where in most places not many trees are left, the HDM was still useful. Depending on the process being investigated, it is therefore important that the two elevation models used to create an HDM originate from the same data source so that accurate elevation differences can be calculated. The HDM was not used for further analysis. However, it could be used to validate the parameters and assess their accuracy. The erosion channels, for example, were already visible in the historical analysis, as well as in the parameter slope and the TRI. The HDM assured these observations. This shows how the combination of different variables and parameters interact to contribute to an analysis in different ways.

The volume calculation turned out to be smaller than initially thought, based on the aerial imagery. As the event analysis of the Buffalora debris flow by Herzog Ingenieure (engineering office in hydraulic engineering) in December 2022 already documented, the debris flow indicated a lot of water and low viscosity, with a large proportion of gravel and sand, but rather few coarse components (Herzog Ingenieure AG, 2022). There are still few trees in the center of the deposits, which also indicates a rather fluid regime. This may also be the reason why the volume based on the elevation model calculations turned out to be rather low, because the water drained and is not considered in an elevation model although it contributes substantially to the distribution and deposition. As for the HDM, the volume was calculated based on two elevation models with different databases. To calculate an accurate volume with fewer uncertainties, pre- and post-DEMs based on lidar would certainly be the most suitable.

8.2 Geomorphometric analysis within SNP

To apply the indices tested on a small scale to a larger scale, the SNP was divided into its catchment areas. In retrospect, it can be said that the catchment areas appear to be a useful division for analyzing debris flows in the SNP in more detail: reasonable size of zoning, limiting the event area for debris flows and the data were already available, although they had to be adapted first. It appeared that the Buffalora event extends over two catchment areas and not within one, which is usually the case. This shows that the landscape has been shaped over decades by countless events in such a way that data sets such as the sub-catchments may have to be recalculated from time to time.

PCA as a standardized and proven method of visualizing and analyzing data proved to be simple and suitable. Of course, much more and a completely different selection of variables could be included in the analysis, which would certainly have a major influence on the result. Nevertheless, the selection of variables for the PCA was a good first approach to analyzing different catchment areas in terms of debris flow hazards. The initial expectation was that clustered catchments would show up directly in the biplot and that similar catchments could be grouped that way. However, when this was not the case, it was decided to use the quadrants of the biplot as classification. The results of the PCA could not predict catchments that are at risk of debris flow hazards. However, it was possible to highlight which catchments are rather not at risk and that these also differ spatially from the others. This also means that the indices as a database are meaningful and suitable for such an analysis. It also shows that one index on its own is not sufficient to make a statement about their classification in geomorphological properties, and certainly not in terms of debris flow risk, e.g., not all catchments with low SPI and TWI are at risk of debris flow. This is shown by quadrant 3 in the PCA biplot (Figure *7.26*). It takes a combination of indices to make a meaningful analysis. Additionally, other characteristics should also be taken into account, such as the local geology or forest cover, which can be of significance for the occurrence of a debris flow.

The analysis was carried out using the SNP as study area. As described in Chapter *4 Study area*, the SNP is located within the mountains and highlands with an overall similar subsoil and terrain. The study area is not composed of very different terrain such as lowlands and highlands or mountains and wetlands. The differentiation of the catchment areas in the final map may therefore be more clear in another area with more varied terrain.

Representing the terrain in the form of elevation models and the parameters and indices derived from them is an abstraction. Including all the necessary variables to imitate nature in its full complexity is almost impossible. It is therefore important to emphasize that the whole analysis is only an approximation of reality. Nevertheless, it has been possible to approximate reality and draw conclusions concerning debris flow hazard risk from a geomorphometric perspective at the example of the SNP.

8.3 Research Questions

With this background in mind, the research questions posed at the beginning of this thesis are now being answered:

Which geomorphometric parameters and indices can be used to show conditions and process interrelationships of a single debris flow event (in the example of Buffalora)?

The research question is answered using the case study of the debris flow event at Buffalora in the Swiss National Park. This thesis showed that a DEM with a resolution of 5 meters proved to be suitable for the application of geomorphometric parameters and indices at this scale. The primary parameters slope, aspect and flow accumulation form the basis. On the one hand, they provide information about the terrain of a debris flow event itself; on the other hand, they are the mandatory basis for further indices. Based on this, the indices SPI, TWI, STI and TRI were calculated, which have proven to show the conditions of a debris flow terrain in different ways. SPI, TWI and STI are visually very similar, but were all able to show the exact course of the debris flow as it happened. In addition to the more hydrological aspect of the other indices, TRI provided a different aspect of terrain, namely where the debris flow can flow more unhindered and where not.

How can geomorphometric indices be applied on a larger scale to describe areas at risk of debris flow hazards (in the example of the SNP)?

Those parameters and indices that have proven themselves on a small scale (see answer to research question 1) form the basis for their application on a larger scale to describe areas at risk of debris flow hazards. To answer this research question, the parameters and indices were expanded from the case study of Buffalora to the whole SNP. It turned out to be adequate to use the same elevation model with a resolution of 5 m and apply the same formulae for calculating the indices on a smaller scale. To evaluate the values in geomorphometric indices, catchment areas proved to be very suitable as units for debris flow event zones. Applying a Principal Component Analysis was very helpful in reducing the many parameters and indices to fewer dimensions and obtaining a better overview. Classes could then be derived from the biplot of the PCA, which results from the intersection points of the x and y axes at the zero point. These 4 classes summarise similar properties in geomorphometric parameters and indices of the individual catchment areas. In this way, similar catchment areas can be identified. Combined with the information in which catchment areas debris flows have already been recorded, a class of the biplot could be determined in which the fewest debris flows have occurred and thus stand out from the others. With this approach, it is therefore not possible to predict catchment areas that are highly susceptible to debris flow hazard but to identify those that have a rather low risk of debris flow hazard. The catchment areas of the other classes, which tend to predict a higher risk, tend to highlight only those catchments in which a debris flow occurs but not necessarily the deposits whose mass and force are just as dangerous. The applied methodology also demonstrated that individual parameters and indices are not sufficient to make an all-encompassing statement on debris flow hazard. A combination of them is always necessary.

9 Conclusion and further work

This thesis has highlighted the value of geomorphometric indices and parameters in assessing debris flow hazards. Each variable impacts the assessment differently, so integrating multiple parameters and indices is recommended for a profound analysis. The use of PCA has proven effective in simplifying and categorizing a large number of parameters and indices. The case study in the SNP demonstrated that PCA could classify catchments based on their geomorphological properties by dividing the biplot into quadrants. This method successfully identified catchments less susceptible to debris flows, showcasing its potential in categorization. Although distinguishing highly susceptible catchments was not possible, and thus the results can not be relied upon as a prevention tool, the findings offer an encouraging approach for application in other case studies.

This analysis was conducted only on parameters and indices based on elevation models. Future studies could benefit significantly from incorporating a wider range of geomorphometric indices to capture even more aspects of terrain dynamics. Variables such as the proportion of forest per catchment area, or indices that account for vegetation cover, land use changes, and soil moisture play a decisive role in preventing the further expansion of debris flow events, and would certainly enhance the comprehensiveness of the analysis. While this thesis focused on the SNP, applying these methodologies to different geographical regions with varying topographical conditions would offer a broader validation of the methodology and findings. This approach would ensure that the developed models and indices are versatile and applicable in various contexts, enhancing their practical utility. Conducting long-term studies that monitor debris flow activities could help validate the indices used in this thesis. Such studies would provide valuable insights into the temporal stability of these indices and their predictive capabilities under different environmental conditions. This is particularly relevant considering the dynamic nature of geomorphometric datasets, as demonstrated by the example of the debris flow at Buffalora, which traverses two catchment areas and therefore requires adjustments to the datasets from time to time. The application of PCA in this thesis demonstrated its potential in approaching debris flow risk assessment. By utilizing PCA and other statistical tools, researchers can simplify complex datasets into more manageable and insightful components, improving the accuracy and utility of debris flow predictions. In connection with ongoing research in the SNP about monitoring the impact of debris flows on biodiversity in the Buffalora area, this master's thesis provides a valuable foundation for further exploration. By understanding how debris flows interact with terrain features and affect the landscape, this work may help prioritize areas for biodiversity monitoring and conservation efforts. By pursuing these research directions, the field of geomorphometric analysis can continue to advance, providing deeper insights and more robust tools for managing and mitigating debris flow hazards in diverse environments.

Bibliography

Ahmad, Imran et al. (July 2019). "Application of hydrological indices for erosion hazard mapping using Spatial Analyst tool". In: *Environmental Monitoring and Assessment* 191. DOI: 10.1007/s10661-019-7614-x.

Barsch, Dietrich and Nel Caine (Nov. 1984). "The Nature of Mountain Geomorphology". In: *Mountain Research and Development* 4.4, p. 287. DOI: 10.2307/3673231. (Visited on 05/29/2024).

Beven, K. J. and M. J. Kirkby (Mar. 1979). "A physically based, variable contributing area model of basin hydrology / Un modèle à base physique de zone d'appel variable de l'hydrologie du bassin versant". In: *Hydrological Sciences Bulletin* 24.1, pp. 43–69. DOI: 10.1080/02626667909491834. (Visited on 11/24/2023).

Borga, Marco et al. (Oct. 2014). "Hydrogeomorphic response to extreme rainfall in headwater systems: Flash floods and debris flows". en. In: *Journal of Hydrology* 518, pp. 194–205. DOI: 10.1016/j.jhydrol.2014.05.022. (Visited on 12/08/2023).

Bovis, Michael J. and Matthias Jakob (1999). "The role of debris supply conditions in predicting debris flow activity". en. In: *Earth Surface Processes and Landforms* 24.11, pp. 1039–1054. DOI: 10.1002/(SICI)1096-9837(199910)24:11<1039::AID-ESP29>3.0.CO;2-U. (Visited on 01/25/2024).

Bundesamt für Meteorologie und Klimatologie Meteoschweiz (2014a). "Das Klima im SNP - Viel Sonne, wenig Niederschlag, extreme Temperaturen". de. In: *Atlas des Schweizerischen Nationalparks. Die ersten 100 Jahre.* Bern: Haupt-Verlag, pp. 22–25. (Visited on 12/20/2023).

— (2014b). "Die Klimaentwicklung im SNP Von den frühen Messungen bis zum Jahr 2099". de. In: *Atlas des Schweizerischen Nationalparks. Die ersten 100 Jahre.* Bern, pp. 214–217. ISBN: 978-3-258-07902-8.

Buttrick, Steve et al. (Feb. 2015). *Conserving Nature's Stage: Identifying Resilient Terrestrial Landscapes in the Pacific Northwest.* Portland: OR: The Nature Conservancy.

Chen, Chien-Yuan and Fan-Chieh Yu (June 2011). "Morphometric analysis of debris flows and their source areas using GIS". In: *Geomorphology* 129, pp. 387–397. DOI: 10.1016/j.geomorph.2011.03.002.

Corominas, Jordi (May 1996). "The angle of reach as a mobility index for small and large landslides". In: *Canadian Geotechnical Journal* 33.2. Publisher: NRC Research Press, pp. 260–271. ISSN: 0008-3674. DOI: 10.1139/t96-005.

Dikau, Richard, Denys Brunsden, et al. (Sept. 1996). *Landslide Recognition: Identification, Movement and Causes.* Englisch. Chichester: John Wiley & Sons Inc. ISBN: 978-0-471-96477-3.

Dikau, Richard, Katharina Eibisch, et al. (2019). "Geomorphologische Systeme und Prozesse". de. In: *Geomorphologie.* Ed. by Richard Dikau et al. Berlin, Heidelberg: Springer, pp. 33–60. ISBN: 978-3-662-59402-5. DOI: 10.1007/978-3-662-59402-5_3.

esri (July 2024). *Flow Accumulation (Spatial Analyst)*. URL: https://pro.arcgis.com/en/pro-app/latest/tool-reference/spatial-analyst/flow-accumulation.htm (visited on 07/29/2024).

Flint, J.J. (1974). "Stream gradient as a function of order, magnitude, and discharge". English. In: *Water Resources Research* 10.5, pp. 969–973. ISSN: 0043-1397. DOI: 10.1029/WR010i005p00969.

França da Silva, Julio, Leonardo Santos, and Chisato Oka-Fiori (June 2019). "Spatial correlation analysis between topographic parameters for defining the geomorphometric diversity index: application in the environmental protection area of the Serra da Esperança (state of Paraná, Brazil)". In: *Environmental Earth Sciences* 78, p. 356. DOI: 10.1007/s12665-019-8357-2.

Furrer, Heinz et al. (2014). "Geologie und Erdgeschichte Lithologisches und zeitliches Fundament des SNP". de. In: *Atlas des Schweizerischen Nationalparks. Die ersten 100 Jahre.* Bern: Haupt-Verlag, pp. 16–17.

Gallant, John C. and John P. Wilson (Aug. 1996). "TAPES-G: A grid-based terrain analysis program for the environmental sciences". In: *Computers & Geosciences* 22.7, pp. 713–722. ISSN: 0098-3004. DOI: 10.1016/0098-3004(96)00002-7.

Greenacre, Michael et al. (Dec. 2022). "Principal component analysis". In: *Nature Reviews Methods Primers* 2, p. 100. DOI: 10.1038/s43586-022-00184-w.

Gregoretti, Carlo and Giancarlo Dalla Fontana (June 2008). "The triggering of debris flow due to channel-bed failure in some alpine headwater basins of the Dolomites: Analyses of critical runoff". In: *Hydrological Processes* 22, pp. 2248–2263. DOI: 10.1002/hyp.6821.

Grelle, Gerardo et al. (Apr. 2019). "Assessment of Debris-Flow Erosion and Deposit Areas by Morphometric Analysis and a GIS-Based Simplified Procedure: A Case Study of Paupisi in the Southern Apennines". en. In: *Sustainability* 11.8, p. 2382. ISSN: 2071-1050. DOI: 10.3390/su11082382.

Grohmann, Carlos, Mike Smith, and Claudio Riccomini (May 2011). "Multiscale Analysis of Topographic Surface Roughness in the Midland Valley, Scotland". In: *Geoscience and Remote Sensing, IEEE Transactions on* 49, pp. 1200–1213. DOI: 10.1109/TGRS.2010.2053546.

Gruber, S. and S. Peckham (2008). "Land-Surface Parameters and Objects in Hydrology". en-GB. In: *Hengl, T. and Reuter, H.I. (Eds), Geomorphometry: Concepts, Software, Applications. Developments in Soil Science*. Vol. 33. Section: Book, pp. 1–28.

Guth, Peter L. et al. (Jan. 2021). "Digital Elevation Models: Terminology and Definitions". en. In: *Remote Sensing* 13.18. Number: 18 Publisher: Multidisciplinary Digital Publishing Institute, p. 3581. ISSN: 2072-4292. DOI: 10.3390/rs13183581.

Harvey, Adrian M. (Feb. 2007). "Geomorphic instability and change–Introduction: Implications of temporal and spatial scales". In: *Geomorphology*. Geomorphic Instability and Change - Introduction:Implications of temporal and spatial scales 84.3, pp. 153–158. ISSN: 0169-555X. DOI: 10.1016/j.geomorph.2006.03.008.

Herzog Ingenieure AG (Dec. 2022). *Gewitter im Raum Buffalora am 25.07.2022 - Ereignisanalyse*. Deutsch. Ereignisanalyse. Graubünden: Amt für Wald und Naturgefahren, purchase only upon inquiry, requested via Swiss National Park.

Hobson, R. D. (1972). "Surface roughness in topography: quantitative approach". en. In: ed. by Richard J. Chorley. London: Methuen, pp. 221–245.

Horn, B.K.P. (Jan. 1981). "Hill shading and the reflectance map". In: *Proceedings of the IEEE* 69.1. Conference Name: Proceedings of the IEEE, pp. 14–47. ISSN: 1558-2256. DOI: 10.1109/PROC.1981.11918.

Hungr, Oldrich, Serge Leroueil, and Luciano Picarelli (Apr. 2014). "The Varnes classification of landslide types, an update". en. In: *Landslides* 11.2, pp. 167–194. ISSN: 1612-510X, 1612-5118. DOI: 10.1007/s10346-013-0436-y.

Ilinca, Viorel (Feb. 2021). "Using morphometrics to distinguish between debris flow, debris flood and flood (Southern Carpathians, Romania)". In: *CATENA* 197, p. 104982. ISSN: 0341-8162. DOI: 10.1016/j.catena.2020.104982.

IUCN (2024). *IUCN Green List Swiss National Park*. en-US. URL: https://iucngreenlist.org/sites/swiss-national-park/ (visited on 07/17/2024).

Jackson, Lionel, Ray Kostaschuk, and Glen MacDonald (1987). "geological Society of America - Reviews in Engineering Geology". In: *Identification of debris flow hazard on alluvial fans in the Canadian Rocky Mountains*. Vol. VII. DOI: 10.13140/2.1.2321.1206.

Kanton Graubünden (2024). *Geoportal der kantonalen Verwaltung Graubünden*. Geoportal. URL: https://edit.geo.gr.ch (visited on 06/03/2024).

Kuckartz, Udo et al. (Sept. 2013). *Statistik: Eine verständliche Einführung*. Deutsch. 2., überarb. Aufl. 2013 Edition. Wiesbaden: VS Verlag für Sozialwissenschaften. ISBN: 978-3-531-19889-7.

Laube, Patrick et al. (2014). "Rothirsche in der Val Foraz Komplexe Karten machen Veränderungen sichtbar". de. In: *Atlas des Schweizerischen Nationalparks. Die ersten 100 Jahre.* Bern: Haupt-Verlag, pp. 154–155.

Lehmann, Johann George (1816). *Die Lehre der Situation-Zeichnung, oder Anweisung zum richtigen Erkennen u. genauen Abbilden der Erd-Oberfläche in topographischen Charten u. Situation-Planen*. 2nd ed. OCLC: 637302005. Dresden: Arnoldi.

Lozza, Hans (2014). "Unberührte Natur als Attraktion Besucherströme zum SNP". de. In: *Atlas des Schweizerischen Nationalparks. Die ersten 100 Jahre.* Bern: Haupt-Verlag, pp. 162–163.

Mani, Peter et al. (Sept. 2023). "Geomorphic Process Chains in High-Mountain Regions—A Review and Classification Approach for Natural Hazards Assessment". In: *Reviews of Geophysics* 61. DOI: 10.1029/2022RG000791.

Marchi, Lorenzo and Giancarlo Dalla Fontana (Jan. 2005). "GIS morphometric indicators for the analysis of sediment dynamics in mountain basins". In: *Environmental Geology* 48, pp. 218–228. DOI: 10.1007/s00254-005-1292-4.

Marthews, T. R. et al. (Jan. 2015). "High-resolution global topographic index values for use in large-scale hydrological modelling". English. In: *Hydrology and Earth System Sciences* 19.1. Publisher: Copernicus GmbH, pp. 91–104. ISSN: 1027-5606. DOI: 10.5194/hess-19-91-2015. URL: https://hess.copernicus.org/articles/19/91/2015/hess-19-91-2015.html (visited on 11/24/2023).

McArdell, Brian, Jacob Hirschberg, et al. (2023). *Illgraben debris-flow characteristics 2019 - 2022 - WSL*. en. csv dataset. URL: https://www.envidat.ch/dataset/illgraben-debris-flow-characteristics-2019-2022 (visited on 04/18/2024).

McArdell, Brian W. and Mario Sartori (2021). "The Illgraben Torrent System". en. In: *Landscapes and Landforms of Switzerland*. Ed. by Emmanuel Reynard. Cham: Springer International Publishing, pp. 367–378. ISBN: 978-3-030-43203-4. DOI: 10.1007/978-3-030-43203-4_25.

Meng, Zhe et al. (Jan. 2023). "Effects of frequent debris flows on barrier lake formation, sedimentation and vegetation disturbance, Palongzangbo River, Tibetan Plateau". en. In: *CATENA* 220, p. 106697. ISSN: 03418162. DOI: 10.1016/j.catena.2022.106697.

MeteoSchweiz (2022). *Klimabulletin Juli 2022*. de. Tech. rep. Zürich, p. 15. URL: https://www.meteoschweiz.admin.ch/wetter/wetter-und-klima-von-a-bis-z/wetterarchiv-der-schweiz.html (visited on 12/21/2023).

Minh, Nguyen Quang et al. (Feb. 2024). "Impacts of Resampling and Downscaling Digital Elevation Model and Its Morphometric Factors: A Comparison of Hopfield Neural Network, Bilinear, Bicubic, and Kriging Interpolations". en. In: *Remote Sensing* 16.5, p. 819. ISSN: 2072-4292. DOI: 10.3390/rs16050819.

Moore, I. D. and G. J. Burch (1986). "Sediment Transport Capacity of Sheet and Rill Flow: Application of Unit Stream Power Theory". en. In: *Water Resources Research* 22.8, pp. 1350–1360. ISSN: 1944-7973. DOI: 10.1029/WR022i008p01350.

Moore, I. D., R. B. Grayson, and A. R. Ladson (1991). "Digital terrain modelling: A review of hydrological, geomorphological, and biological applications". en. In: *Hydrological Processes* 5.1, pp. 3–30. ISSN: 1099-1085. DOI: 10.1002/hyp.3360050103.

Oguchi, T. and Thad Wasklewicz (Jan. 2011). "Geographic information systems in geomorphology". In: *The SAGE Handbook of Geomorphology*, pp. 227–245. DOI: 10.4135/9781446201053.n13.

Olaya, V. (Jan. 2009). "Basic Land-Surface Parameters". In: *Developments in Soil Science*. Ed. by Tomislav Hengl and Hannes I. Reuter. Vol. 33. Geomorphometry. Elsevier, pp. 141–169. DOI: 10.1016/S0166-2481(08)00006-8.

Ortega, Rengifo (June 2012). "Modelling potential debris flows from SRTM data in the upper Chama river watershed, northwestern Venezuela". In: *Revista Geografica Venezolana* 53, pp. 93–108.

Otto, Jan-Christoph et al. (Dec. 2017). "GIS Applications in Geomorphology". In: *Reference Module in Earth Systems and Environmental Sciences*. Journal Abbreviation: Reference Module in Earth Systems and Environmental Sciences. ISBN: 978-0-12-409548-9. DOI: 10.1016/B978-0-12-409548-9.10029-6.

Patton, PC (1988). "Drainage basin morphometry and floods." In: *Baker VR, Kochel RC, Patton PC (eds) Flood geomorphology.* Wiley, New York, pp. 51–65.

Peres-Neto, Pedro, Donald Jackson, and Keith Somers (June 2005). "How Many Principal Components? Stopping Rules for Determining the Number of Non-Trivial Axes Revisited". In: *Computational Statistics & Data Analysis* 49, pp. 974–997. DOI: 10.1016/j.csda.2004.06.015.

Pike, R.J., I.S. Evans, and T. Hengl (2008). "Geomorphometry: A Brief Guide". In: *Hengl, T. and Reuter, H.I. (Eds), Geomorphometry: Concepts, Software, Applications. Developments in Soil Science*. Vol. 33. Section: Book, pp. 1–28.

Pike, R.J. and Stephen E Wilson (Apr. 1971). "Elevation-Relief Ratio, Hypsometric Integral, and Geomorphic Area-Altitude Analysis". In: *GSA Bulletin* 82.4, pp. 1079–1084. ISSN: 0016-7606. DOI: 10.1130/0016-7606(1971)82[1079:ERHIAG]2.0.CO;2.

PIX4D Documentation (2024). *Ground sampling distance (GSD) in photogrammetry*. en. URL: https://support.pix4d.com/hc/en-us/articles/202559809 (visited on 07/23/2024).

Rey, Peter et al. (2002). "Der Spöl - Lebensraum und Energielieferant". In: *Cratschla 2/02: Luftgeschichten* -.2, pp. 20–23. (Visited on 07/23/2024).

Rickenmann, Dieter (Jan. 1999). "Empirical Relationships for Debris Flows". en. In: *Natural Hazards* 19.1, pp. 47–77. ISSN: 1573-0840. DOI: 10.1023/A:1008064220727.

Rist, Armin et al. (2014). "Langsam, aber stetig Die Solifluktionsloben am Munt Chavagl". de. In: *Atlas des Schweizerischen Nationalparks. Die ersten 100 Jahre.* Bern: Haupt-Verlag, pp. 208–209. ISBN: 978-3-258-07902-8.

Röber, S. and R. Schmidt (2014). "Erosion - Transport - Ablagerung - Eine Landschaft wird geformt". de. In: *Atlas des Schweizerischen Nationalparks. Die ersten 100 Jahre.* Bern: Haupt-Verlag, pp. 34–35. ISBN: 978-3-258-07902-8.

Sappington, J. Mark, Kathleen M. Longshore, and Daniel B. Thompson (2007). "Quantifying Landscape Ruggedness for Animal Habitat Analysis: A Case Study Using Bighorn Sheep in the Mojave Desert". en. In: *The Journal of Wildlife Management* 71.5, pp. 1419–1426. ISSN: 1937-2817. DOI: 10.2193/2005-723.

Schumm, S.A. (1979). "The fluvial system". en. In: *Earth Surface Processes* 4.1, p. 338. ISSN: 1931-8065. DOI: 10.1002/esp.3290040121.

Sevgen et al. (Sept. 2019). "A Novel Performance Assessment Approach Using Photogrammetric Techniques for Landslide Susceptibility Mapping with Logistic Regression, ANN and Random Forest". In: *Sensors* 19, p. 3940. DOI: 10.3390/s19183940.

Singh, Ajay Pratap, Ajay Arya, and Dhruv Singh (Feb. 2020). "Morphometric Analysis of Ghaghara River Basin, India, Using SRTM Data and GIS". In: *Journal of the Geological Society of India* 95, pp. 169–178. DOI: 10.1007/s12594-020-1406-3.

Smith, Michael John De, Michael F. Goodchild, and Paul Longley (2007). *Geospatial Analysis: A Comprehensive Guide to Principles, Techniques and Software Tools*. en. Troubador Publishing Ltd. ISBN: 978-1-905886-60-9.

SNP (May 2022). *Buffalora Murgang Ortophoto*. Schweizerischer Nationalpark (SNP), Samuel Wiesmann, Zernez.

— (2024). *Der Schweizerische Nationalpark im Engadin*. en. URL: https://www.nationalpark.ch/de/ (visited on 12/19/2023).

Speight, J. (Apr. 1980). "The role of topography in controlling throughflow generation: A discussion". In: *Earth Surface Processes* 5, pp. 187–191. DOI: 10.1002/esp.3760050209.

Staley, Dennis M., Thad A. Wasklewicz, and Jacek S. Blaszczynski (Mar. 2006). "Surficial patterns of debris flow deposition on alluvial fans in Death Valley, CA using airborne laser swath mapping data". In: *Geomorphology* 74, pp. 152–163. ISSN: 0169-555X. DOI: 10.1016/j.geomorph.2005.07.014.

Stäubli, Anina et al. (2018). "Analysis of Weather- and Climate-Related Disasters in Mountain Regions Using Different Disaster Databases". en. In: *Climate Change, Extreme Events and Disaster Risk Reduction*. Ed. by Suraj Mal, R.B. Singh, and Christian Huggel. Cham: Springer International Publishing, pp. 17–41.

Stoffel, Markus et al. (Jan. 2014). "Possible impacts of climate change on debris-flow activity in the Swiss Alps". en. In: *Climatic Change* 122.1-2, pp. 141–155. ISSN: 0165-0009, 1573-1480. DOI: 10.1007/s10584-013-0993-z.

Strahler, Arthur N (1968). "Quantitative geomorphology". In: *Fairbridge, R.W. (ed.) Encyclopedia of Geomorphology*. New York: Reinhold Book Corporation.

swisstopo (2020). *swissALTI3D, Bundesamt für Landestopografie*. de. URL: https://www.swisstopo.admin.ch/de/home.html.

— (2023). *Bundesamt für Landestopografie*. de. URL: https://www.swisstopo.admin.ch/de/home.html (visited on 12/21/2023).

— (Aug. 2024). *Bundesamt für Landestopografie swisstopo*. de. URL: https://www.swisstopo.admin.ch/de/hoehenmodell-swisssurface3d (visited on 04/17/2024).

Tilahun, Abayneh and Hayal Desta (Dec. 2023). "Soil erosion modeling and sediment transport index analysis using USLE and GIS techniques in Ada'a watershed, Awash River Basin, Ethiopia". In: *Geoscience Letters* 10.1, p. 57. ISSN: 2196-4092. DOI: 10.1186/s40562-023-00311-9.

Umar, Z., W. Akib, and A. Ahmad (Feb. 2014). "Analysis of Debris Flow Kuranji River in Padang City Using Rainfall Data, Remote Sensing and Geographic Information System". In: *IOP Conference Series: Earth and Environmental Science* 18, p. 012122. DOI: 10.1088/1755-1315/18/1/012122.

USGS (Jan. 2006). *Fact Sheet 2004-3072: Landslide Types and Processes*. URL: https://pubs.usgs.gov/fs/2004/3072/ (visited on 12/07/2023).

Veitinger, J., B. Sovilla, and R. S. Purves (Apr. 2014). "Influence of snow depth distribution on surface roughness in alpine terrain: a multi-scale approach". English. In: *The Cryosphere* 8.2, pp. 547–569. ISSN: 1994-0416. DOI: 10.5194/tc-8-547-2014.

Wilford, David et al. (Mar. 2004). "Recognition of debris flow, debris flood and flood hazard through watershed morphometrics". In: *Landslides* 1, pp. 61–66. DOI: 10.1007/s10346-003-0002-0.

Wilson, John P. and John C. Gallant (Aug. 2000). *Terrain Analysis: Principles and Applications*. Englisch. New York: John Wiley & Sons Inc. ISBN: 978-0-471-32188-0.

Wipf, Sonja, Christian Rixen, and Veronika Stöckli (2013). "Veränderung der Gipfelfloren". In: *Cratschla 2/13: Klimawandel vor der Tür* -.2, pp. 12–13.

Wipf, Sonja, Christian Rossi, et al. (Mar. 2024). *Murgang Buffalora - von tabula rasa zu neuem Leben*. en-US. URL: https://nationalpark.ch/en/forschung/murgang-buffalora/ (visited on 07/23/2024).

Wipf, Sonja and Thomas Scheurer (2016). "Gipfeltreffen im SNP". In: *Cratschla 1/16: Gipfeltreffen im SNP* -.1, pp. 4–5. (Visited on 07/23/2024).

Wood, Eric F., Murugesu Sivapalan, and Keith Beven (1990). "Similarity and scale in catchment storm response". en. In: *Reviews of Geophysics* 28.1, pp. 1–18. ISSN: 1944-9208. DOI: 10.1029/RG028i001p00001.

WSL (2006). "Informationen zu: "Murgang" (Mure, Rüfe)". de. In: *Definitionen "Murgang"*.

— (Mar. 2018). *Unwetter und Bergstürze 2017: Acht Todesopfer und hohe Sachschäden*. URL: https://www.wsl.ch/de/news/unwetter-und-bergstuerze-2017-acht-todesopfer-und-hohe-sachschaeden/ (visited on 04/18/2024).

— (2024). *Murgangtestgelände Illgraben*. de-CH. URL: https://www.wsl.ch/de/ueber-die-wsl/versuchsanlagen-und-labors/naturgefahren-anlagen/murgang-anlagen/murgangtestgelaende-illgraben-susten-leuk-vs/ (visited on 04/18/2024).

Zevenbergen, Lyle W. and Colin R. Thorne (1987). "Quantitative analysis of land surface topography". en. In: *Earth Surface Processes and Landforms* 12.1, pp. 47–56. ISSN: 1096-9837. DOI: 10.1002/esp.3290120107.

Personal declaration: I hereby declare that the submitted thesis results from my own independent work. All external sources are explicitly acknowledged in the Thesis.

Zurich, July 29, 2024

Fabienne Koenig